DEPARTMENT OF ENERGY
Environmental Management Los Alamos Field Office (EM-LA)
Los Alamos, New Mexico 87544

January 14, 2021

EMLA-2021-0128-02-001

Mr. Kevin Pierard
Bureau Chief
Hazardous Waste Bureau
New Mexico Environment Department
2905 Rodeo Park Drive East, Building 1
Santa Fe, NM 87505-6313

Subject: Submittal of the Geophysical Letter Report, Revised Pothole Location Maps, and Independent Review Comments for the Middle DP Road Site Solid Waste Management Unit Assessment Work Plan

Dear Mr. Pierard:

Enclosed please find two hard copies with electronic files of the “Geophysical Letter Report” for the Middle DP Road (MDPR) Site (Enclosure 1). Also enclosed are two revised proposed potholing location maps associated with the “Solid Waste Management Unit Assessment Work Plan for Middle DP Road Site” (Enclosures 2 and 3). These documents are being provided in response to the New Mexico Environment Department’s (NMED’s) request to receive these documents in early January 2021 in order to complete the review of the solid waste management unit assessment work plan.

Based on the geophysical survey results, seven additional pothole locations are proposed at the MDPR Site. As indicated in the “Geophysical Letter Report,” five geophysical anomaly areas were identified based on the combined survey results from time domain electromagnetics (TDEM) and vertical gradient magnetometry (VGM). Linear features identified by frequency domain electromagnetic (FDEM) surveys will be evaluated using existing proposed pothole locations. The two enclosed figures include the five geophysical anomaly areas and the seven additional proposed pothole locations to evaluate these anomalies.

At the request of the U.S. Department of Energy, Environmental Management, Los Alamos Field Office (DOE EM-LA), the Oak Ridge Institute for Science and Education (ORISE) performed an independent review of the December 3, 2020, draft “Solid Waste Management Unit Assessment Work Plan for Middle DP Road Site” and provided comments dated December 18, 2020. To provide transparency, DOE EM-LA is including the ORISE comments as Enclosure 4. Revisions to the work plan as a result of these comments will be evaluated concurrently with comments received from NMED.

If you have any questions, please contact Duane Parsons at (505) 551-2961 (duane.parsons@em-la.doe.gov) or Cheryl Rodriguez at (505) 414-0450 (cheryl.rodriguez@em.doe.gov).

Sincerely,

Arturo Q. Duran

Digitally signed by Arturo Q. Duran
Date: 2021.01.14 13:21:48 -07'00'

Arturo Q. Duran
Compliance and Permitting Manager
Environmental Management
Los Alamos Field Office

Enclosure(s): Two hard copies with electronic files:

1. Geophysical Letter Report, Project 20-184, Middle Delta Prime Road Site Geophysical Investigation
2. Figure 4.1-1, Proposed Potholing Locations and Excavation Areas at Tract A-8-a
3. Figure 4.2-2, Proposed Potholing Locations and Excavation Areas at Tract A-16-a
4. Independent Review of the Solid Waste Management Unit Assessment Work Plan for Middle DP Road Site Associated with the Los Alamos National Laboratory, Los Alamos, New Mexico, DCN 5352-LT-02-0

CC (letter and enclosure[s] emailed):
Laurie King, EPA Region 6, Dallas, TX
Chris Catechis, NMED-DOE-OB
Steve Yanicak, NMED-DOE-OB
William Alexander, N3B
Emily Day, N3B
Michael Erickson, N3B
Jeff Holland, N3B
Kim Lebak, N3B
Joseph Legare, N3B
Dana Lindsay, N3B
Pamela Maestas, N3B
Glenn Morgan, N3B
Joseph Murdock, N3B
Duane Parsons, N3B
Kent Rich, N3B
Joseph Sena, N3B
Troy Thomson, N3B
M. Lee Bishop, EM-LA
Stephen Hoffman, EM-LA
Kirk D. Lachman, EM-LA

David Nickless, EM-LA
Cheryl Rodriguez, EM-LA
emla.docs@em.doe.gov
n3brecords@em-la.doe.gov
Public Reading Room (EPRR)
PRS website

Enclosure 1

Geophysical Letter Report, Project 20-184,
Middle Delta Prime Road Site Geophysical Investigation

January 5, 2021

Luke Hill

Banda Group International, LLC
9664 Eagle Ranch Road NW, Suite 5
Albuquerque, NM 87114

Email: lukeh@bandagroupintl.com

RE: Geophysical Letter Report | Project 20-184
Middle Delta Prime Road Site Geophysical Investigation

Collier Geophysics, LLC (Collier) conducted a geophysical investigation on behalf of Banda Group International, LLC (BGI), located in Los Alamos, New Mexico (Figure 1). The Middle Delta Prime Road (MDPR) Area project site is located at the Los Alamos National Laboratory (LANL) facilities. The site property is currently owned by Los Alamos County. This geophysical investigation was performed under RFP N3B MSA PO-000635-03. The primary objective of the geophysical investigation is to define the presence and limits of buried debris within the defined Area of Interest (AOI). The purpose of this geophysical investigation is to assist BGI in defining the boundaries of historic trench/disposal areas within the AOI. In addition to defining the boundaries, these data will be used for determining, to the extent possible, the distribution of metallic objects. A secondary set of objectives is to identify bedrock conditions, and to the extent possible, identify contaminated materials.

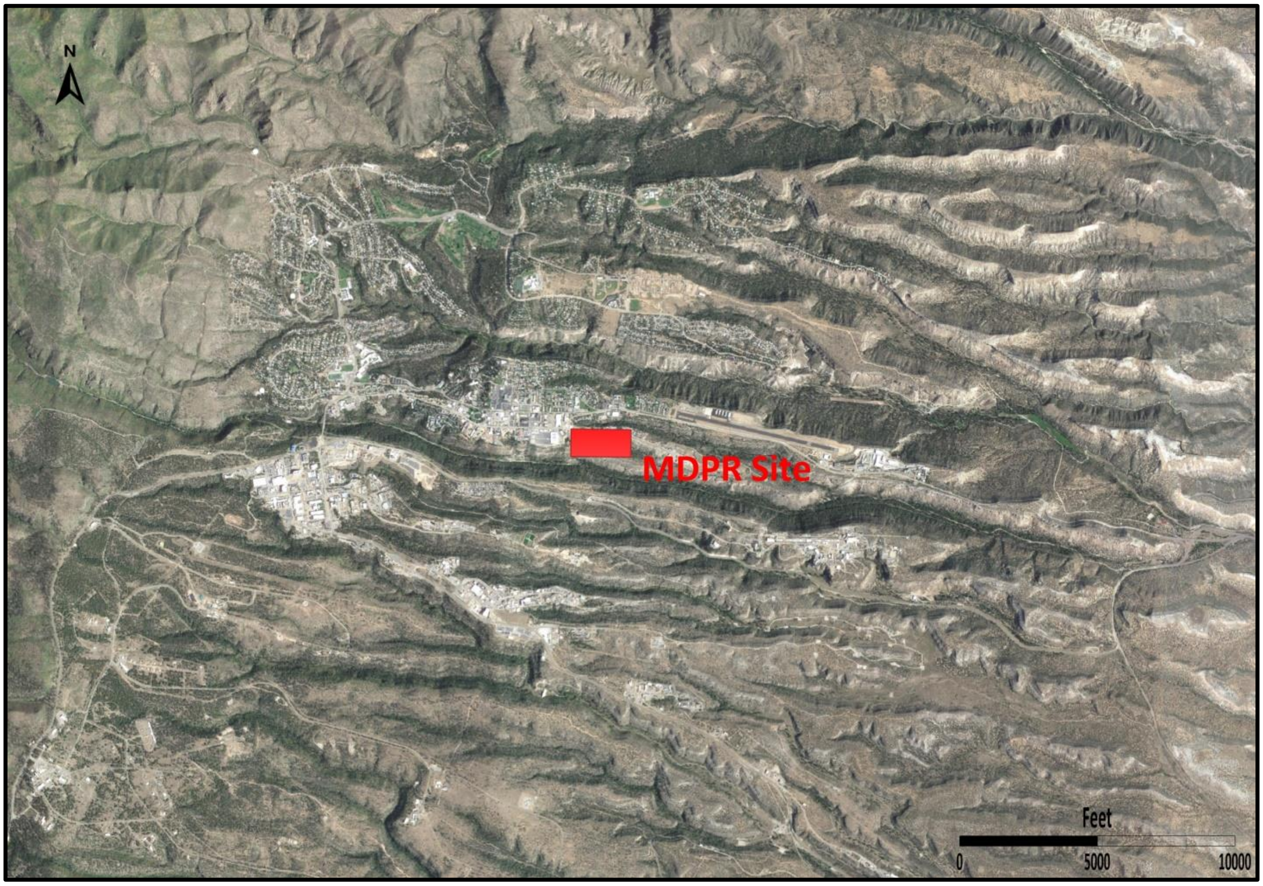

Figure 1. MDPR Site location map (base image from Google Map Tiles).

Site Description

The MDPR Site as identified is an area covering approximately 5.5 acres that potentially has buried solid waste, anticipated to be placed within excavated cells or trenches. The AOI was operational for LANL and contains an unknown quantity or type of buried metallic objects and other debris. Based on historical records, the vertical extent of the buried materials is expected to be in the upper 15 ft below ground surface (bgs); that is, generally within the overburden soils that overly bedrock (Upper Bandelier Tuff) and they are likely covered with clean fill materials.

The AOI is divided into two zones, a north zone and a south zone (Figure 2). Active county operations within the AOI included material loading operations (asphalt pile) in the north half of the north zone and installation of a lift station in the eastern half of the south zone. The site was bounded by fences (ranging from metal T-post and wire to metal chain link security fencing). A number of covered piles of excavated materials were located within the north zone, and the south zone included county construction equipment.

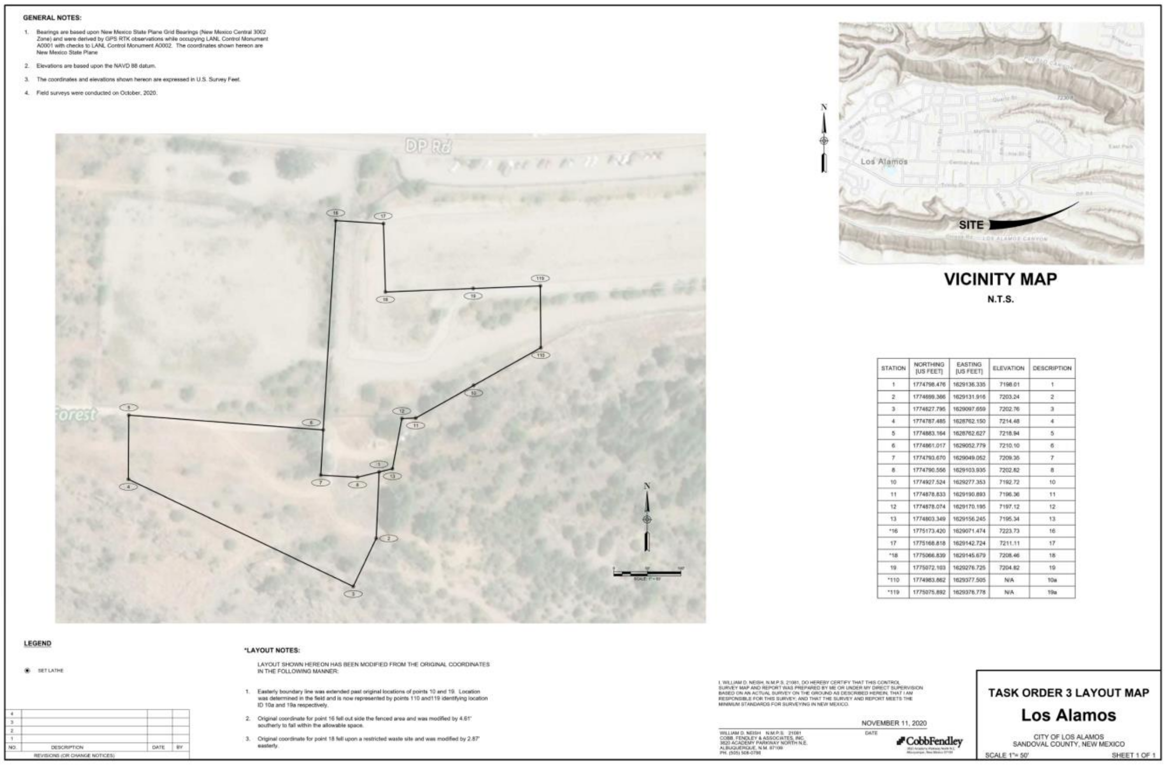

Figure 2. MDPR Site AOI (black outline) as provided by BGI.

Data Acquisition

As outlined in the geophysical work plan, the geophysical data were acquired in three phases: 1) acquire electromagnetic (EM) and magnetic data over 100% of the MDPR Site AOI using Time Domain Electromagnetics (TDEM), Frequency Domain Electromagnetics (FDEM), and Vertical Gradient Magnetometry (VGM); 2) acquire 2D ground penetrating radar (GPR) transects over anomalies identified in the phase 1 data and other areas of interest designated by BGI; 3) perform multiple 2D seismic refraction tomography (SRT) transects across the AOI to create 2D compressional wave velocity (Vp) sections. Based on the size of the AOI and surface conditions at the site, all geophysical data were collected using portable instrumentation. A brief description of each method is proved below. For further information regarding the details of these techniques, Collier can submit a method addendum to this report upon request.

Time Domain Electromagnetics (TDEM)

TDEM data were acquired using an EM61-MK2, by Geonics Limited. The EM61-MK2 instrument is a high-sensitivity metal detector and is an industry standard instrument for shallow metal detection (i.e. UXO surveys, landfill investigations, UST locates, etc.). The EM61 will detect most electrically conductive metals (i.e. copper, aluminum, brass, steel, etc.). The effective depth of detection varies with the size (mass and surface area) of the buried metal object. As a general reference range, the EM61-MK2 can typically detect a one-inch diameter steel pipe four inches in length up to maximum burial depth of about 16 inches, while a 55-gallon steel drum has a maximum detection depth of about 10 feet.

The EM61 consists of a coincident transmitter/receiver main coil 1 m by 0.5 m in size, and an equivalent-sized second receiver coil mounted approximately 0.5 m above the primary coil. A

primary magnetic field is generated by imparting a current through the primary coil which is then shut off (unipolar rectangular current), resulting in decaying eddy currents in the subsurface. These eddy currents decay over time, generating a decaying secondary magnetic field. The instrument records the response induced in the coils generated by the secondary magnetic fields in millivolts (mV) in a series of four time-gates up to 1,266 µs after the primary shutoff. The instrument continuously repeats this process and records data at a rate of 10 Hz. The instrument is highly sensitive to all metallic objects in the subsurface, whether ferrous or non-ferrous, as its primary sensitivity is to electrical conductivity. GPS position data were logged simultaneously recording the NEMA string output from a Trimble Geo7x GPS into the EM61 Allegro data logger. GPS data were logged at a rate of 1 Hz. EM61 data were acquired along roughly parallel profile lines with a nominal 8-foot spacing and along-line data spacing of approximately 0.1 ft.

Frequency Domain Electromagnetics (FDEM)

An FDEM instrument consists of at least one pair of transmitting and receiving coils. A primary magnetic field of a constant frequency is generated using an alternating current in the transmitter coil, and a secondary magnetic field is detected in the receiving coil as a result of the interaction of the primary field with the subsurface. The FDEM instrument allows for simultaneous measurements of both the in-phase and quadrature components of the secondary magnetic field. The in-phase component is measured in parts-per-thousand (ppt) of the amplitude of the primary magnetic field. The in-phase response is primarily sensitive to magnetic susceptibility, generally due to the presence of metallic or ferromagnetic material in the subsurface. The quadrature component (90-degrees out of phase with the primary signal) is primarily sensitive to electrical conductivity due to changes in lithology, moisture, and/or fines (clay) content. The quadrature response is calibrated and measured as apparent bulk conductivity in milliSiemens per meter (mS/m). Note that these are the primary sensitivities, but that both components can be affected by buried metal or geologic features.

FDEM data were acquired using a CMD-Explorer, by GF Instruments. The CMD-Explorer consists of a boom with three sets of FDEM coil pairs, at three separations; 1.4 m (4.5 ft), 2.8 m (9.2 ft), and 4.5 m (14.8 ft). The effective depth of sensitivity of the FDEM method is a function of the antenna spacing between the transmitter and receiver, the antenna orientation, the frequency of the primary field, and the bulk electromagnetic properties of the subsurface. Data were acquired using a vertical dipole orientation, which results in the greatest depth of investigation. The depth of investigation is not precise, but as a rule of thumb when using a vertical dipole orientation, is approximately equal to the antenna spacing. In this case using the CMD-Explorer, the values recorded would correspond to the bulk electromagnetic properties in approximately the upper 5 feet, 10 feet, and 15 feet, of the subsurface respective to each antenna separation. CMD-Explorer data were collected at a rate of 10 Hz, using a primary field frequency of 10 kHz at all three antenna spacings simultaneously. GPS position data were logged simultaneously recording the NEMA string output from a Trimble Geo7x GPS into the CMD data logger. GPS data were logged at a rate of 1 Hz. CMD data were acquired along roughly parallel profile lines with a nominal 8-foot spacing and along line data spacing of approximately 0.1 ft.

Vertical Gradient Magnetometry (VGM)

Magnetometry data were acquired using a Geometrics G-858 magnetometer system. The magnetometer was configured with two sensors mounted on a vertical aluminum pole with a separation of 2.4 feet. Each magnetometer sensor measures the strength of Earth's magnetic field in nanoteslas (nT), called the Total Field Intensity (TFI). With two sensors, the difference in the TFI is calculated to obtain the vertical gradient (VGM). The advantage of measuring the vertical gradient is the elimination of the need for a base magnetometer station to provide drift corrections for the diurnal variation in the total magnetic field intensity. The presence of ferrous materials causes distortions in the magnetic field that are detected by the sensors. The effective depth of investigation of the G858 is highly variable as it

depends on the cumulative effect of many factors including the size, mass, shape and orientation of the metal object, the orientation of the remnant magnetic field of the object and the magnetic properties of the materials surrounding the object. In general, the G-858 is capable of detecting large ferrous metal objects, such as pipelines, well casings and tanks, at significantly greater depths than either the EM61 or CMD.

VGM data were collected at a sample frequency of 10 Hz. GPS position data were logged simultaneously recording the NEMA string output from a Juniper Systems Geode GPS into the G-858 console data logger. GPS data were logged at a rate of 1 Hz. VGM data were acquired along roughly parallel profile lines with nominal 8-foot spacing and along line data spacing of approximately 0.1 ft.

Ground Penetrating Radar (GPR)

The GPR method is based on the recording of reflected electromagnetic waves that are transmitted into the subsurface using a transmitter (TX) and receiver (RX) antenna pair (*inset image, below*).

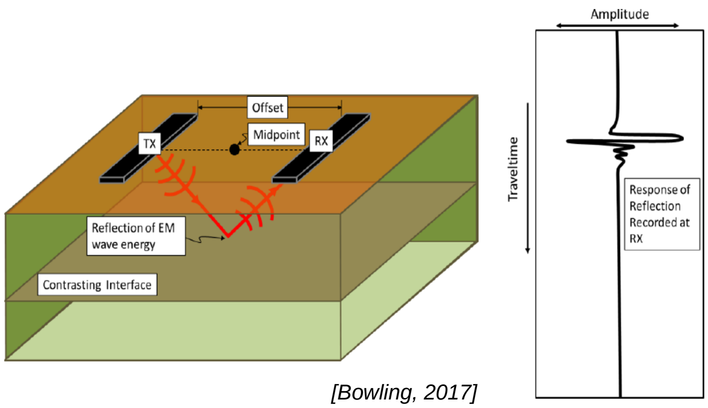

[Bowling, 2017]

The reflections are stored as a time series (known as traces) representing reflection “strength” or amplitude as a function of travel-time. Travel-time is the time required for the transmitted energy to travel down from the transmitting antenna into the subsurface, reflect off an interface of contrasting electromagnetic impedance, and travel back up to the surface to be recorded by the GPR receiver antenna. Therefore this time is often referred to as two-way travel-time (TWT).

As the GPR instrument is moved to different locations on the surface, different reflection series are recorded which represent changes in the subsurface EM impedance/reflectivity distribution. GPR signals are sensitive to the presence of a variety of subsurface materials including: buried objects (metallic and nonmetallic), air-filled voids, water saturated sediments, and geologic boundaries.

For this project GPR data were acquired over geophysical anomalies selected from the TDEM, FDEM and VGM datasets, and in other areas of concern as delineated by BGI onsite personnel. Spacing between GPR transect lines varied depending on ground conditions and the area to be covered. The in-line trace spacing was nominally 1 inch.

A GSSI SIR-4000 GPR system with a digital monostatic 350 MHz antenna was utilized for the data acquisition. GPS position data were logged simultaneously recording the NEMA string output from a Juniper Systems Geode GPS into the SIR4000 GPR console and written into the trace headers. The GPS antenna was mounted on a tripod directly over the center of the 350 MHz GPR antenna. GPS data were logged at a rate of 1 Hz. The effective depth of investigation is strongly affected by the site-specific soil properties such as clay content, water content and metal content. In areas where the bulk conductivity of the soils is greater than about 25 - 30 milliSiemens/meter, GPR effective depth of investigation will be severely limited. The manufacturer's specification for depth of investigation range for the digital 350 MHz antenna is listed as 0 to 40 feet; however, the high end of this range is only possible under ideal conditions. For typical good soil site conditions, the maximum effective depth of investigation is generally 5 -10 ft.

Seismic Refraction Tomography (SRT)

Seismic data were collected using a gimballed land streamer receiver array. Three seismic profile lines were surveyed within the AOI. The land streamer consists of twenty-four 30 Hz geophones suspended within a metal cylindrical enclosure at 3.3 ft (1 meter) spacing. The land streamer is ideally suited to work on smooth ground surfaces, as the weighted gimballed sensors provide good coupling to the ground without the need for inserting a metal spike, and the entire array can be advanced along the profile line by dragging the assembly.

Seismic data were acquired using a Geometrics Geode 24 channel seismograph. This recording system utilizes a state-of-the-practice seismograph connected to a field laptop via an ethernet cable. Analog data from the geophones are collected in the seismograph where the data are digitized, transmitted to the laptop computer, and then recorded on the computer's hard drive. Geophone positions were measured with a Trimble Geo7x, a handheld GPS unit with sub-meter accuracy.

SRT data were acquired using an active seismic impact source (16-lb sledgehammer and HDPE strike plate). Shot points were spaced every 13.1 feet (four receiver stations) along line. Off-end shots for each profile line were also collected to increase ray path coverage beneath the ends of the line(s). Each seismic profile was recorded in overlapping individual segments (24-channel spreads). After source data were recorded at 13.1 feet spacing along each 24-channel spread up through geophone #13 of 24 active, the land streamer was advanced half the spread length (39.4 ft [*12 geophone stations*]) and source recording was repeated at 13.1 ft intervals. This progression continued until the end of the profile line was reached.

The maximum depth of investigation for SRT is a function of the size of the active receiver array (23 meters), the seismic source (sledgehammer) and the subsurface velocity structure, in particular the depth to the top of the first refractor. Additionally, the seismic refraction method assumes the seismic velocity increases with depth. If a high velocity layer overlies a lower velocity layer, the low velocity layer will not be directly detected by refraction methods. Generally, maximum depth of investigation using these acquisition parameters is up to 30 ft.

Data Processing

Time Domain Electromagnetics (TDEM)

The raw TDEM data were downloaded and converted to tabular data files using TrackMaker61 MK2 (version 1.65), by Geomar Software Inc. All further data processing and gridding of the TDEM data was performed using Geosoft Oasis montaj, version 9.3 (Seequent). Within Geosoft, data were analyzed for instrument latency, the presence of drop-outs or spikes, and any drift in the background readings over time (instrument drift), which can be produced by changes in ambient conditions during operation. Data quality for the TDEM data was fair to good, with significant amounts of background electromagnetic noise that required filtering. In order to maximize the data quality, data from each of the four time gates was leveled using the following procedure: First surgically edit outlier data points from the dataset, then fit the remaining data using a smooth curve (via a BSpine filter), and finally remove the smooth curve from the full dataset.

Following the steps described above, the four different time gates were summed together. Geosoft was then used to grid and view the summed TDEM data using the minimum curvature method, and export the result as a plan view map image.

Frequency Domain Electromagnetics (FDEM)

Raw FDEM data were exported in tabular format using CMD Data Transfer, version 1.6.1, by GF Instruments. Positions for each measurement are interpolated for each record from GPS positions using the data transfer software. The data were then processed using Geosoft Oasis montaj, version 9.3 (Seequent). Data were checked for quality then gridded using a minimum curvature method, and export the result as a plan view map image.

Aarhus Workbench, version 5.9.3.0 was used to generate an earth resistivity model based on the FDEM bulk conductivity values. This process includes: decoupling the recorded EM response from surface features by removing affected data, using a 4-meter moving-window average to generate a pseudo-FDEM sounding every 25 cm along the acquired transects, and geophysical inversion of the processed pseudo-soundings. The geophysical inversion process iteratively fits a subsurface electrical resistivity model to each of the pseudo-soundings generated from the first processing steps, subject to lateral smoothing constraints (i.e., along data collection profiles). Resistivity models from the geophysical inversion are then exported in x-y-z-v format (3D position and value) to Geosoft Oasis montaj for final visualization.

Vertical Gradient Magnetometry (VGM)

The VGM raw data were positioned and converted to tabular data files using MAGMAP 2000 (version 5.04), by Geometrics, Inc. All further data processing and gridding of the VGM data was performed using Geosoft Oasis montaj version 9.7.1, by Seequent. The primary step required for VGM data processing is to remove data dropouts that can occur during data acquisition. These data dropouts occur when the magnetometer is aligned at a particular angle with respect to the Earth's magnetic field, or is very close to a large above ground metal object. These occurrences are typically less than one second in duration, and can be easily removed from the data with no detrimental effects on the final results. No further corrections or filtering were required, as the data quality was good to very good. Geosoft was used to grid the VGM data using the minimum curvature method. In addition, an analytic signal (AS) filter was applied to the VGM data grid. AS is an amplitude gradient computation which effectively compensates for the positive/negative magnetic dipole effects in raw VGM data, in order to place magnetic anomalies over their causative bodies.

Ground Penetrating Radar (GPR)

The GPR data processing was performed using Radan v.7 by GSSI Inc. GPR Data processing followed a standard workflow, taking the raw data and applying several filtering and gaining procedures to produce interpretable images. These steps included:

- Mute the direct wave
- Apply exponential gain function
- Apply background removal filter

Seismic Refraction Tomography (SRT)

The 2D refraction data from this investigation were processed using Rayfract®, version 4.01, by Intelligent Resources Inc. The two processing steps involved with SRT processing are first arrival picking and tomographic inversion. The first arrival picking step consists of picking the time on each signal trace where the first arrival energy from the seismic source is observed at each geophone position for each shot record . After picking is completed, a data inversion is performed generating a two-dimensional (2D) P-wave velocity (Vp) model that best fits the arrival picks by iteratively modifying an initial velocity grid model until the misfit between the modeled and measured travel-time values is minimized, subject to smoothing constraints.

GPS Surveying and Positional Data

The location of the surface features were surveyed on the first day of geophysical data acquisition using a Trimble Geo7x handheld GPS. The surface feature GPS data, and the SRT survey data, were differentially corrected in post-processing using Trimble Pathfinder and local permanent GPS base data. GPS data differentially corrected in post-processing typically has a horizontal accuracy better than 0.5 meters under good conditions. A number of control points were GPS surveyed by Collier on the first field day and post-processed as part of the surface feature survey. Comparing Collier's GPS surveyed locations of the control points with BGI's provided locations show that most (9 control points) are within 0.5 ft, one is within 0.75 ft and two outliers are offset by approximately 3 ft. There is approximately a 1.5 meter average offset to the northwest between the real-time GPS positions and the Trimble Pathfinder post-processed GPS positions for the surface feature GPS survey dataset.

GPS positional data recorded simultaneously with instrument data (TDEM, FDEM, VGM and GPR data) were linked in real-time and as such were not differentially corrected in post-processing. The real-time GPS survey data will typically have sub-meter horizontal accuracy or better under good conditions.

Results and Discussion

Time Domain Electromagnetics (TDEM)

A color contoured plan view map of the summed TDEM response for all four time gates is shown in Figure A-1 in the upper left-hand plot window and in Figure A-2. The color contours range from blue to red (low mV response to high mV response). In this plot blue contours represent areas with background readings and little or no buried metal detected. Color contours from green to red represent areas where the EM61 instrument detected the likely presence of metal. The darkest red areas, representing the largest TDEM response, indicate areas containing metal – above or below ground. The detected metal could range from a single large metal object, such as a steel drum, to a number of smaller individual metallic objects clustered beneath or adjacent to the TDEM instrument. Distinguishing between a single large metallic object and a cluster of smaller metallic objects, using only the TDEM data, is difficult. Burial pits or trenches filled with debris containing metallic objects will typically appear in the TDEM plan map as broad areas with variability of the elevated response, and often with vague outlines in shape or a group of irregular clusters of smaller anomalies. Smaller isolated anomalies are generally associated with individual random pieces of buried metal and would not be considered high priority anomalies if searching for a metallic debris-filled burial pit.

As discussed in the Data Acquisition section above, the maximum depth of investigation using the EM61-MK2 instrument varies depending on the mass of the metal object, and other factors. However, this instrument is generally not significantly affected by soil conditions, except in unusual circumstances which are not expected at this site. The only buried metal object at this site of known depth was the culvert beneath the access road (labeled “Buried Metal Culvert” near the northeast corner of Figure A-22). The maximum burial depth to the top of this culvert is approximately 4-5 ft-bgs and this feature was easily detected by the EM61-MK2 creating a high amplitude response (Figure A-2). Large metal surface objects, such as construction vehicles or metal chain link fences, may obscure the signal from buried objects in the TDEM data when those data are acquired within 5 – 10 ft of the surface metal object. Even though they are not beneath the sensor, these surface metal features are also detected by the instrument, which records the sum of all the responses to metal within the volume of the active EM field.

Frequency Domain Electromagnetics (FDEM)

A color contoured plan view map of the FDEM In-Phase and Quadrature response is shown in Figure A-1 in the lower left- and lower right-hand plot windows, respectively, with full page plan maps shown in Figures A-3 and A-4. The In-Phase response is primarily sensitive to larger volume or linear metallic features, while the Quadrature Phase (Bulk Conductivity) is primarily sensitive to ground conductivity (which can also be elevated due to the presence of metal in the subsurface). In Figure A-4, note that the Bulk Conductivity data (mS/m) have been converted to Bulk Resistivity (ohm-m) for easier comparison with the inverted FDEM earth model shown in Figure A-5. The FDEM data identified multiple linear anomalies. Long linear anomalies that appear in both the In-Phase and Bulk Conductivity are likely associated with buried metallic pipes or electrical utilities. However, the east-west and north-south large and obvious response anomalies along the edges of the south and north areas, respectively, are located relatively close to the perimeter fence. The FDEM anomalies do not exactly mimic the fence position, nor do they have equal response along the entire length of the fence; therefore, they are called out as FDEM anomalies (Figures A-3, A-4 and A-22). Linear anomalies that are only evident in the Bulk Resistivity may represent non-metallic pipes or excavations that have been backfilled with non-native soil or trapped moisture in the fill materials.

A pseudo-3D resistivity earth model was developed from the FDEM quadrature data and is presented in Figure A-5 as resistivity depth slices (i.e., 2D plan maps) at 2.5-foot depth intervals. The earth resistivity model was affected by the significant presence of metal at this site, both surface metal and subsurface metal. This impact to the FDEM data required increased smoothing to minimize the localized effects of metal on the measurements. While this improves the inversion results for the resistivity earth model in terms of characterizing the bulk soil electrical properties (vertical variation), it also limits the lateral resolution of small-scale features or objects of interest such as buried debris. Linear features are better represented in the plan view map of the bulk resistivity data (Figure A-4).

As discussed in the Data Acquisition section above, the maximum depth of investigation using the CMD instrument is generally about 15 ft for the largest transmitter – receiver coil separation. This may be reduced if the near surface soils are very conductive (low resistivity). Significant amounts of subsurface or surface metal in close proximity to the instrument can affect the depth of investigation due to their influence on the measured bulk conductivity. As with the EM61-MK2, the known culvert was easily detected by the CMD resulting in strong lows in both the In-Phase and bulk resistivity measurements (Figures A-3 and A-4).

Vertical Gradient Magnetometry (VGM)

Two different color contoured plan view maps of the VGM data are presented to highlight the use of magnetometry surveys. Figure A-1 presents the vertical gradient in the upper right-hand plot; and, Figure A-6 presents a full page plan view map of the VGM analytic signal result. The vertical magnetic gradient is the difference in the total magnetic field intensity measurements between two magnetic sensors relative to the vertical offset distance between the sensors. VGM is only sensitive to magnetic objects, predominantly ferrous metals, unlike TDEM which is sensitive to all conductive metallic objects. Comparison of the responses of larger anomalies in the TDEM and VGM data are used to provide some differentiation between ferrous metal objects and non-ferrous metallic objects. Using VGM data, magnetic anomalies typically appear as dipoles (a magnetic low “blue” adjacent to a magnetic high “red” - see Figure A-1), the orientation of a dipole depends on the shape and orientation of the ferrous metal object. Figure A-6 shows the vertical magnetic gradient data after applying the analytic signal filter, as discussed in the data processing section above. In the AS plot (Figure A-6), the location of the detected ferrous metal object would theoretically be directly beneath the peak amplitude of the anomaly (for an isolated subsurface target passing directly beneath the magnetometer sensors).

VGM is a potential field method which does not use an active signal source; therefore, the depth of investigation is dependent on the magnitude and orientation of the variation (vector property) in the remnant magnetism of ferrous metal objects at the site. Additionally, as a potential field method, the instrument is sensitive to the local perturbations of the earth’s magnetic field caused by all ferrous metal objects, both above ground and below ground, within the detection limit of the instrument. Therefore, the measured total field data at each sensor are the sum of all of the vector contributions of the earth's magnetic field and all the remnant magnetic fields of magnetic objects within the detection limits of the sensors. Using the magnetic vertical gradient will help to reduce the effects of offline surface ferrous metal objects adjacent to the sensor location to some degree, but the VGM data are more sensitive to surface metal features than the TDEM or FDEM data. The location of the known metal culvert correlates with a strong response in the VGM AS data (Figure A-6); however, the shape of the feature is not as well defined as in the TDEM and FDEM data. This may be due to the geometry of the data collection line paths over the culvert or to other ferrous metal objects (surface and/or subsurface) located in the vicinity of the culvert.

Ground Penetrating Radar (GPR)

Figure A-7 shows a plan view map with the locations of the GPR scan lines. The GPR profile sections are shown in Figures A-8 through A-19. GPR data collected over a known buried metal culvert in the North Zone did not detect the culvert at an estimated burial depth of 3 to 4 ft-bgs. The GPR data collected in the vicinity of SRT Line 3 (GPR Line 32) shows a clear shallow reflection to a maximum depth of approximately 3 ft-bgs. This reflection horizon likely represents a layer change within the unconsolidated overburden, possibly the contact between surface fill materials and native soils. Therefore, with the exception of the area around GPR Line 32, the effective depth of investigation for GPR at this site was limited to less than 2 ft-bgs. The GPR data in this excepted area also show some distinct diffractions in multiple parallel GPR profiles. These diffractions likely represent buried pipelines.

The GPR data collected along the SRT profile lines (GPR Lines 32, 36, and 38) are shown in Figures A-12, A-13 and A-14 respectively, and with the SRT profiles in Figure A-21. The plots in Figure A-21 show that the GPR data do not image to the depth of the interpreted top of bedrock horizon (dashed black contour) shown in the SRT Vp sections (Figure A-20). SRT results are discussed in the following section.

To a much greater degree than any of the other geophysical methods deployed at this site, the effectiveness of GPR is heavily dependent on the site-specific ground conditions. Therefore, the effective depth of investigation cannot be determined prior to data collection at a given site. Typically, high bulk ground conductivity, often due to high clay content in the soils, is a common limiting factor in GPR depth of investigation. At this site, the mean bulk conductivity of the surface soil layer is approximately 24 mS/m, as measured by the shortest offset receiver coil (1.4 meter separation) of the CMD instrument which is most sensitive to the upper few feet of soil. This value is approaching the general rule of thumb limit of 25 – 30 mS/m and is likely a contributing factor in limited GPR depth of investigation at this site. This is also supported by the observation that the best GPR data were collected in an area where the near surface bulk conductivity (measured by the 1.4 m separation coils on the CMD) was less than 14 mS/m. Based on approximately 5,930 linear feet of GPR data collected at this site, we have not fully identified the boundaries of areas where near-surface soil properties limit the depth of investigation when using a new, state-of-the-art, 350 MHz GPR digital antenna. This antenna was selected to identify the depth of buried objects in the overburden soils, and had an anticipated depth of investigation of 5 to 10 feet bgs.

Seismic Refraction Tomography (SRT)

The SRT results are shown as color contoured 2D P-wave velocity (Vp) cross sections beneath the three seismic lines in Figure A-20. Horizontal and vertical scales and color contour scales for each line are the same. An inset image showing a 3D perspective view of the 2D lines (as viewed from the southeast) is included in Figure A-20. The P-wave velocity (Vp) results tie very well at the line intersections, based on the 3D seismic fence diagram. Cool colors show low velocities (i.e., blues) which are generally loose, unconsolidated and unsaturated soils. Hot colors (i.e., orange/red) show more competent, generally harder materials, which can be interpreted as bedrock. Vp values are an indication of the bulk compressibility of the subsurface materials.

Based on information provided by BGI, bedrock (Upper Bandelier Tuff) was anticipated to be shallow beneath the SRT profile lines but with a variable thickness. Based on the good signal quality and SRT model results, a Vp of 2,300 ft/s has been selected to represent the transition from unconsolidated or weathered materials to bedrock. Borehole geologic information is not yet available to confirm this velocity interface as bedrock; that is, to calibrate these model results with the interpretation. But, based on experience and the high gradient in the Vp contours, we are led to this interpretation, which is shown as the black-dashed lines on each 2D SRT section. The three lines of SRT show an interpreted overburden soil layer (undifferentiated fill and native materials) that ranges from less than 5 feet thick (Line 1 – distance ~0-20 ft) to a maximum observed thickness of just greater than 20 feet (Line 1 – distance ~340 ft). This interpreted bedrock velocity is quite low for competent bedrock, indicating the tuff is either poorly welded, highly fractured and/or a thick weathering zone is present. Drill hole information will be valuable to confirm the Vp interpretation. However, the general shape / geometry of the soil-rock interface, and the overall depth will not be expected to change significantly. Bedrock outcrops at the surface along the southern edge of the South Zone in the AOI (i.e., beyond the southern extent of SRT Line 2). The thickest section of overburden observed beneath both Lines 1 and 2, in the southern part of the AOI, is easily observed in the 2D seismic sections and the inset 3D perspective view (Figure A-20).

The depth of investigation of the SRT method is primarily controlled by the length of the active receiver array (75.5 ft) and the subsurface velocity structure (Vp). At this site, the first refractor encountered in the data, indicated by a change in slope of the first arrivals of signal from the sledgehammer at each receiver, is interpreted as the dashed black line (2,300 ft/s Vp contour) in Figures A-20 and A-21. In the refraction method, the highest ray path density will be associated with this boundary and the highest subsurface resolution will be in the area with the highest raypath data density. Beneath this impedance boundary, raypath density is lower and results in a reduction of resolution. The depth to this interpreted refractor in the SRT profiles ranges from about 5 ft to 20 ft-bgs. This is within the normal depth range expected for this array geometry and thin overburden over bedrock site conditions.

Anomaly Selection

Figure A-22 shows a combined layer map of the interpreted TDEM (red), FDEM (yellow) and VGM (dark blue) data overlain on the Google Earth site image, with posted surface features. Based on the observed trends in each data set, anomaly identification and selection was prioritized for overlapping TDEM and VGM anomalies (e.g., isolated areas), and then FDEM anomalies (e.g., linear features). In Figure A-22, the selected and co-located TDEM and VGM anomalies are outlined in light blue; and the selected linear FDEM anomalies are shown as yellow lines. These selected anomalies are listed below in Tables 1A and 1B:

Table 1A. Center location of selected & co-located TDEM and VGM anomalies (WGS84, DD.dd)

TDEM/VGM Anomaly	Center Latitude	Center Longitude
A	35.87761504	-106.28821691
B	35.87792493	-106.28806758
C	35.87879473	-106.28822083
D	35.87845266	-106.28792178
E	35.87759928	-106.28872777

Table 1B. End points of selected FDEM linear anomalies (WGS84, DD.dd)

FDEM Anomaly	Latitude	Longitude
F (west end)	35.87775373	-106.28905950
F (east end)	35.87772656	-106.28862619
G (west end)	35.87796342	-106.28955097
G (bend)	35.87784105	-106.28912646
G (east end)	35.87785909	-106.28820294
H (west end)	35.87806432	-106.28932634
H (east end)	35.87798395	-106.28820621
I (south end)	35.87810284	-106.28830189
I (north end)	35.87882467	-106.28821913

FDEM Anomaly	Latitude	Longitude
J (west end)	35.87850304	-106.28749026
J (east end)	35.87852784	-106.28728092
K (west end)	35.87846560	-106.28750909
K (east end)	35.87843543	-106.28727387

The selected TDEM and VGM anomalies represent areas with a coincident and larger lateral extent and are apparent in both the TDEM and VGM data. These anomaly areas are of the size and shape generally associated with burial pits and/or trenches. Anomaly A may represent a single buried metal object or a small number of clustered buried metal objects. Anomalies B, C and D are interpreted to reflect multiple metallic objects within the outlined area. While Anomalies B, C and D have marked above-ground metallic surface features and/or marked buried utilities within the anomaly extent, these known cultural features alone do not fully account for the elevated instrument response or spatial extents for these anomalous locations. Anomaly E may represent a single buried metal object based on the shape of the TDEM anomaly.

The selected FDEM linear anomalies represent long linear features typical of narrow trenches or buried utilities (e.g., non-metallic or low conductivity pipe). Over the majority of the extents of these linear FDEM anomalies shown in Figure A-22, there are no apparent or corresponding TDEM/VGM anomalies. This indicates that these features do not likely contain significant amounts of conductive metal. These linear FDEM anomalies, most apparent in the FDEM bulk resistivity measurements (Figure A-4), suggest that the native in-situ soils along these alignments may have been disturbed and possibly replaced with non-native or backfilled materials characterized by a difference in bulk resistivity. Two of these linear higher bulk resistivity anomalies are very close to the boundary fence on the north edge of the southern AOI and the west edge of the northern AOI (previously discussed); as such, their proximity is noteworthy for investigation. Linear Anomaly H is in close proximity, and roughly parallels the mapped alignment of a buried sewer utility shown in Figure A-22. However, the western end of Anomaly H diverges from the mapped sewer utility to the north and then fades out, suggesting that this anomaly may not be fully attributable to the buried sewer utility as mapped. Anomaly I is located between the alignments of a mapped electrical utility and a mapped sewer utility (Figure A-22); however, the shape, character and length of Anomaly I may not totally be attributable to these buried utilities. Linear Anomalies F, G, and K are not located near known or mapped buried utilities. The western portion of Anomaly J is likely associated with the buried corrugated metal culvert, while the eastern portion of the anomaly is not located near any mapped buried utility or linear surface metal features. Elsewhere, the in-phase FDEM data (Figure A-3) clearly detects the buried corrugated metal culvert and detects the perimeter metal fencing at this site, which generally impacts the quadrature values next to the fences as well.

One GPR anomaly is identified on the eastern end of the North AOI Zone, in an area with better depth of investigation (green line, Figure A-22). This anomaly is listed in Table 1C below.

Table 1C. Center location of selected GPR anomaly (WGS84, DD.dd)

GPR Anomaly	Center Latitude	Center Longitude
L	35.8783617	-106.287448

This anomaly has a length of approximately 30 ft and is characterized by a cluster of irregularly spaced small diffractions located beneath a reflecting horizon at a depth of approximately 3 ft-bgs (GPR Line 32, Figures A-12 and A-21). The width of the anomaly (off-line extent) cannot be determined from the single GPR profile. This GPR anomaly has the general in-line extent and characteristics of a potential debris pit. In this location, the VGM shows only background response, indicating no ferrous metal was detected. The TDEM plan map for this area shows two small clusters of low to moderate response above background indicating the presence of metal. The TDEM metal detector is a profiling tool (mapping in X, Y), such that the size and depth of the metal detected cannot be directly determined from the instrument data.

The selected geophysical anomalies discussed above represent the most likely locations of potential debris filled pits or trenches, if present, identified in the geophysical data. An intrusive field investigation is necessary to determine the nature and cause of these geophysical anomalies. The site, in general, contains an abundance of metal, both above and below ground surface that was detected by the geophysical instruments. Geophysical coverage gaps are present beneath the existing debris piles, large surface metal and surface obstructions which are noted on Figure A-22.

Closure

Overall FDEM and VGM data quality were very good, with high signal-to-noise data acquired over the AOI. TDEM data quality was good, although intermittent noise was detected during static instrument testing at a location near the parking area, east of the North AOI Zone. This type of TDEM noise may have been a result of nearby radar (airport) and/or radio signals. SRT data quality was very good with high signal-to-noise levels recorded for most records. SRT Line 1 data had some elevated ambient noise from an operating generator located just north of the fence line in the South AOI Zone, but this did not significantly impact data processing. While GPR data quality was moderate to good, the effective depth of investigation was variable across the site, with the best depth penetration in the southwest corner of the North AOI Zone over regions covered by fill materials. It is determined that the GPR signal penetration of 2 to 3 feet bgs, renders much of the GPR data ineffective for depth imaging of buried objects/debris. Apart from the GPR data/results, there is a high degree of confidence in the results presented herein.

The geophysical methods and field procedures defined in this report were applicable to the project objectives and have been successfully applied by Collier geophysicists to investigations of similar size and nature. However, sometimes field or subsurface conditions are different from those anticipated and the resultant data may not achieve the investigation objectives. Collier warrants that our services were performed within the limits prescribed for this project, with the usual thoroughness and competence of the geophysical profession. Collier conducted this project using the current standards of the geophysical industry and utilized in house quality control standards to produce a reliable geophysical survey.

Collier is very appreciative of the support provided by BGI staff and for the assistance in data collection and site logistics. If you have any questions regarding the field procedures, data analyses, or the interpretive results presented herein, please do not hesitate to contact us. We appreciate working with you and look forward to providing BGI with geophysical services in the future.

Respectfully Submitted,

Collier Geophysics, LLC

J. Pfeiffer

Jim Pfeiffer, PGp, PG
Senior Geophysicist

Phil Sirles

Phil Sirles
Senior Geophysicist

(1 copy e-mailed PDF format)

FIGURES

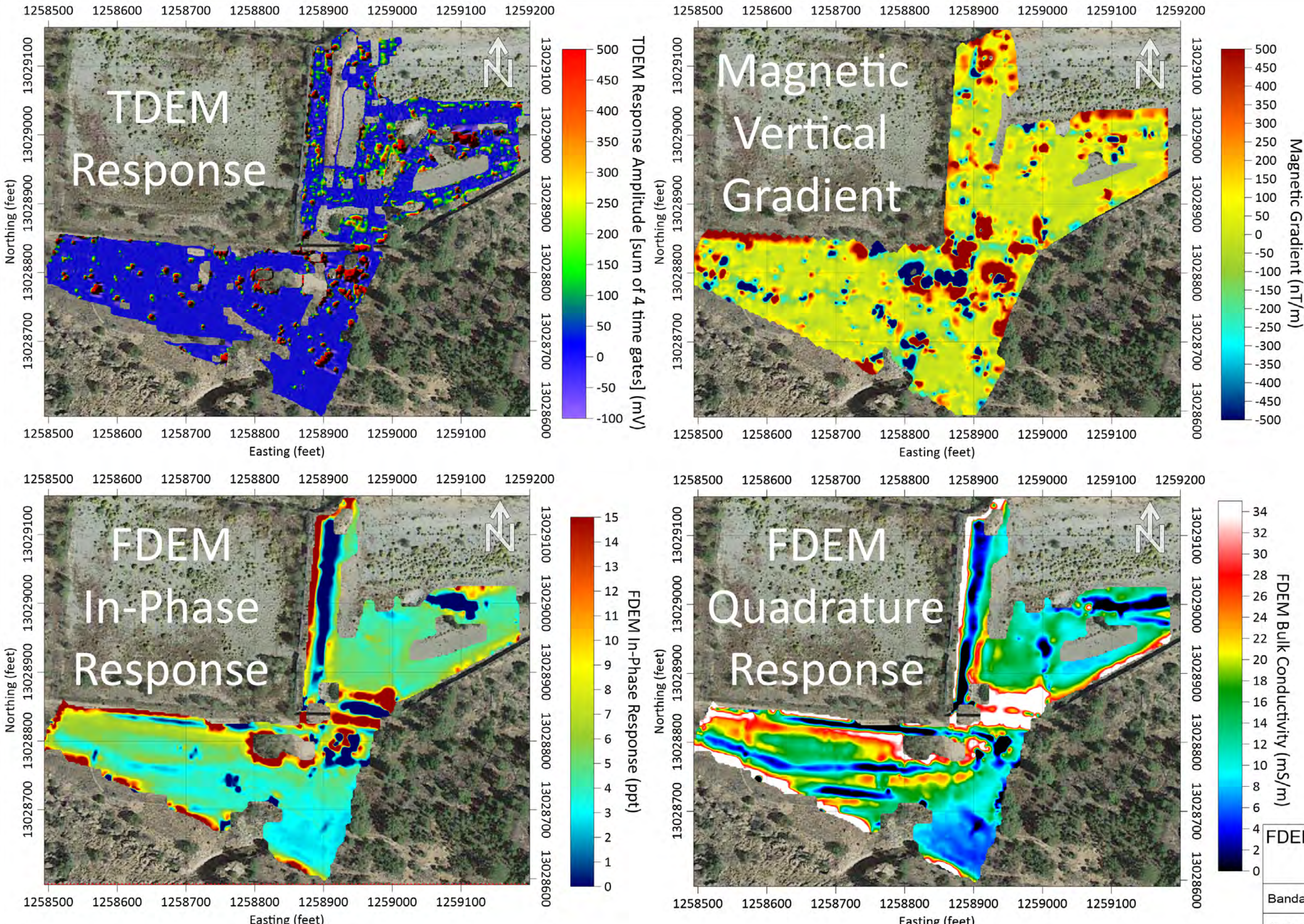

UTM 13N NAD83 Feet

FDEM, TDEM and VGM Results MDPR Site Investigation Los Alamos, NM	
Banda Group International, LLC	COLLIER GEOPHYSICS
Project #: 20-184	January 2021
Drafted by: J. Sheehan	Checked by: P. Sirles
	Fig. A-1

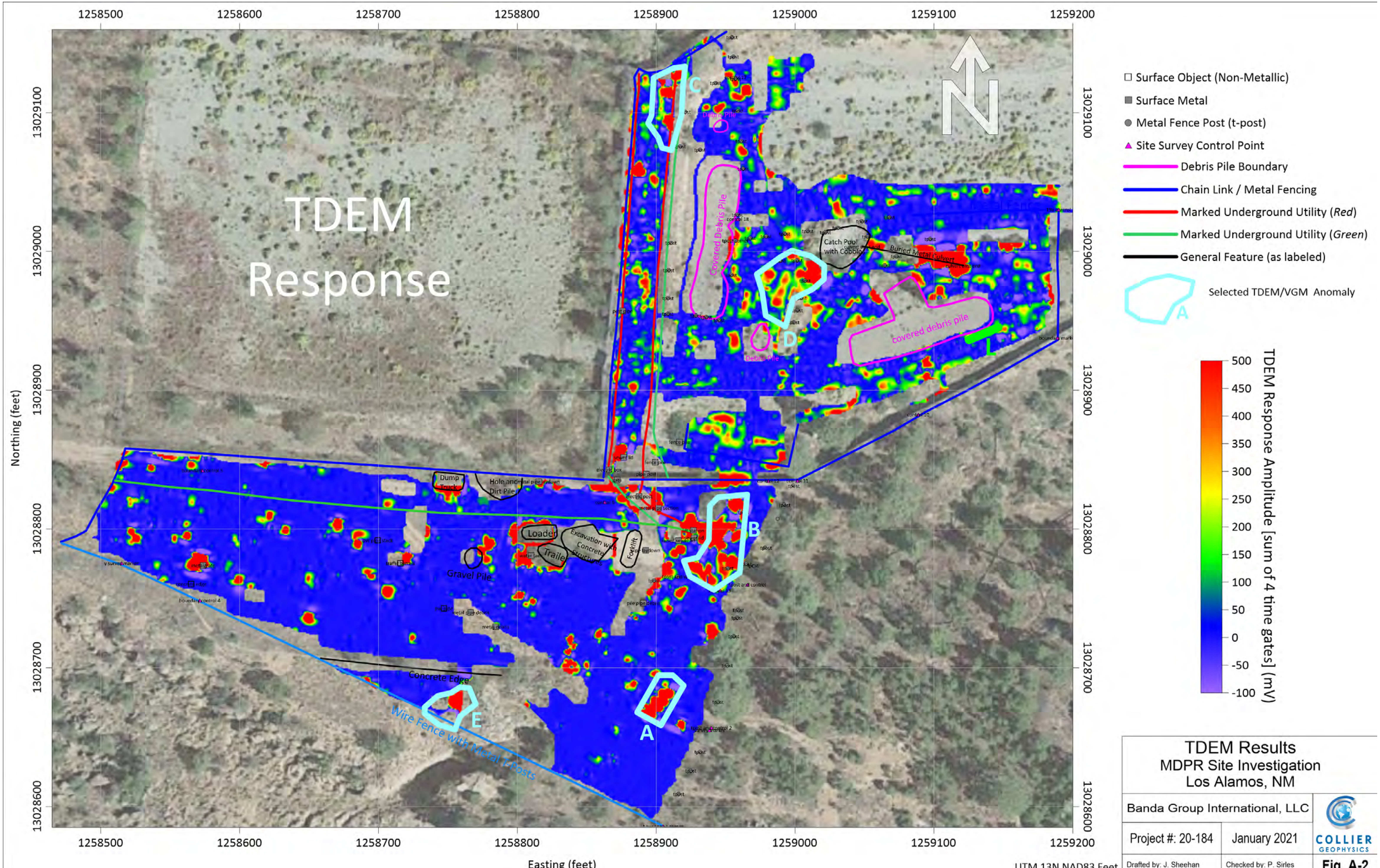
TDEM Response
Surface Object (Non-Metallic)
Surface Metal
Metal Fence Post (t-post)
Site Survey Control Point
Debris Pile Boundary
Chain Link / Metal Fencing
Marked Underground Utility (Red)
Marked Underground Utility (Green)
General Feature (as labeled)
Selected TDEM/VGM Anomaly
TDEM Response Amplitude [sum of 4 time gates] (mV)
500
450
400
350
300
250
200
150
100
50
0
-50
-100
Easting (feet)
Northing (feet)
UTM 13N NAD83 Feet
Covered Debris Pile
covered debris pile
Debris Pile
Catch Pool with Cobble
Buried Metal Culvert
Dump Truck
Hole and Dirt Pile
Loader
Excavation with Concrete Structure
Trailer
Forklift
Gravel Pile
Concrete Edge
Wire Fence with Metal T-posts
A
B
C
D
E
TDEM Results
MDPR Site Investigation
Los Alamos, NM
Banda Group International, LLC
Project #: 20-184
January 2021
COLLIER GEOPHYSICS
Drafted by: J. Sheehan
Checked by: P. Sirles
Fig. A-2

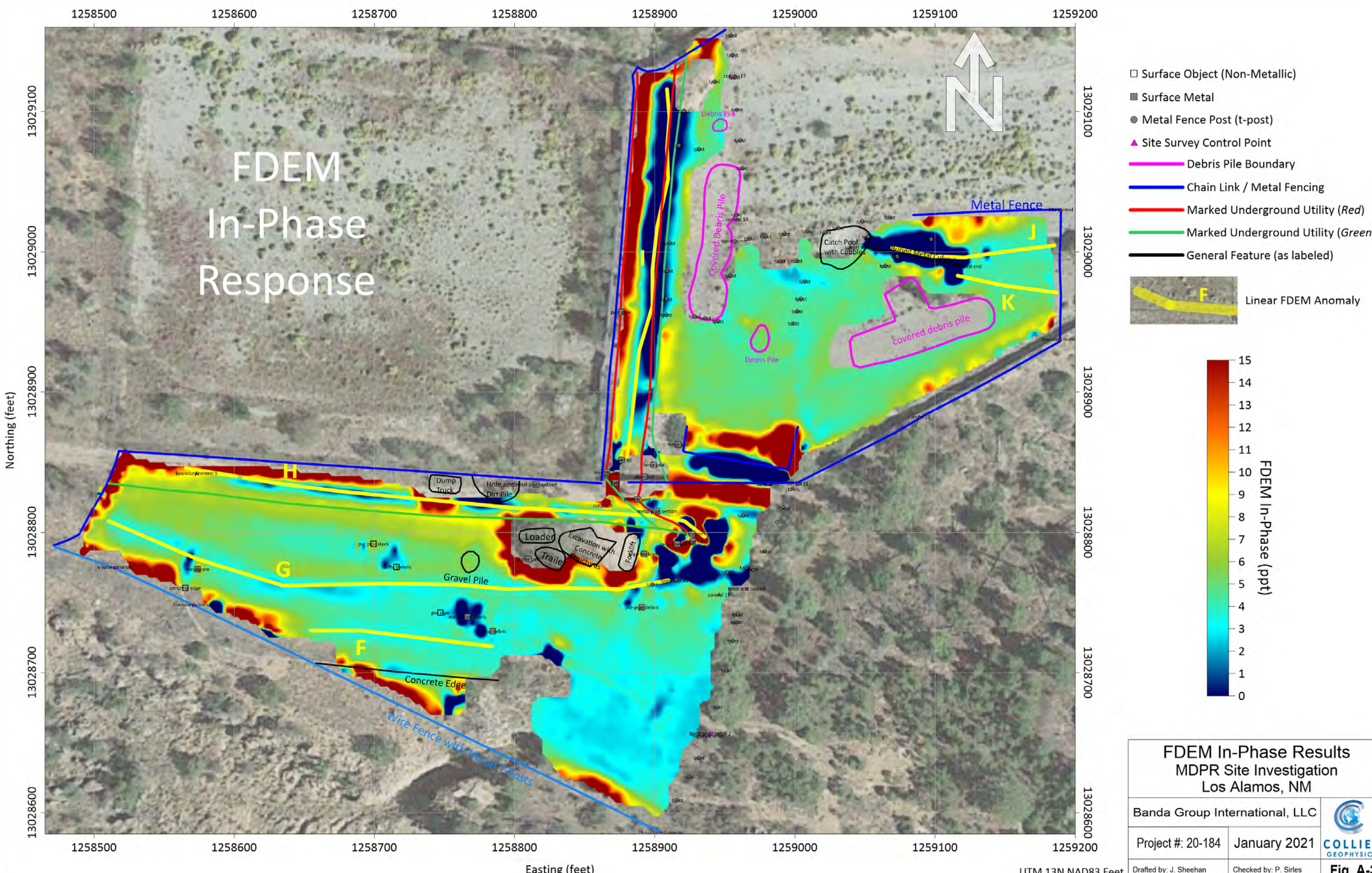

FDEM In-Phase Results
MDPR Site Investigation
Los Alamos, NM

Banda Group International, LLC

Project #: 20-184 | January 2021

COLLIER GEOPHYSICS

Drafted by: J. Sheehan | Checked by: P. Sirles | Fig. A-3

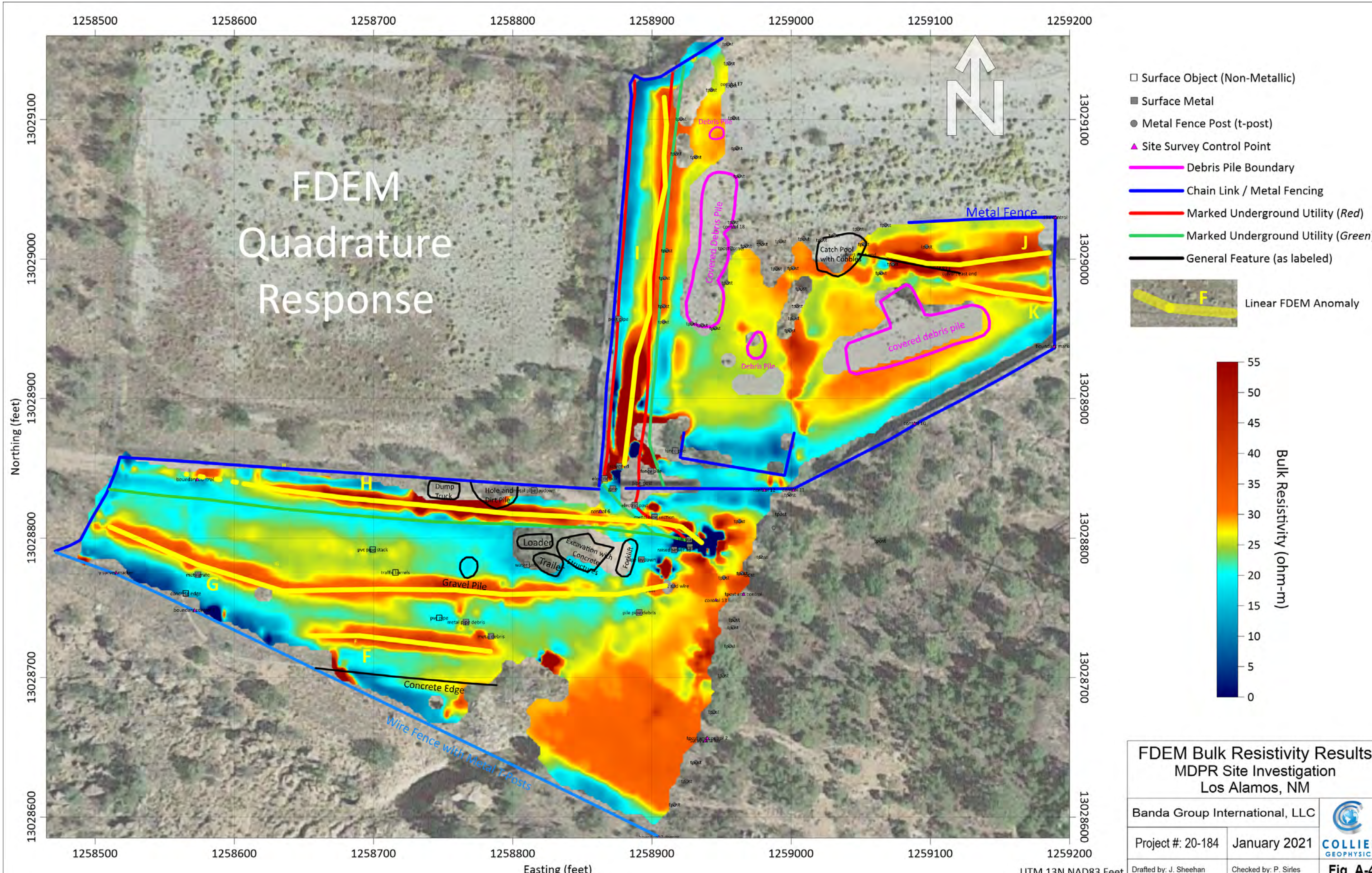
FDEM
Quadrature
Response
Surface Object (Non-Metallic)
Surface Metal
Metal Fence Post (t-post)
Site Survey Control Point
Debris Pile Boundary
Chain Link / Metal Fencing
Marked Underground Utility (*Red*)
Marked Underground Utility (*Green*)
General Feature (as labeled)
Linear FDEM Anomaly
Bulk Resistivity (ohm-m)
55
50
45
40
35
30
25
20
15
10
5
0
Easting (feet)
Northing (feet)
1258500
1258600
1258700
1258800
1258900
1259000
1259100
1259200
13028600
13028700
13028800
13028900
13029000
13029100
Metal Fence
Wire Fence with Metal T-posts
Catch Pool with Cobbles
Covered Debris Pile
covered debris pile
Debris Pile
Dump Truck
Hole and Dirt Pile
Loader
Trailer
Excavation with Concrete Structures
Forklift
Gravel Pile
Concrete Edge
F
G
H
I
J
K
UTM 13N NAD83 Feet
FDEM Bulk Resistivity Results
MDPR Site Investigation
Los Alamos, NM
Banda Group International, LLC
Project #: 20-184
January 2021
Drafted by: J. Sheehan
Checked by: P. Sirles
COLLIER GEOPHYSICS
Fig. A-4

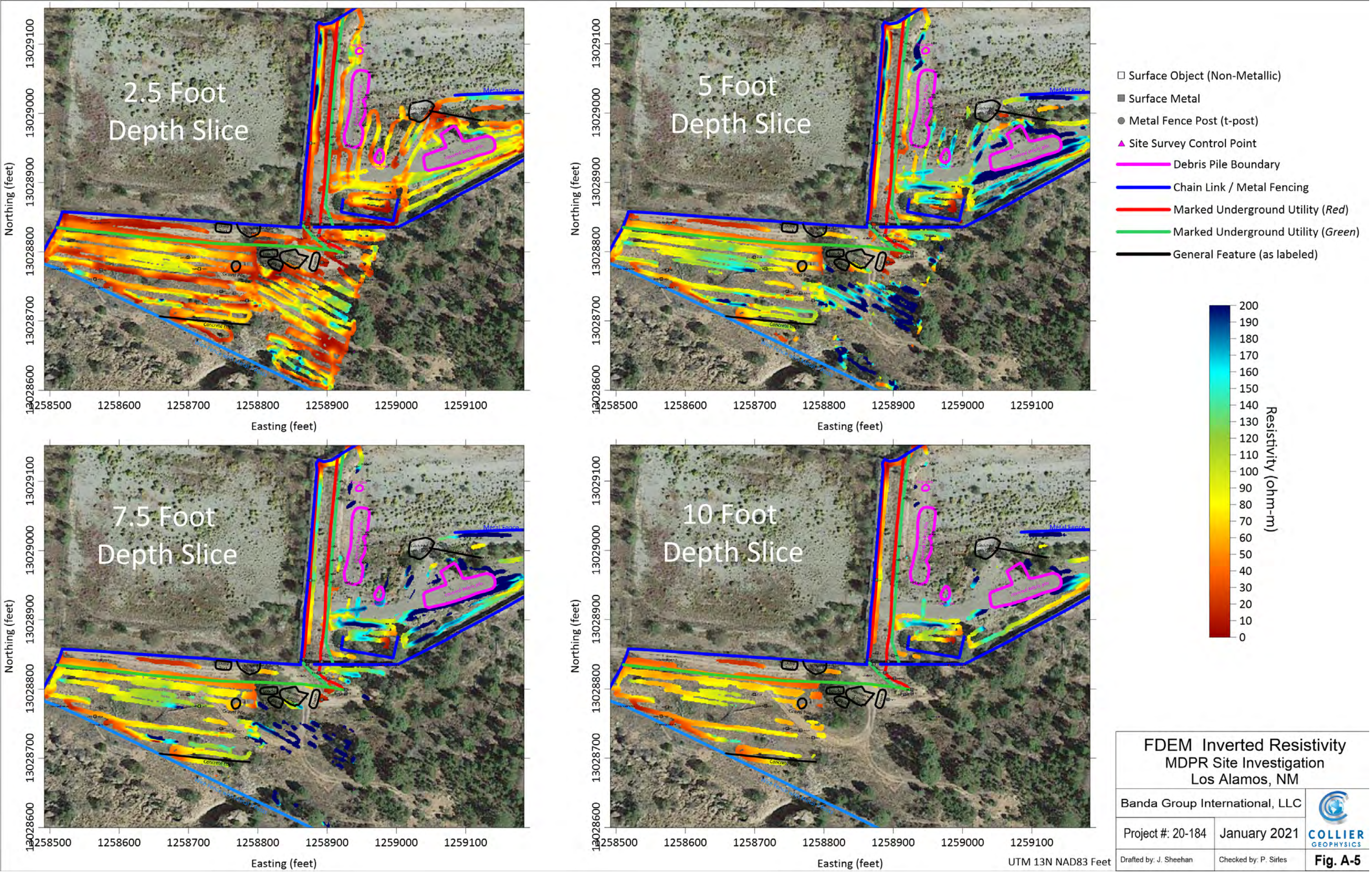
2.5 Foot Depth Slice
5 Foot Depth Slice
7.5 Foot Depth Slice
10 Foot Depth Slice
Northing (feet)
Easting (feet)
13028600
13028700
13028800
13028900
13029000
13029100
1258500
1258600
1258700
1258800
1258900
1259000
1259100
Metal Fence
Gravel Pile
Concrete
Surface Object (Non-Metallic)
Surface Metal
Metal Fence Post (t-post)
Site Survey Control Point
Debris Pile Boundary
Chain Link / Metal Fencing
Marked Underground Utility (Red)
Marked Underground Utility (Green)
General Feature (as labeled)
Resistivity (ohm-m)
200
190
180
170
160
150
140
130
120
110
100
90
80
70
60
50
40
30
20
10
0
UTM 13N NAD83 Feet
FDEM Inverted Resistivity
MDPR Site Investigation
Los Alamos, NM
Banda Group International, LLC
Project #: 20-184
January 2021
COLLIER GEOPHYSICS
Drafted by: J. Sheehan
Checked by: P. Sirles
Fig. A-5

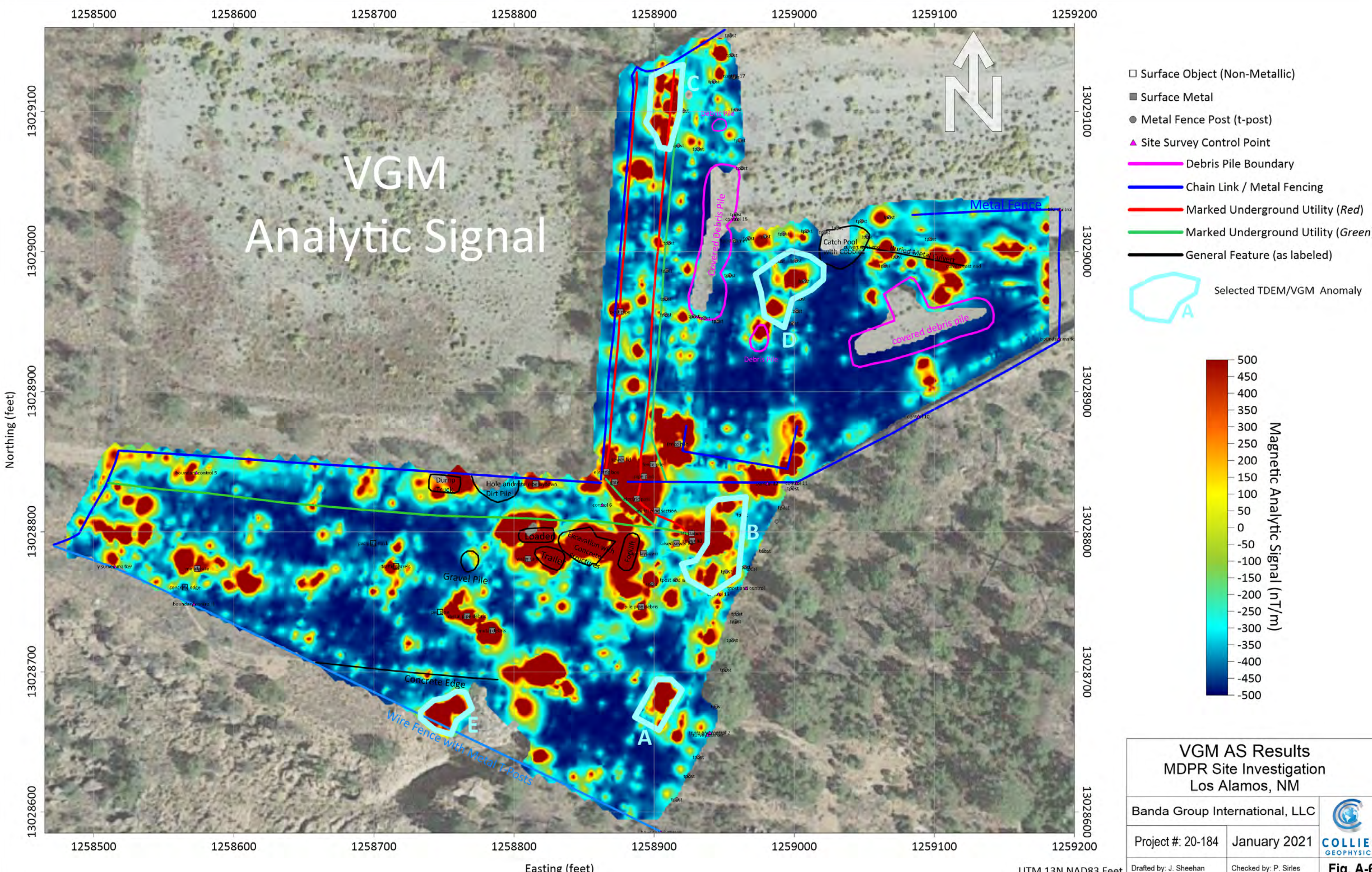

VGM AS Results
MDPR Site Investigation
Los Alamos, NM

Banda Group International, LLC		COLLIER GEOPHYSICS
Project #: 20-184	January 2021	
Drafted by: J. Sheehan	Checked by: P. Sirles	Fig. A-6

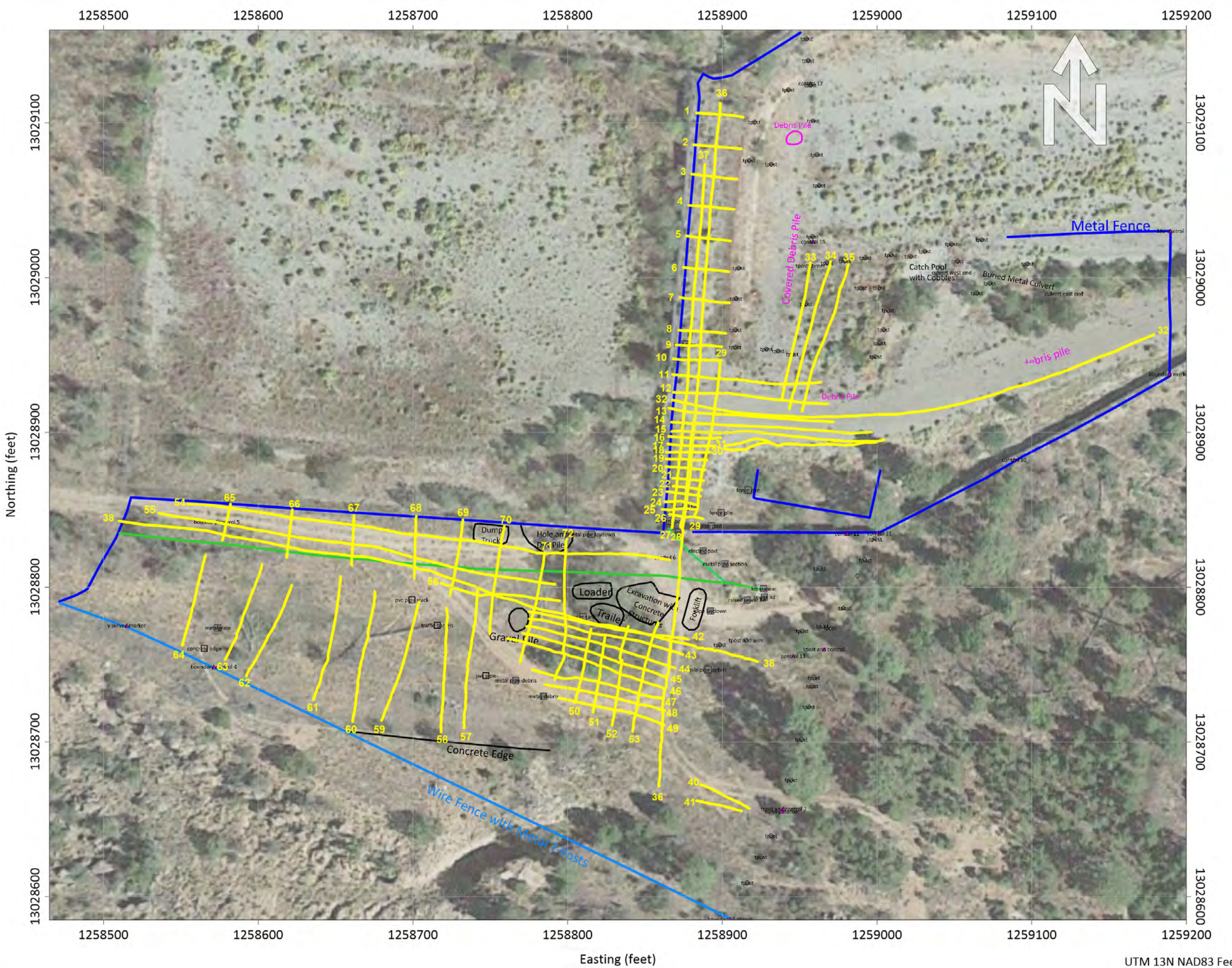

- Surface Object (Non-Metallic)
- Surface Metal
- Metal Fence Post (t-post)
- Site Survey Control Point
- Debris Pile Boundary
- Chain Link / Metal Fencing
- Marked Underground Utility (*Red*)
- Marked Underground Utility (*Green*)
- General Feature (as labeled)
- GPR Survey Lines

GPR Survey Line Paths MDPR Site Investigation Los Alamos, NM	
Banda Group International, LLC	COLLIER GEOPHYSICS
Project #: 20-184	January 2021
Drafted by: J. Sheehan	Checked by: P. Sirles

Fig. A-7

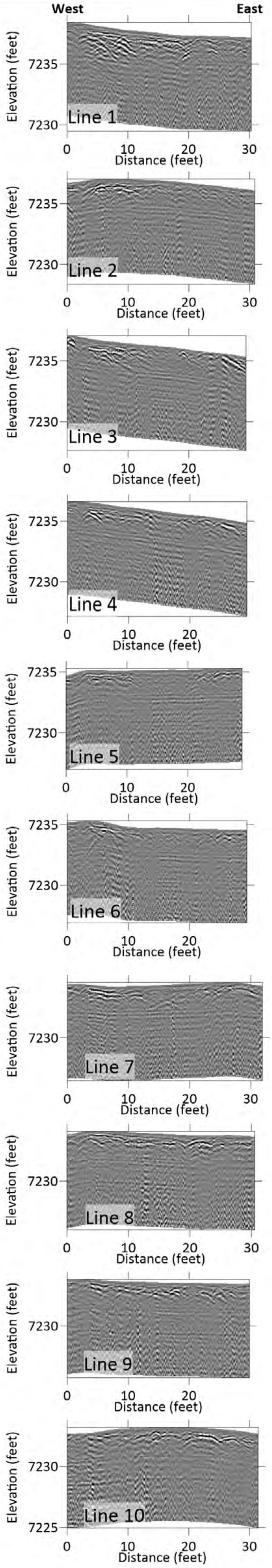

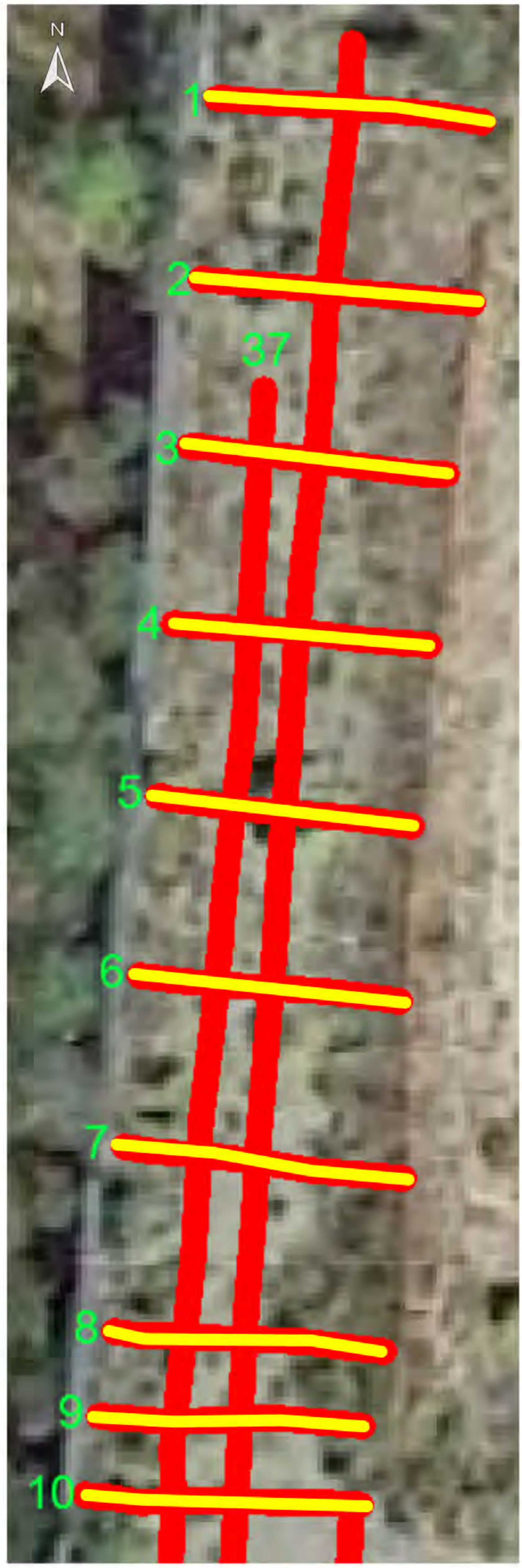

GPR Results (1 of 12)
MDPR Site
Los Alamos, NM

Banda Group International, LLC		COLLIER GEOPHYSICS
Project #: 20-184	January 2021	
Drafted by: J. Sheehan	Checked by: P. Sirles	Fig. A-8

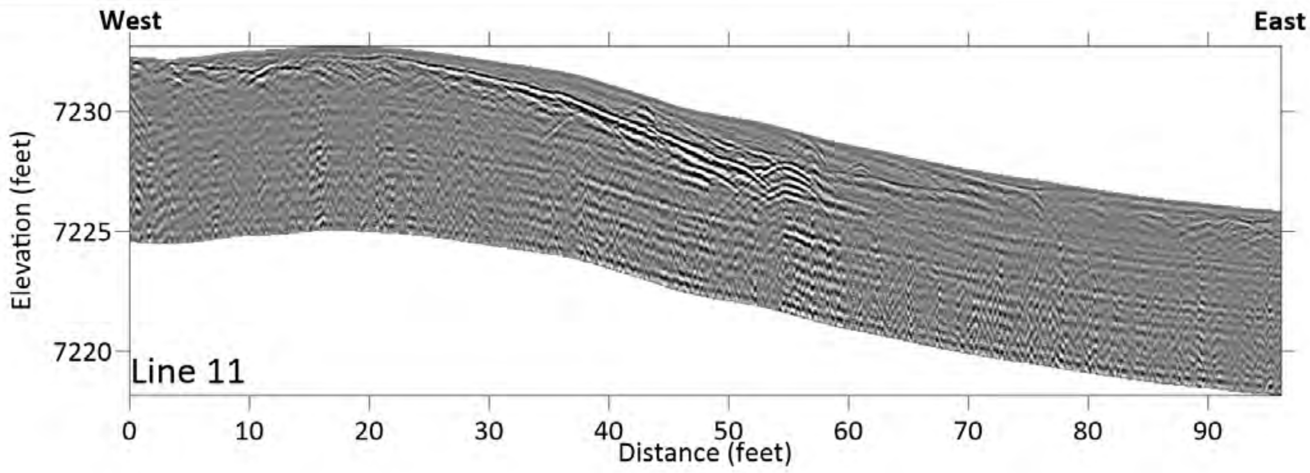

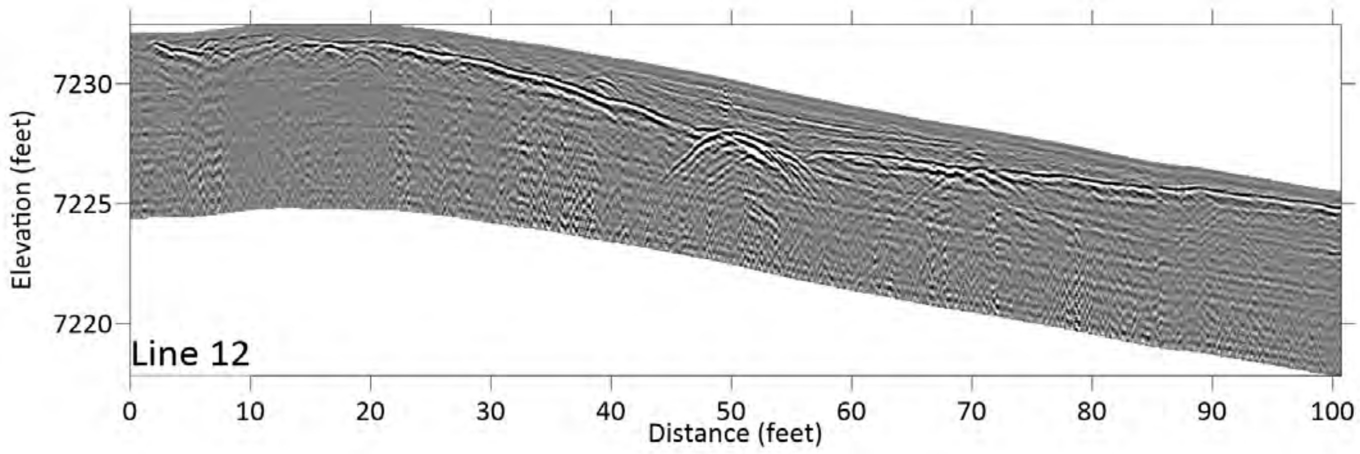

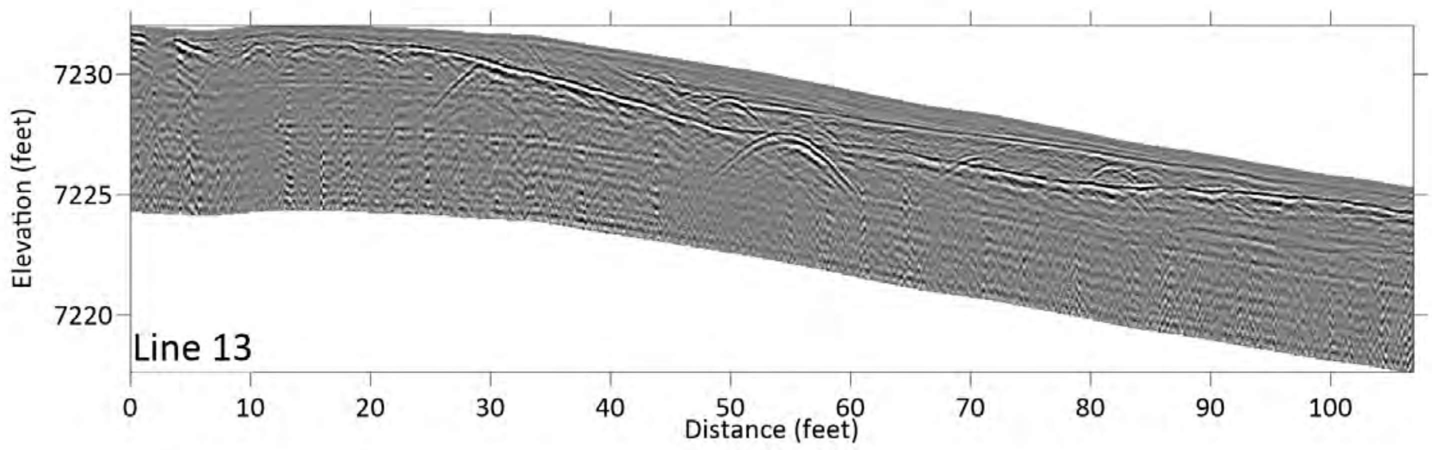

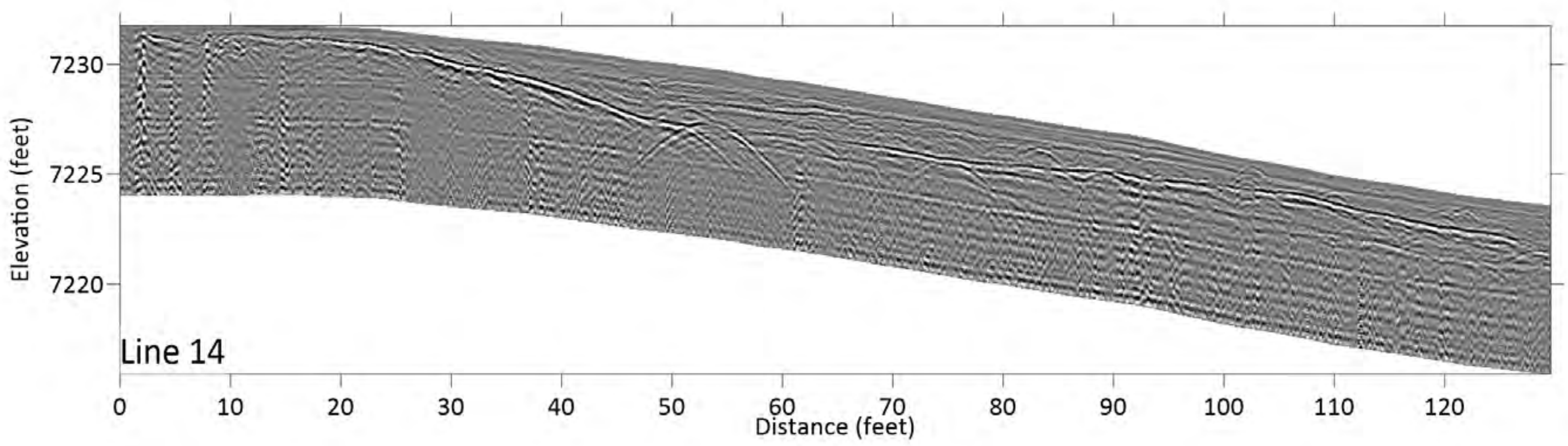

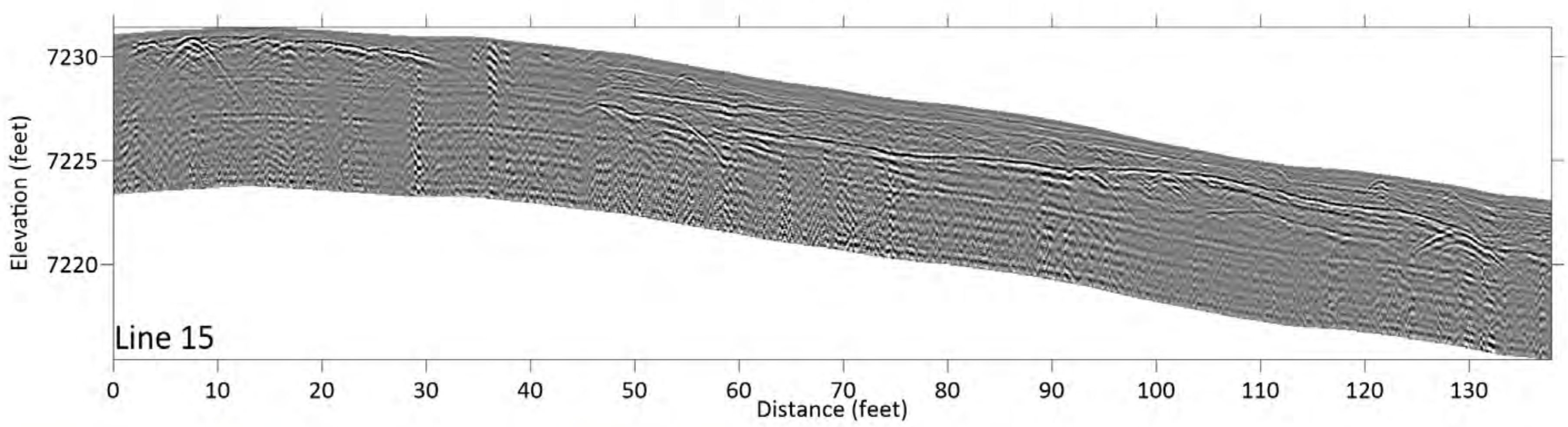

GPR Results (2 of 12)
MDPR Site
Los Alamos, NM

Banda Group International, LLC	COLLIER GEOPHYSICS
Project #: 20-184	January 2021
Drafted by: J. Sheehan	Checked by: P. Sirles

Fig. A-9

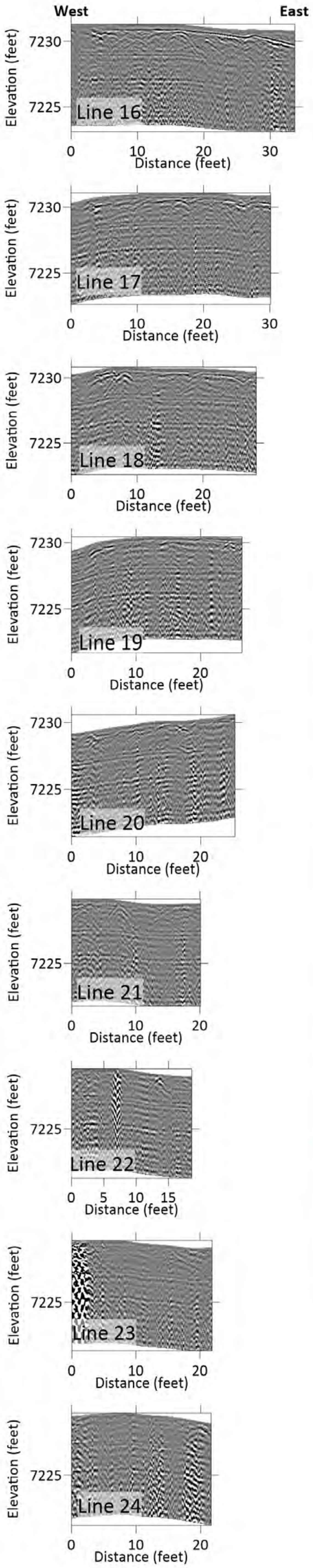

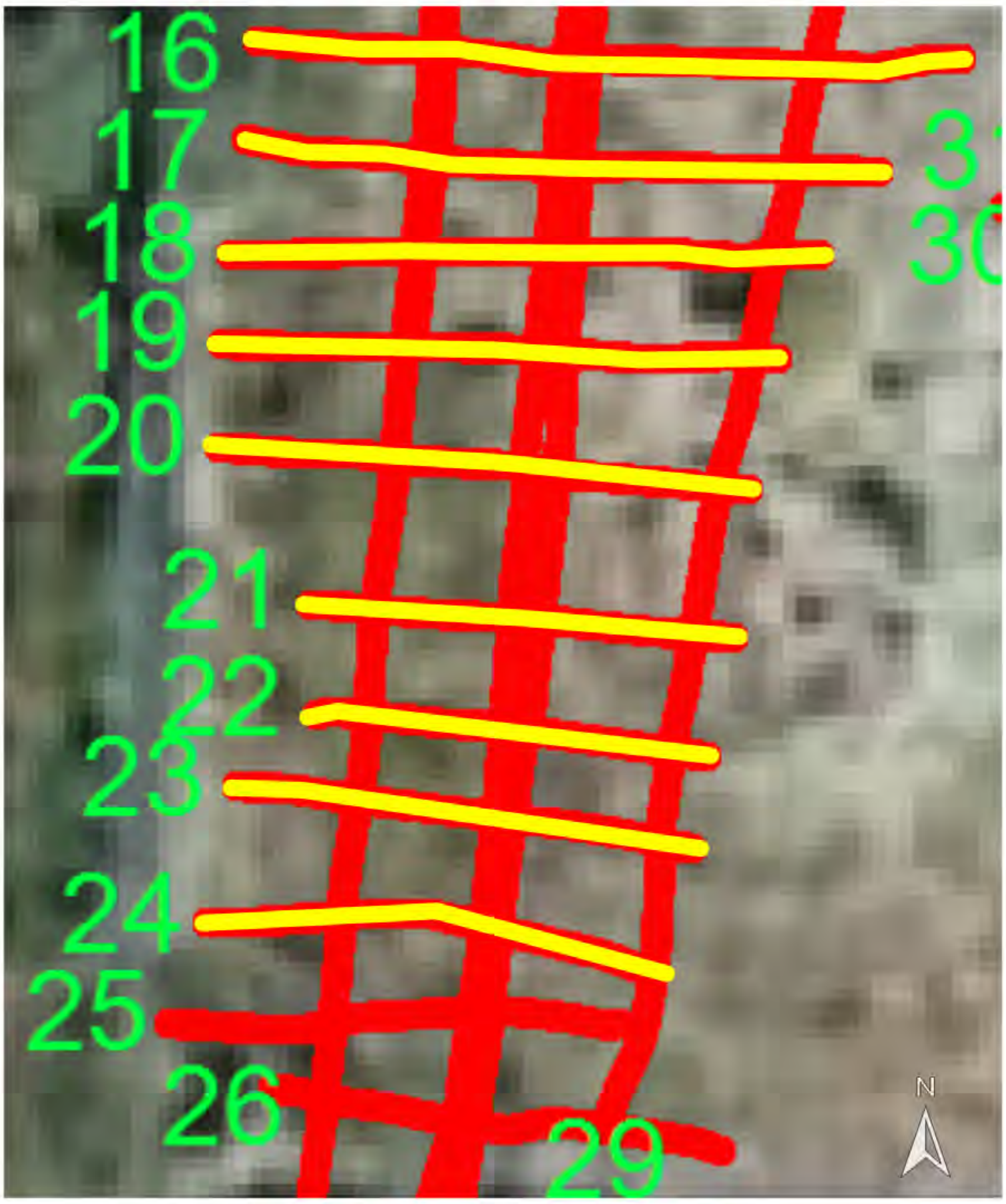

GPR Results (3 of 12)
MDPR Site
Los Alamos, NM

Banda Group International, LLC

Project #: 20-184	January 2021
Drafted by: J. Sheehan	Checked by: P. Sirles

COLLIER GEOPHYSICS

Fig. A-10

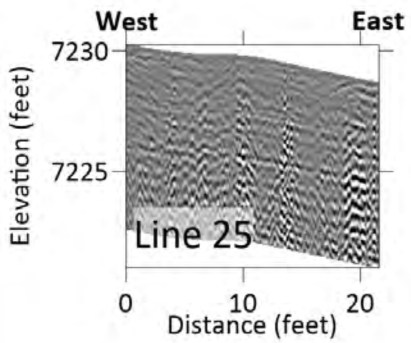

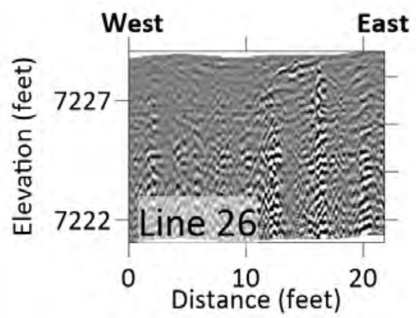

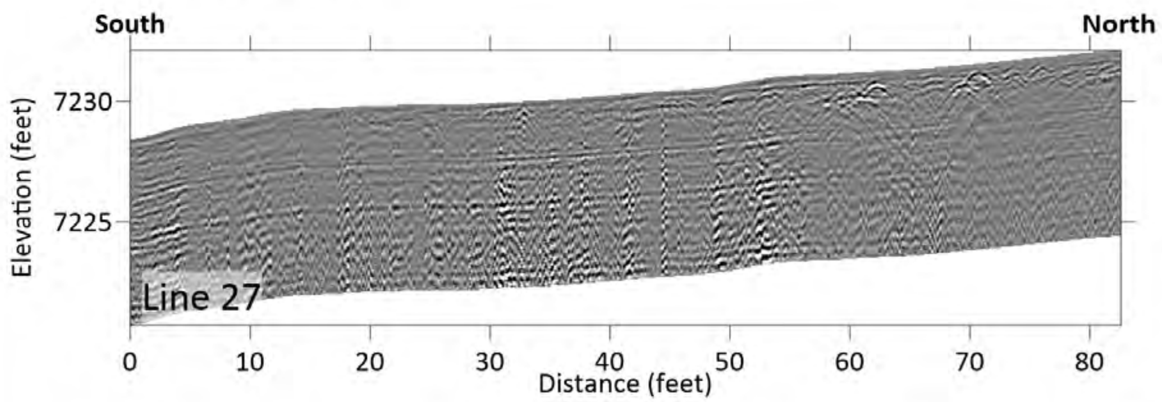

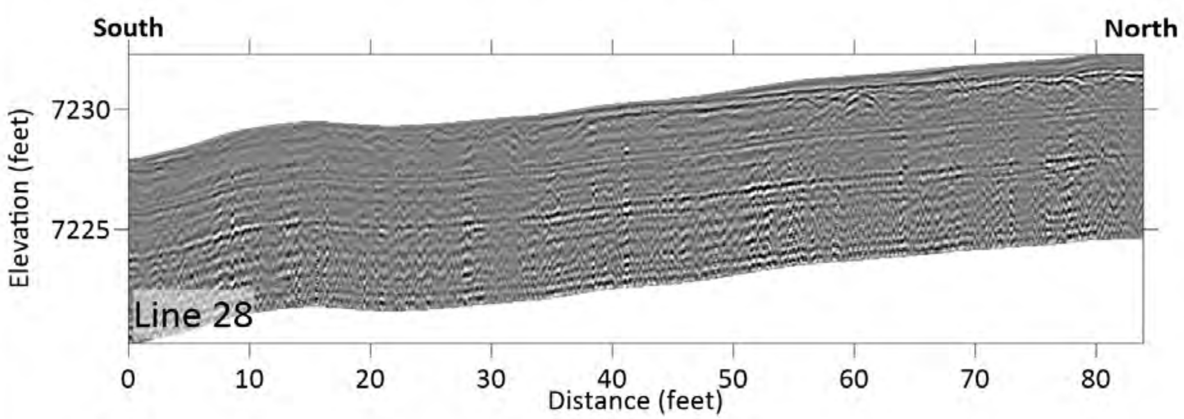

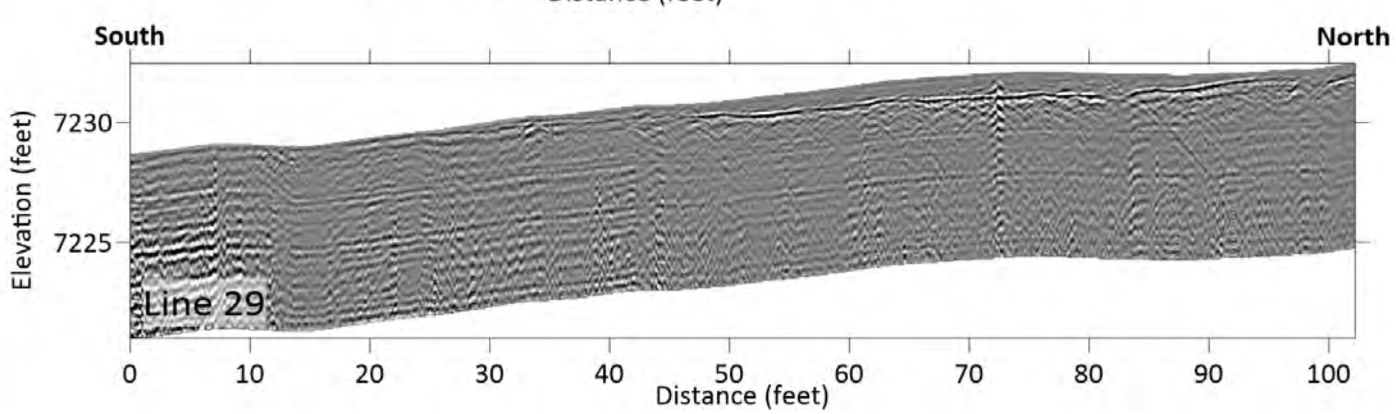

GPR Results (4 of 12)
MDPR Site
Los Alamos, NM

Banda Group International, LLC

Project #: 20-184	January 2021
Drafted by: J. Sheehan	Checked by: P. Sirles

COLLIER GEOPHYSICS

Fig. A-11

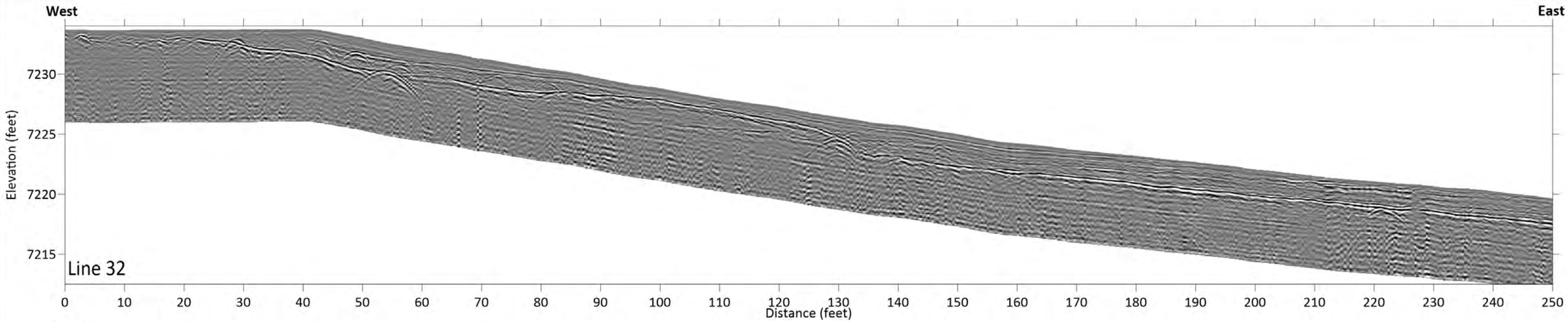

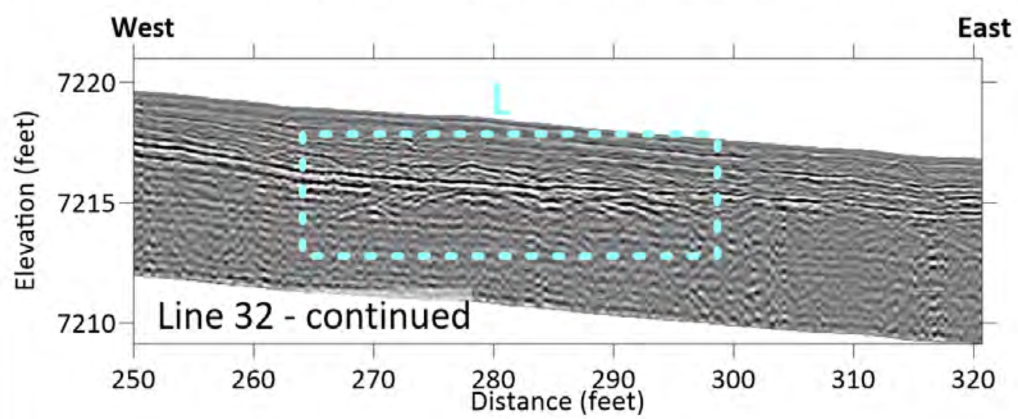

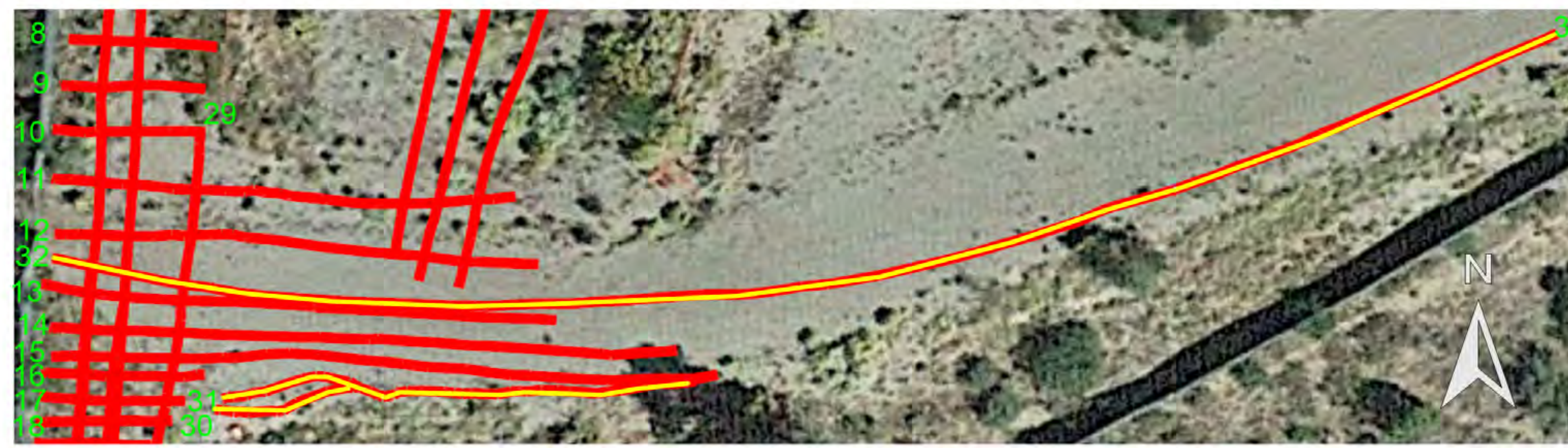

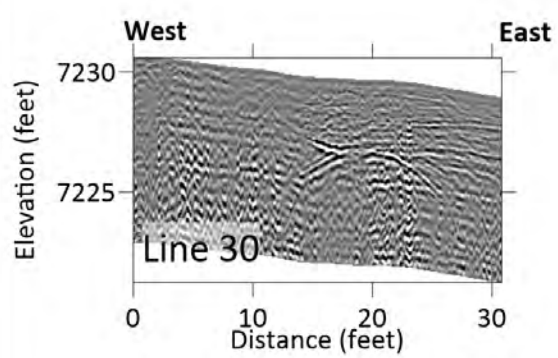

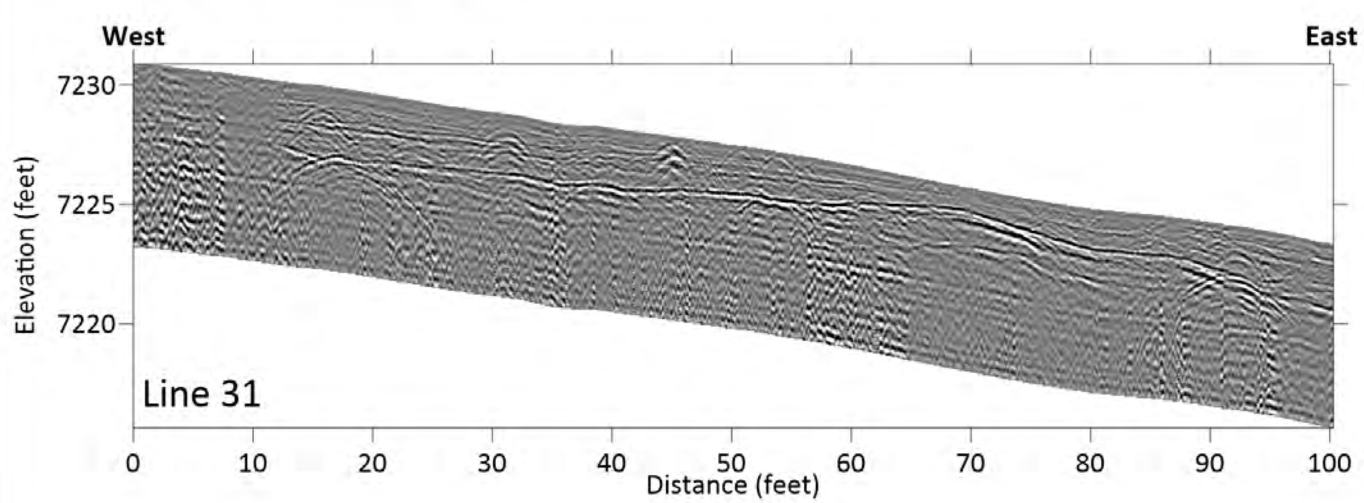

L Selected GPR Anomaly

GPR Results (5 of 12)
MDPR Site
Los Alamos, NM

Banda Group International, LLC

Project #: 20-184	January 2021
Drafted by: J. Sheehan	Checked by: P. Sirles

COLLIER GEOPHYSICS

Fig. A-12

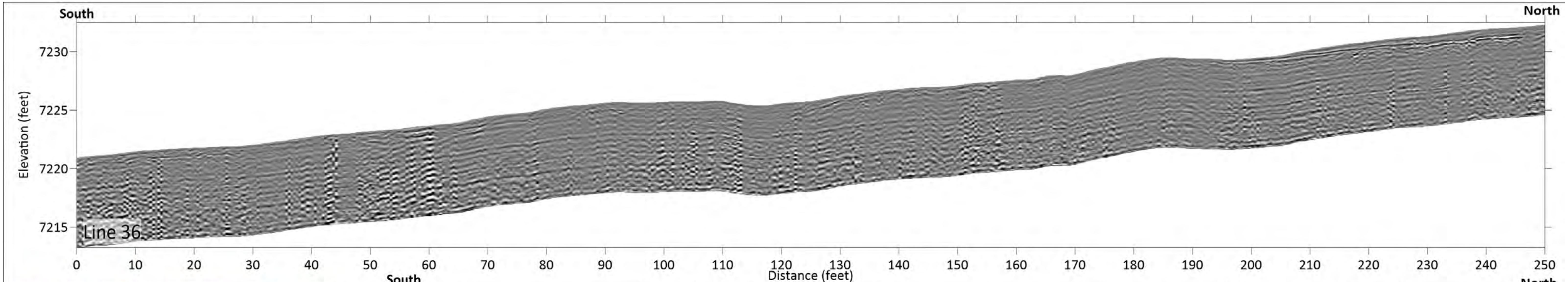

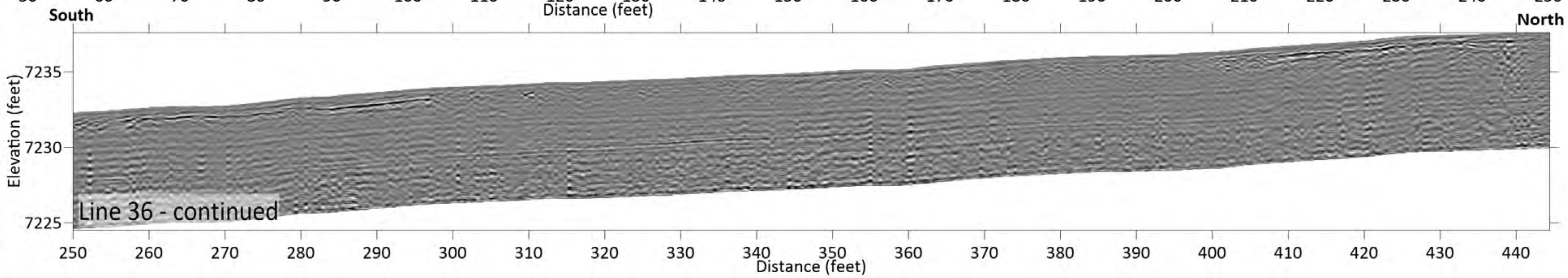

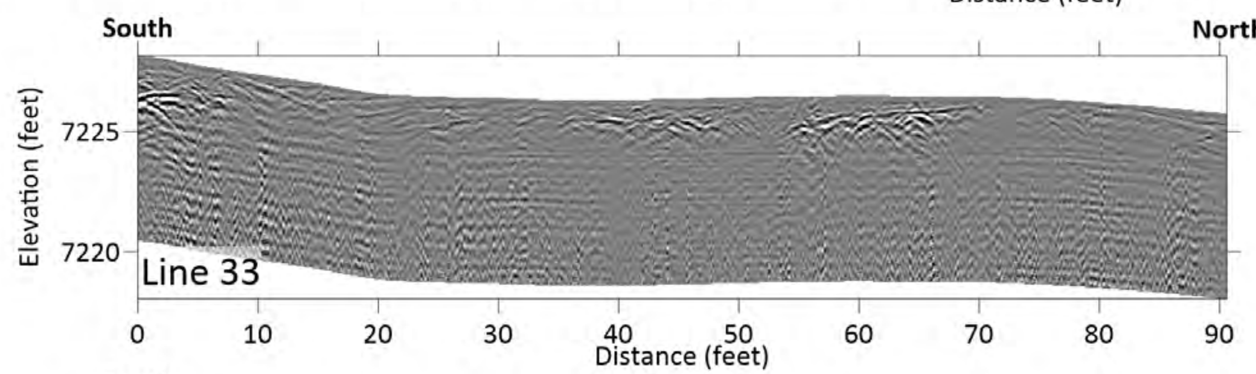

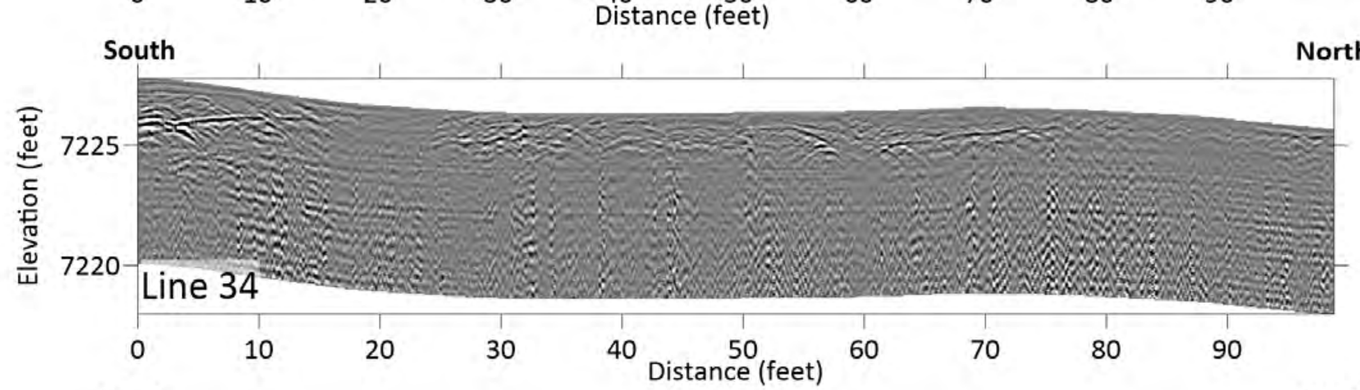

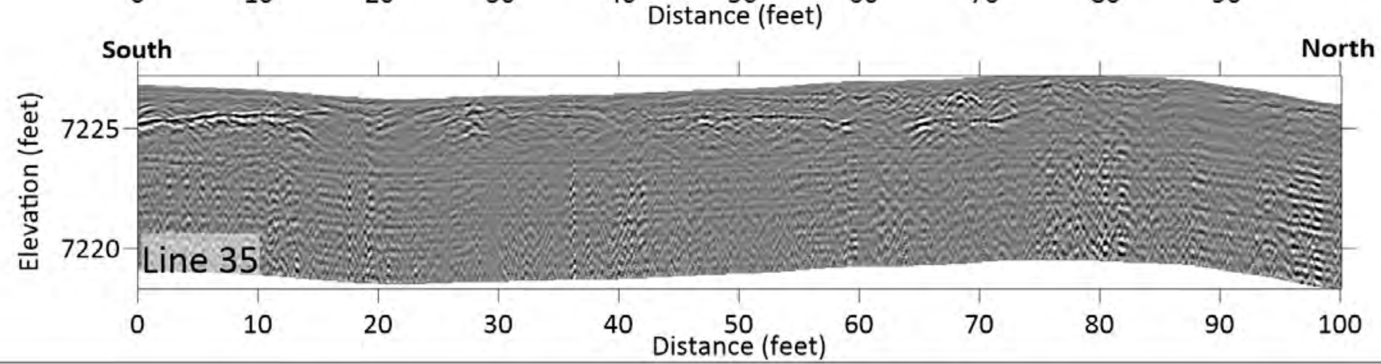

GPR Results (6 of 12)
MDPR Site
Los Alamos, NM

Banda Group International, LLC	COLLIER GEOPHYSICS
Project #: 20-184	January 2021
Drafted by: J. Sheehan	Checked by: P. Sirles

Fig. A-13

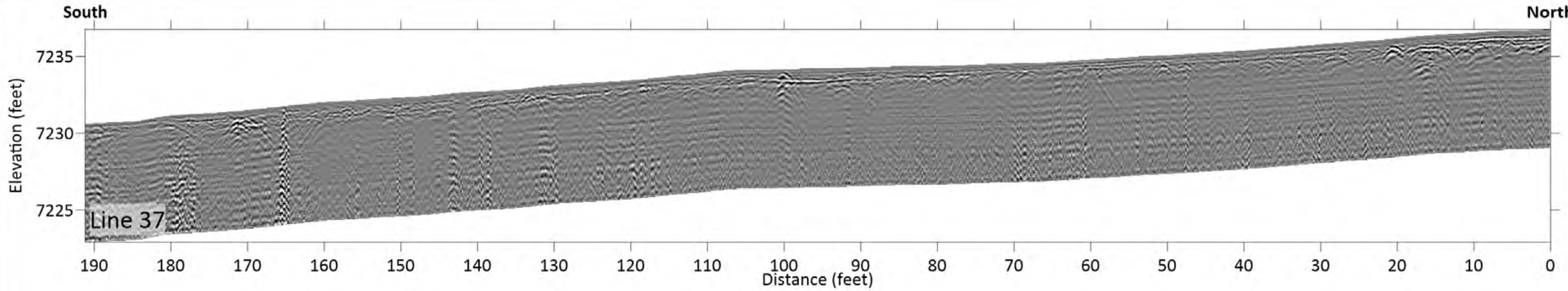

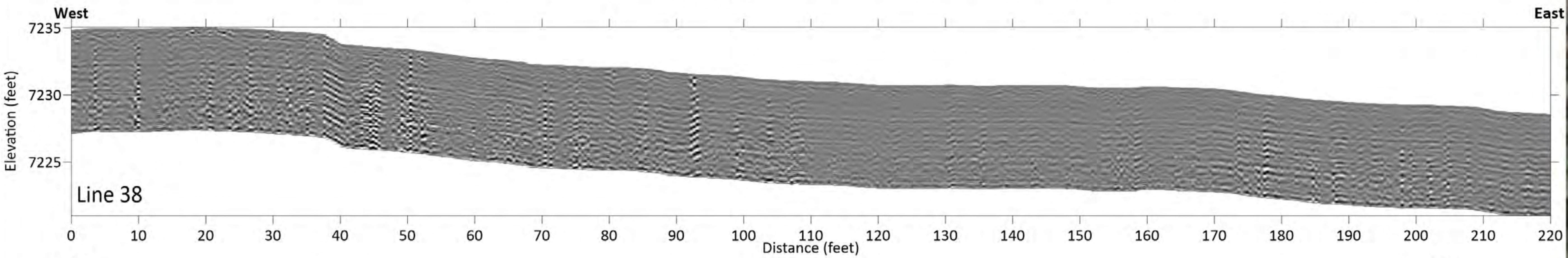

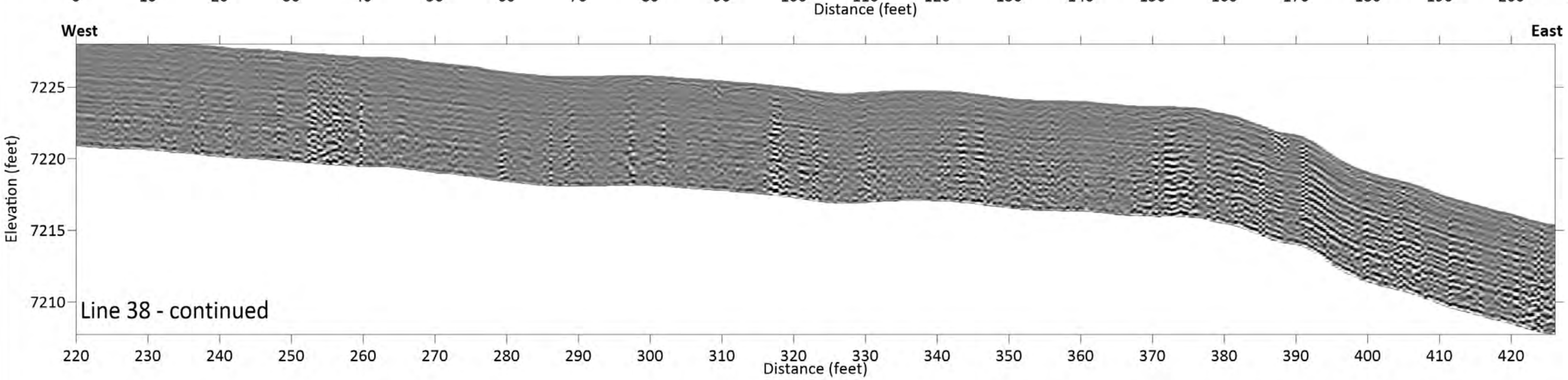

GPR Results (7 of 12)
MDPR Site
Los Alamos, NM

Banda Group International, LLC		COLLIER GEOPHYSICS
Project #: 20-184	January 2021	
Drafted by: J. Sheehan	Checked by: P. Sirles	Fig. A-14

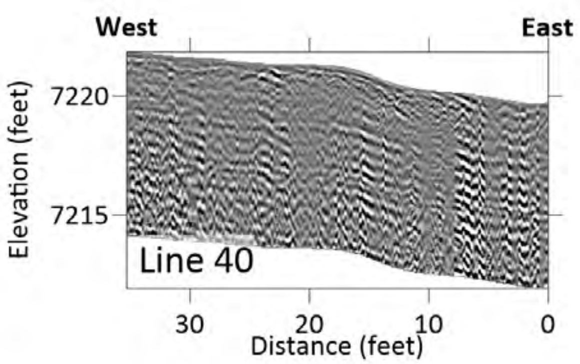

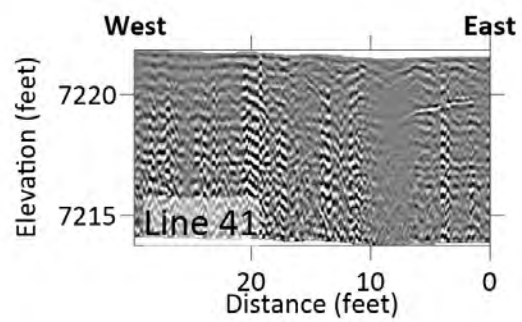

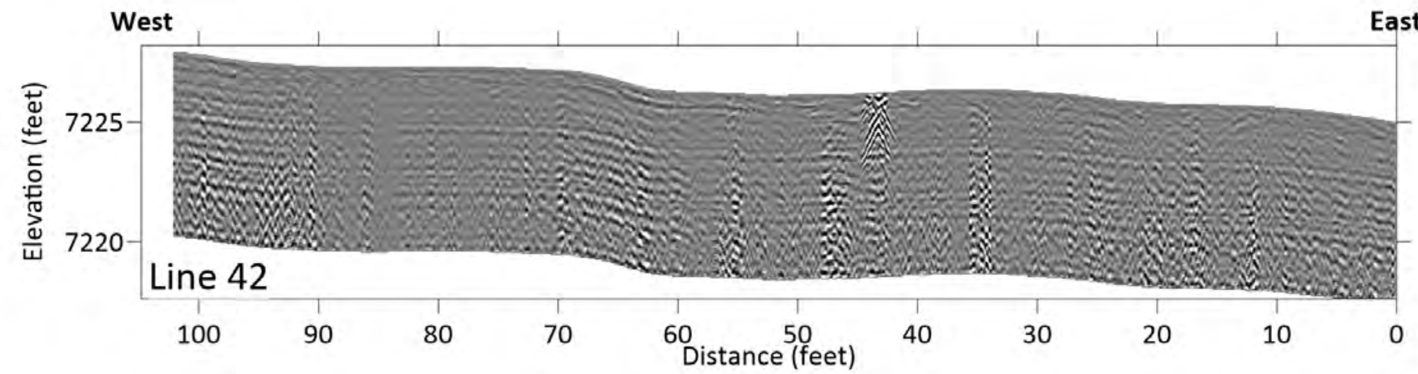

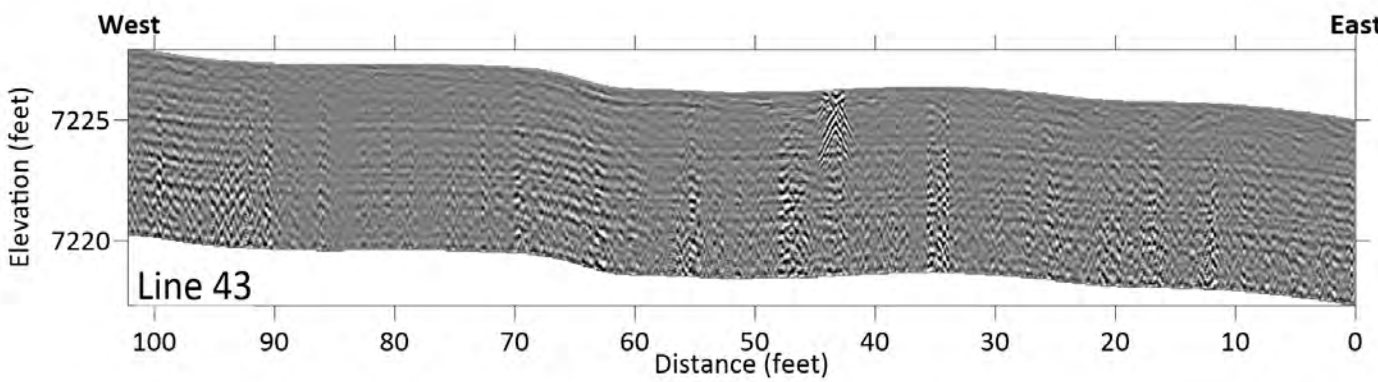

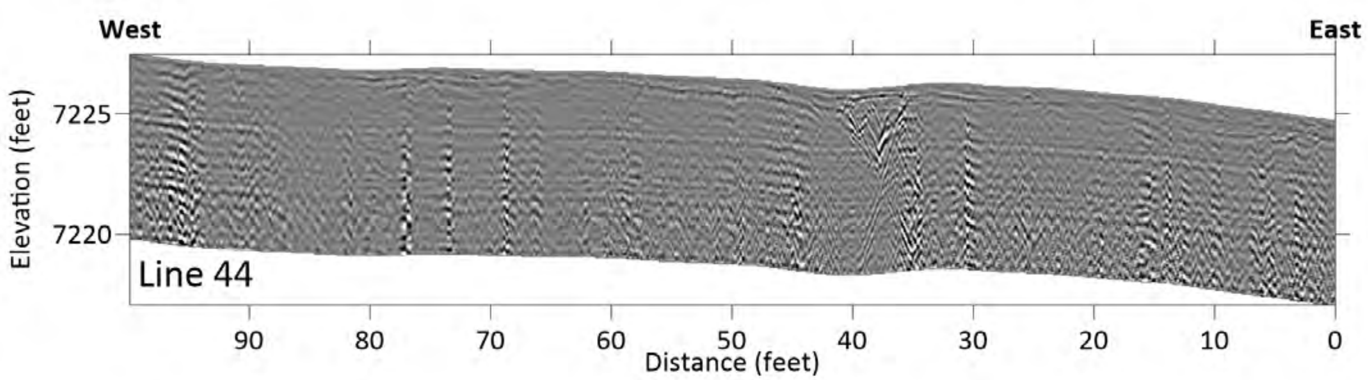

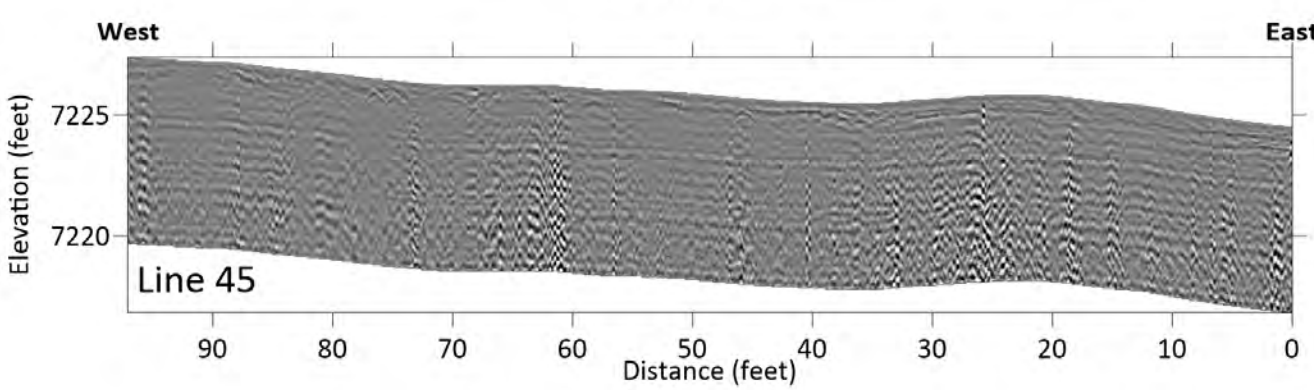

GPR Results (8 of 12)
MDPR Site
Los Alamos, NM

Banda Group International, LLC		COLLIER GEOPHYSICS
Project #: 20-184	January 2021	
Drafted by: J. Sheehan	Checked by: P. Sirles	Fig. A-15

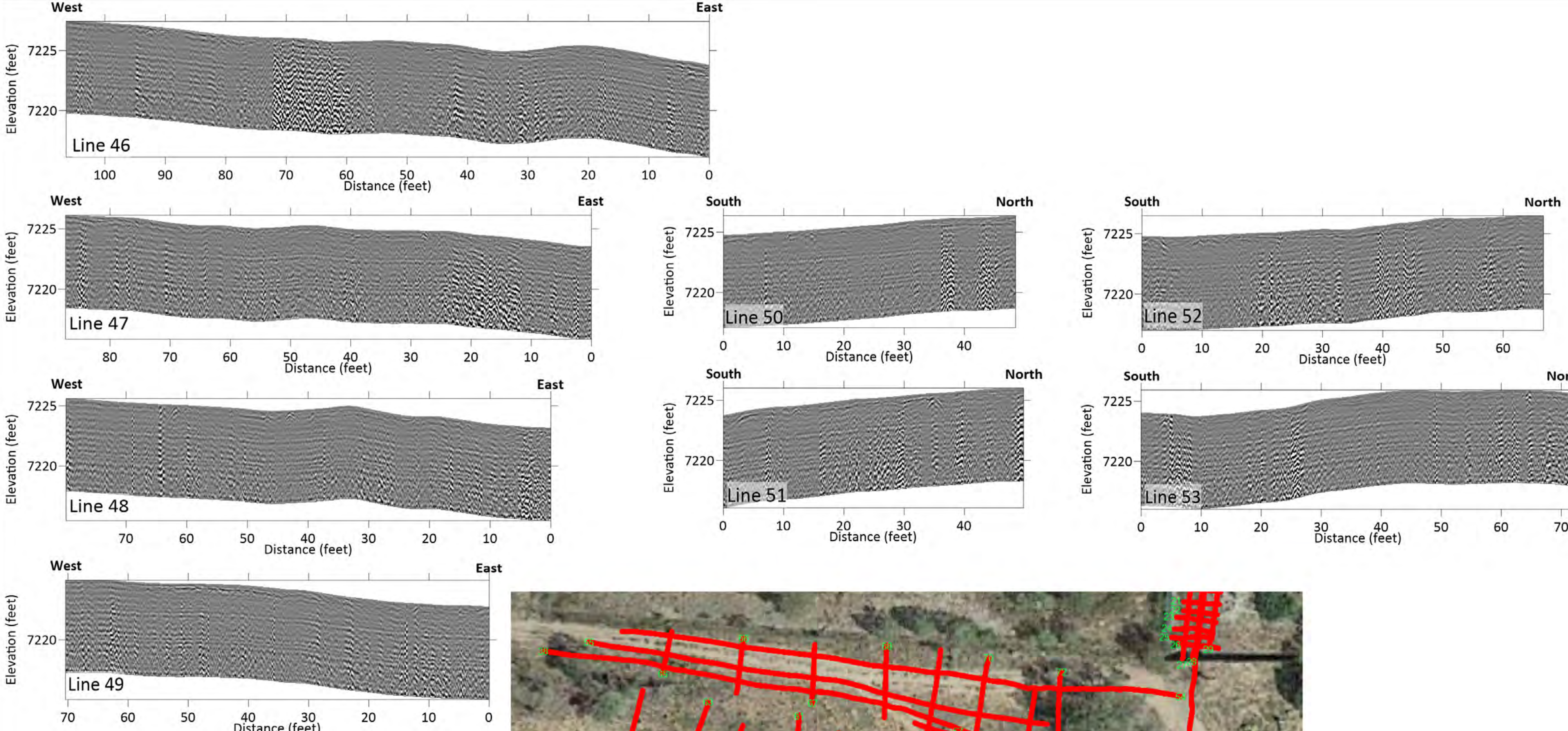

GPR Results(9 of 12)
MDPR Site
Los Alamos, NM

Banda Group International, LLC

COLLIER GEOPHYSICS

Project #: 20-184	January 2021
Drafted by: J. Sheehan	Checked by: P. Sirles

Fig. A-16

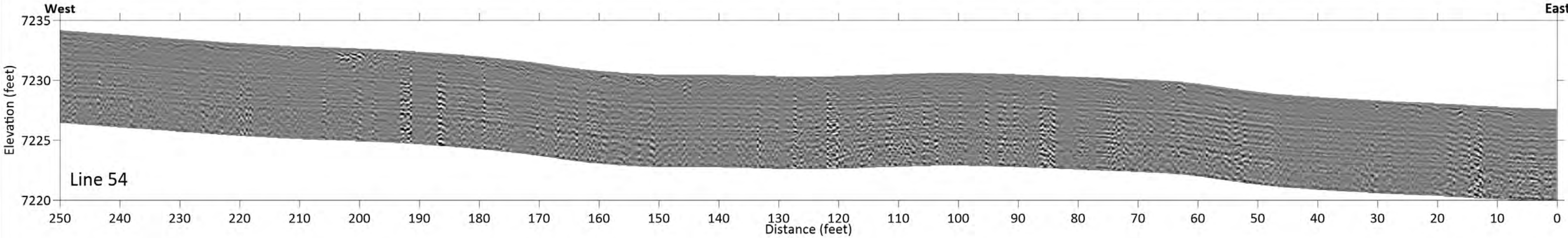

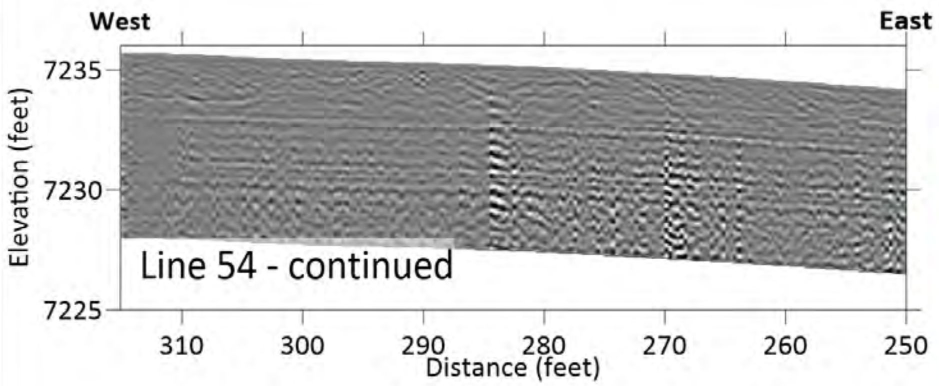

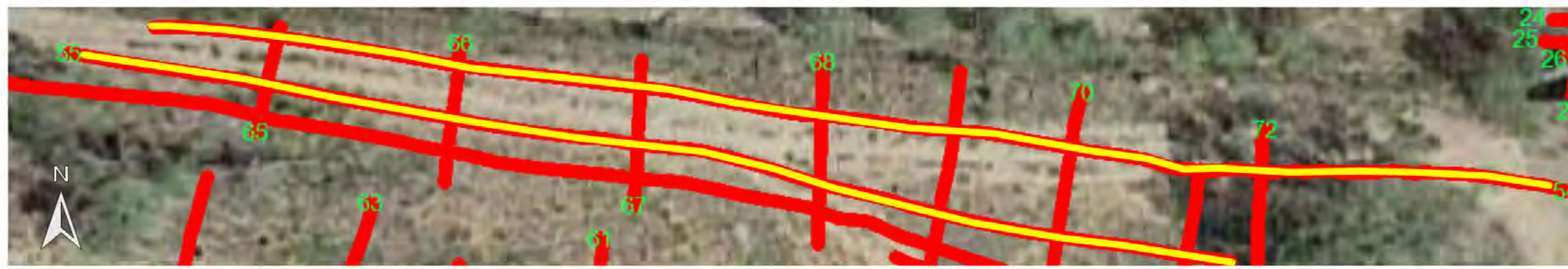

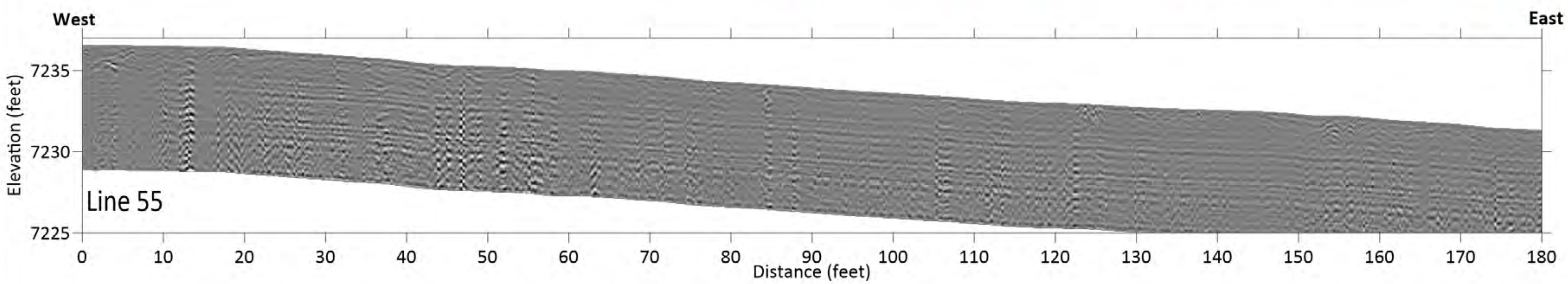

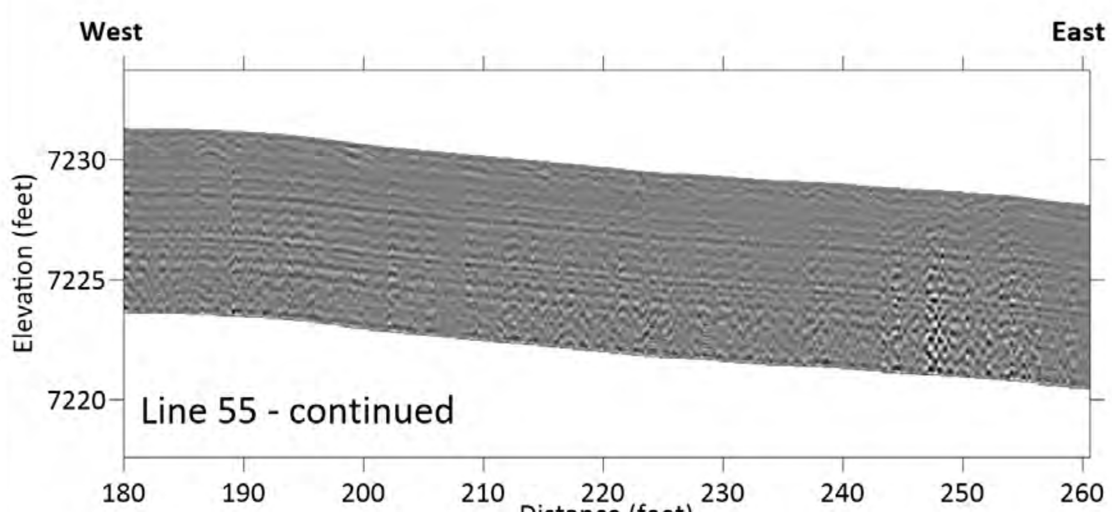

GPR Results (10 of 12) MDPR Site Los Alamos, NM		
Banda Group International, LLC		COLLIER GEOPHYSICS
Project #: 20-184	January 2021	
Drafted by: J. Sheehan	Checked by: P. Sirles	Fig. A-17

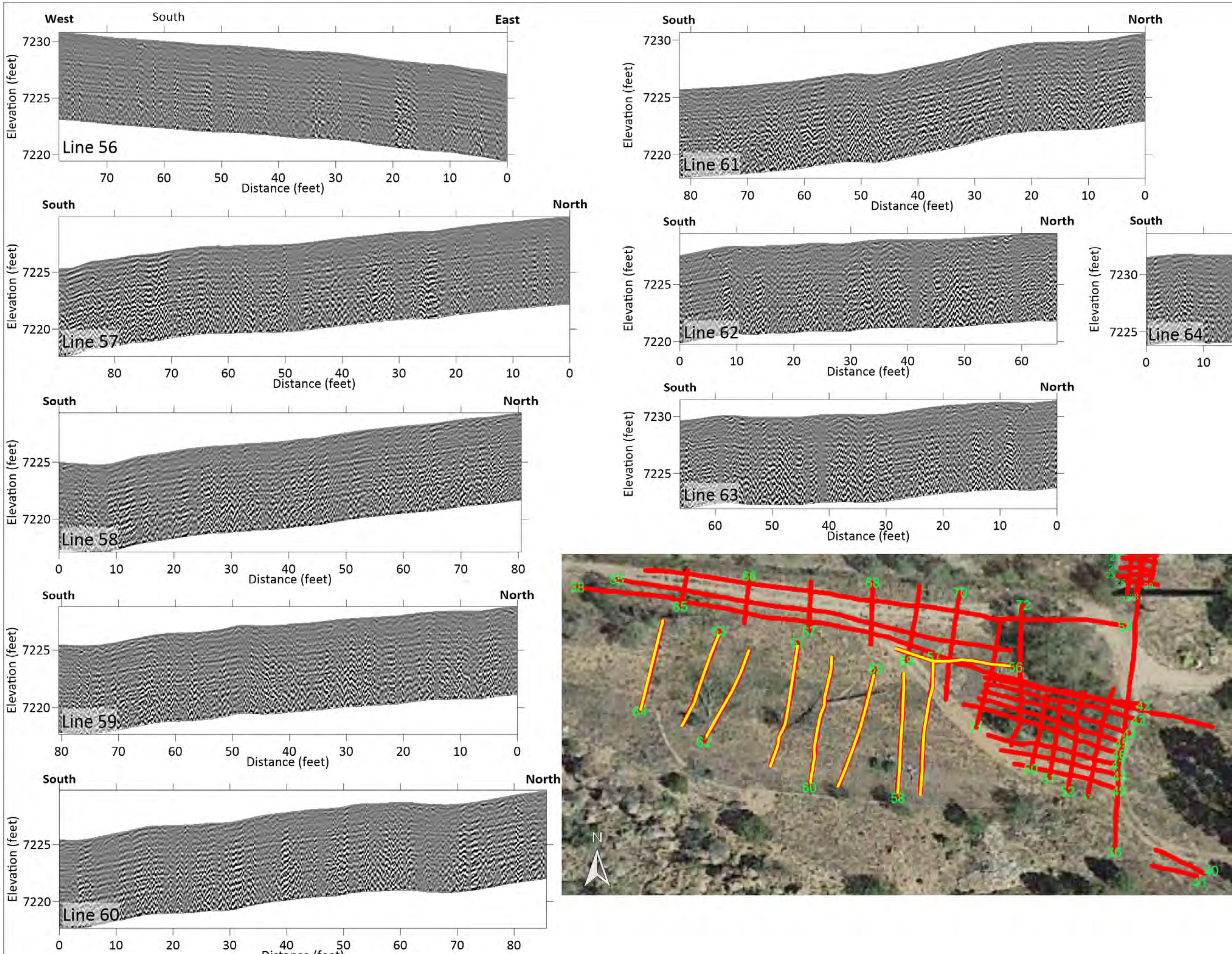

GPR Results (11 of 12)
MDPR Site
Los Alamos, NM

Banda Group International, LLC

COLLIER GEOPHYSICS

Project #: 20-184	January 2021	
Drafted by: J. Sheehan	Checked by: P. Sirles	Fig. A-18

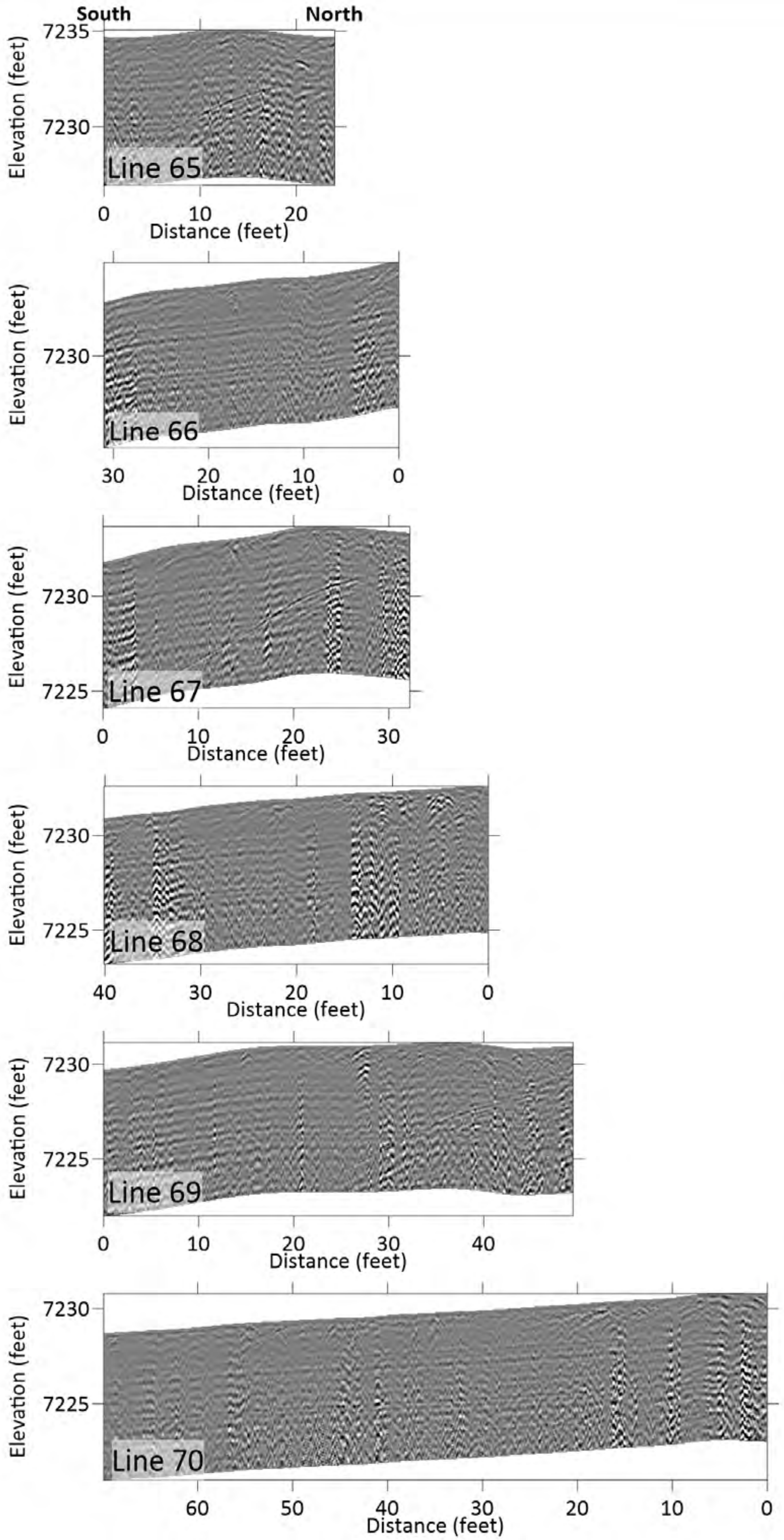

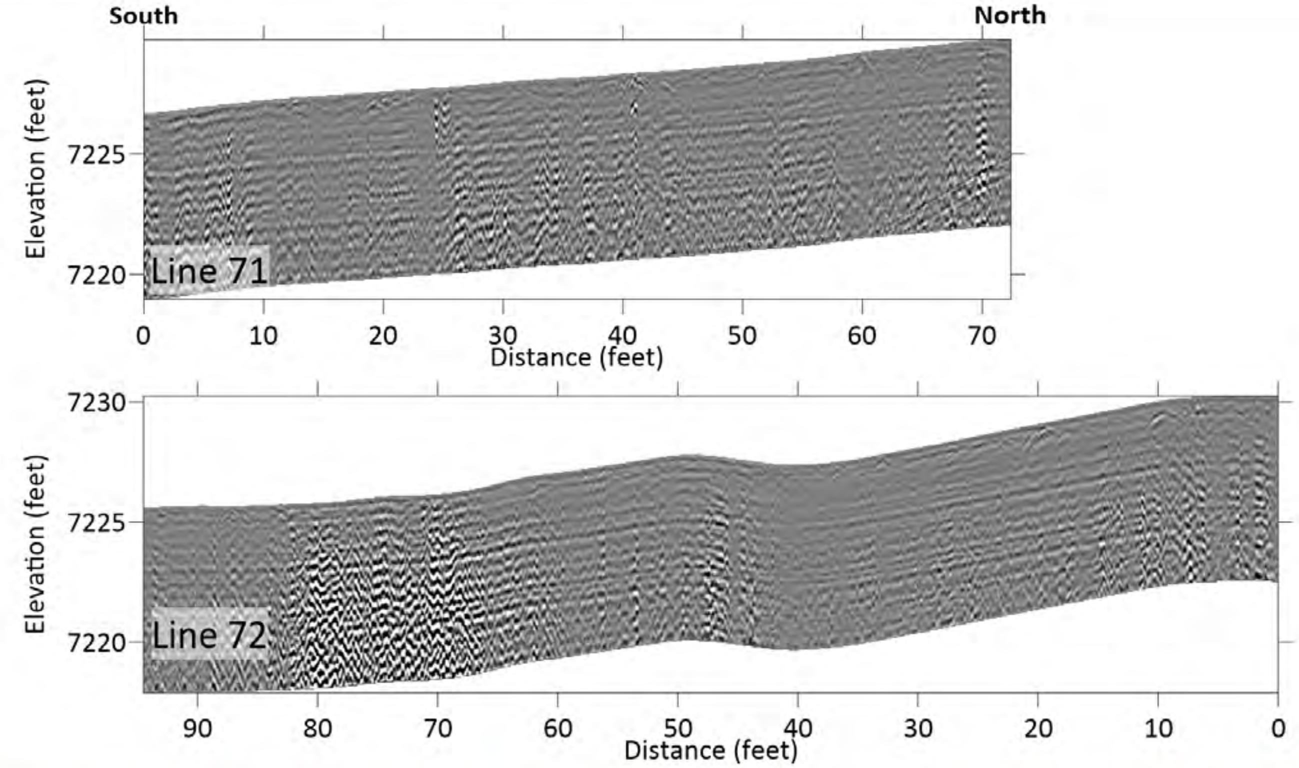

GPR Results (12 of 12)
MDPR Site
Los Alamos, NM

Banda Group International, LLC

Project #: 20-184	January 2021
Drafted by: J. Sheehan	Checked by: P. Sirles

Fig. A-19

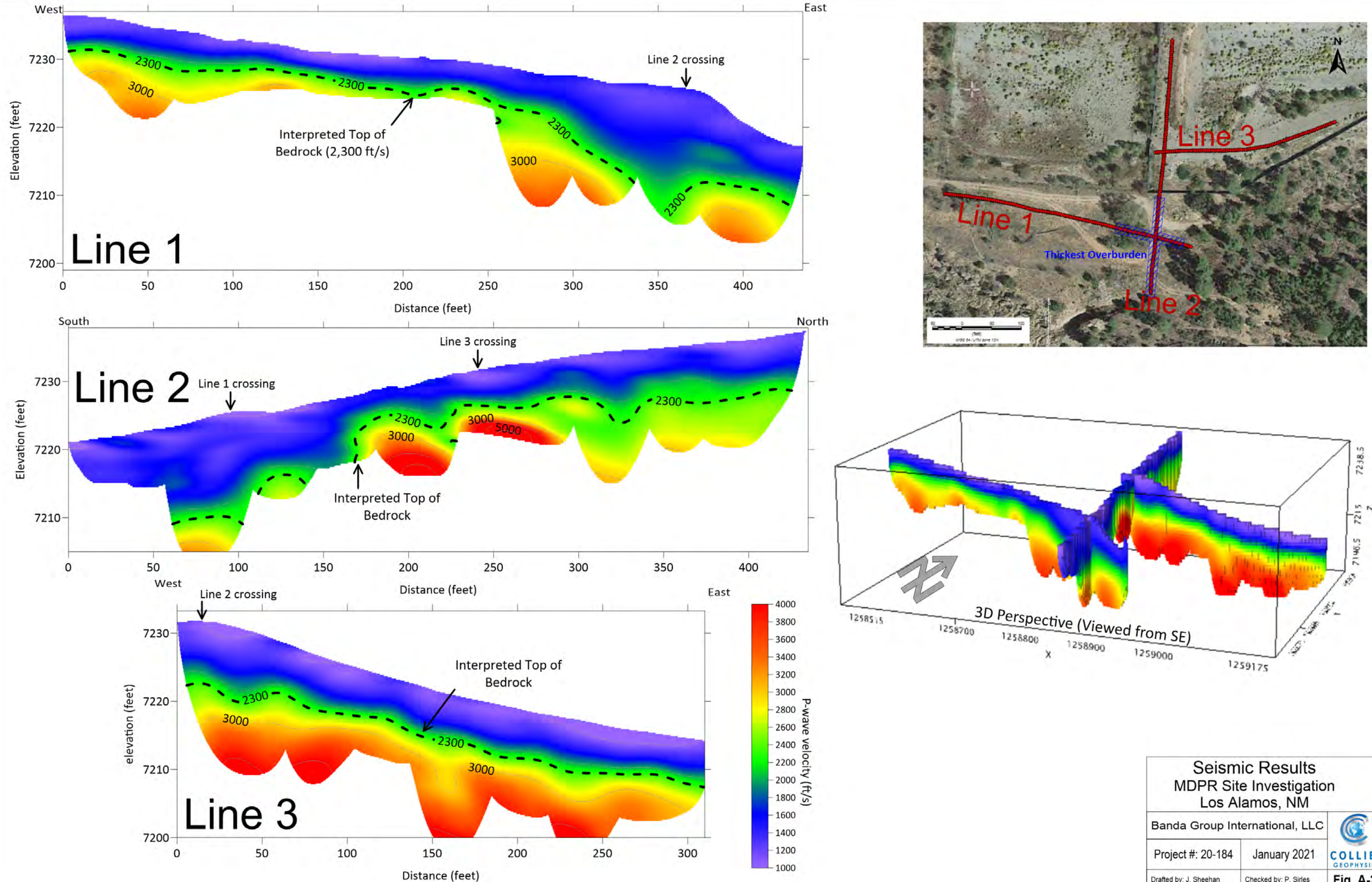

Seismic Results
MDPR Site Investigation
Los Alamos, NM

Banda Group International, LLC

Project #: 20-184 | January 2021

Drafted by: J. Sheehan | Checked by: P. Sirles

COLLIER GEOPHYSICS

Fig. A-20

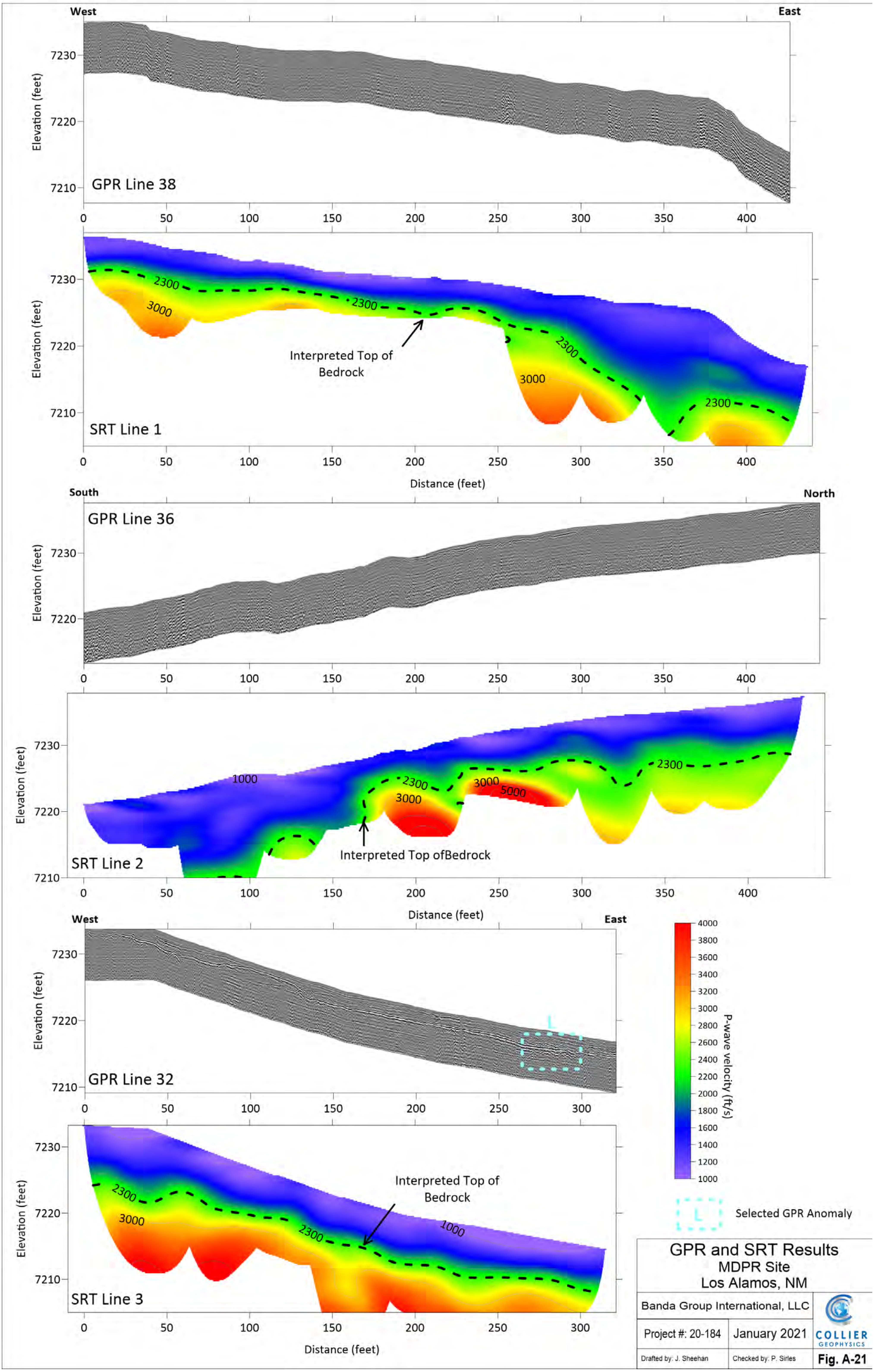
West
East
GPR Line 38
Elevation (feet)
7230
7220
7210
0
50
100
150
200
250
300
350
400
2300
3000
2300
2300
3000
2300
Interpreted Top of
Bedrock
SRT Line 1
Distance (feet)
South
North
GPR Line 36
1000
2300
3000
3000
5000
2300
Interpreted Top ofBedrock
SRT Line 2
West
East
GPR Line 32
2300
3000
2300
1000
Interpreted Top of
Bedrock
SRT Line 3
P-wave velocity (ft/s)
4000
3800
3600
3400
3200
3000
2800
2600
2400
2200
2000
1800
1600
1400
1200
1000
Selected GPR Anomaly
GPR and SRT Results
MDPR Site
Los Alamos, NM
Banda Group International, LLC
Project #: 20-184
January 2021
COLLIER
GEOPHYSICS
Drafted by: J. Sheehan
Checked by: P. Sirles
Fig. A-21

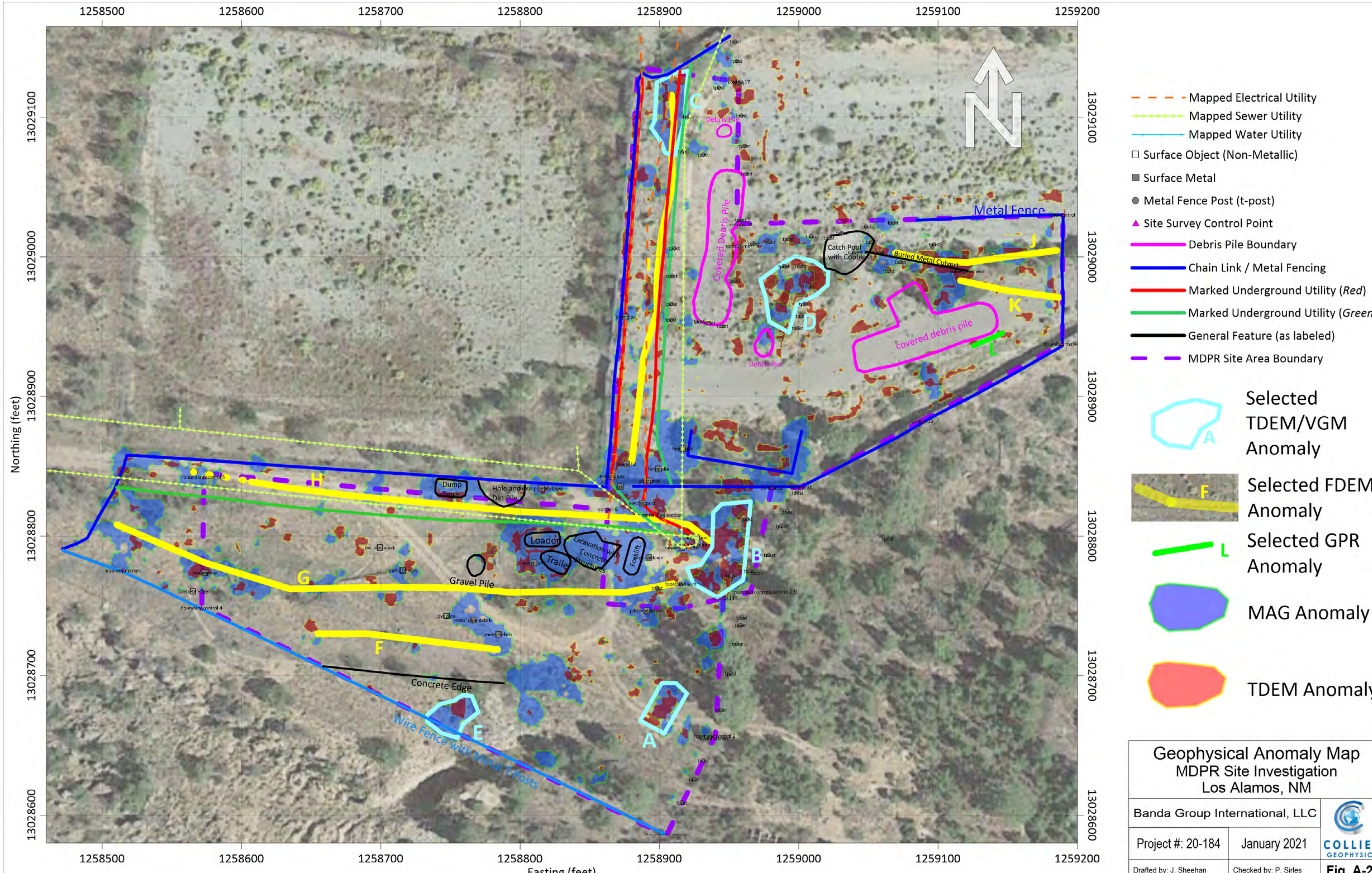

Geophysical Anomaly Map
MDPR Site Investigation
Los Alamos, NM

Banda Group International, LLC

Project #: 20-184	January 2021
Drafted by: J. Sheehan	Checked by: P. Sirles

COLLIER GEOPHYSICS

Fig. A-22

Enclosure 1

Geophysical Letter Report, Project 20-184,
Middle Delta Prime Road Site Geophysical Investigation

7711 W. 6th Ave., Ste G/H | Lakewood, CO 80217 | (720) 487-9200

January 5, 2021

Luke Hill

Banda Group International, LLC
9664 Eagle Ranch Road NW, Suite 5
Albuquerque, NM 87114

Email: lukeh@bandagroupintl.com

RE: Geophysical Letter Report | Project 20-184
Middle Delta Prime Road Site Geophysical Investigation

Collier Geophysics, LLC (Collier) conducted a geophysical investigation on behalf of Banda Group International, LLC (BGI), located in Los Alamos, New Mexico (Figure 1). The Middle Delta Prime Road (MDPR) Area project site is located at the Los Alamos National Laboratory (LANL) facilities. The site property is currently owned by Los Alamos County. This geophysical investigation was performed under RFP N3B MSA PO-000635-03. The primary objective of the geophysical investigation is to define the presence and limits of buried debris within the defined Area of Interest (AOI). The purpose of this geophysical investigation is to assist BGI in defining the boundaries of historic trench/disposal areas within the AOI. In addition to defining the boundaries, these data will be used for determining, to the extent possible, the distribution of metallic objects. A secondary set of objectives is to identify bedrock conditions, and to the extent possible, identify contaminated materials.

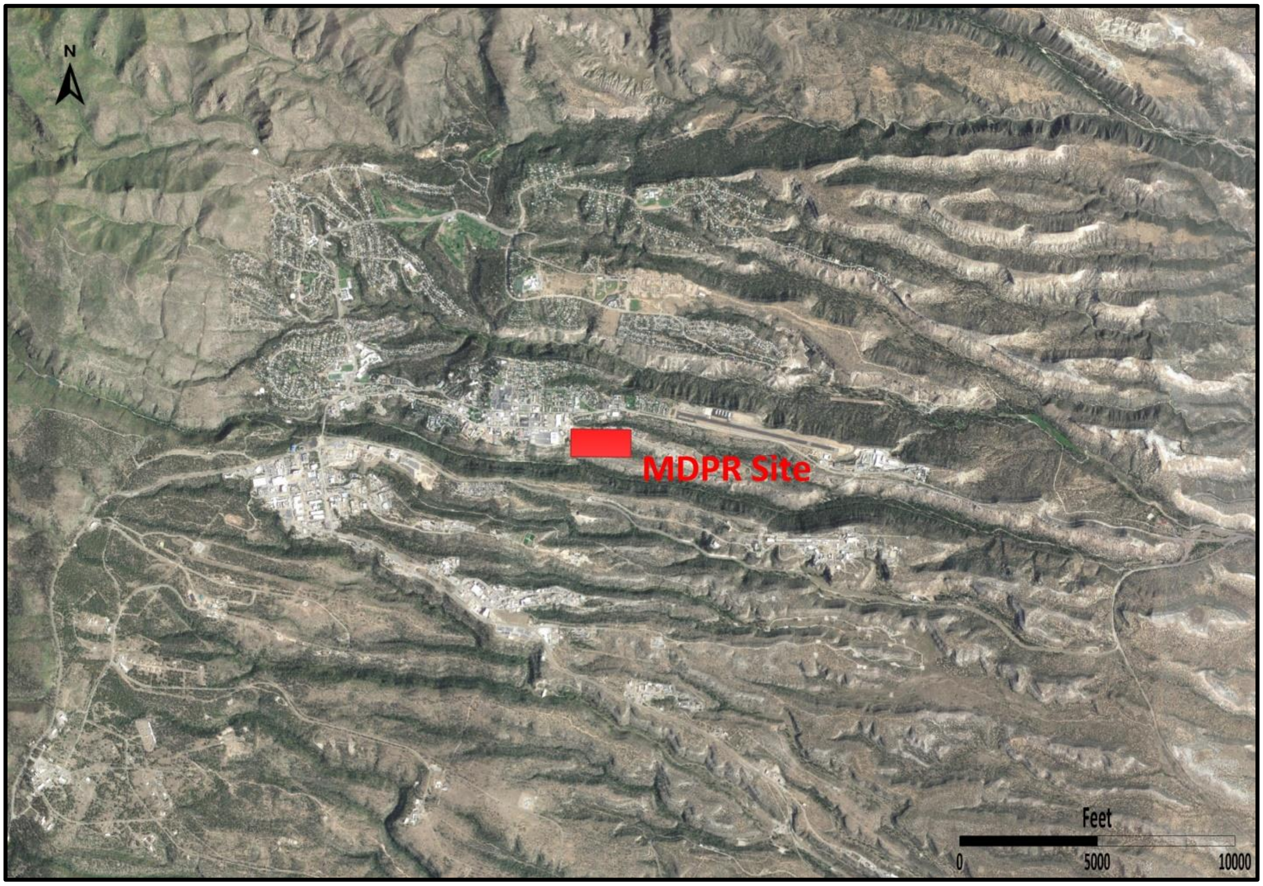

Figure 1. MDPR Site location map (base image from Google Map Tiles).

Site Description

The MDPR Site as identified is an area covering approximately 5.5 acres that potentially has buried solid waste, anticipated to be placed within excavated cells or trenches. The AOI was operational for LANL and contains an unknown quantity or type of buried metallic objects and other debris. Based on historical records, the vertical extent of the buried materials is expected to be in the upper 15 ft below ground surface (bgs); that is, generally within the overburden soils that overly bedrock (Upper Bandelier Tuff) and they are likely covered with clean fill materials.

The AOI is divided into two zones, a north zone and a south zone (Figure 2). Active county operations within the AOI included material loading operations (asphalt pile) in the north half of the north zone and installation of a lift station in the eastern half of the south zone. The site was bounded by fences (ranging from metal T-post and wire to metal chain link security fencing). A number of covered piles of excavated materials were located within the north zone, and the south zone included county construction equipment.

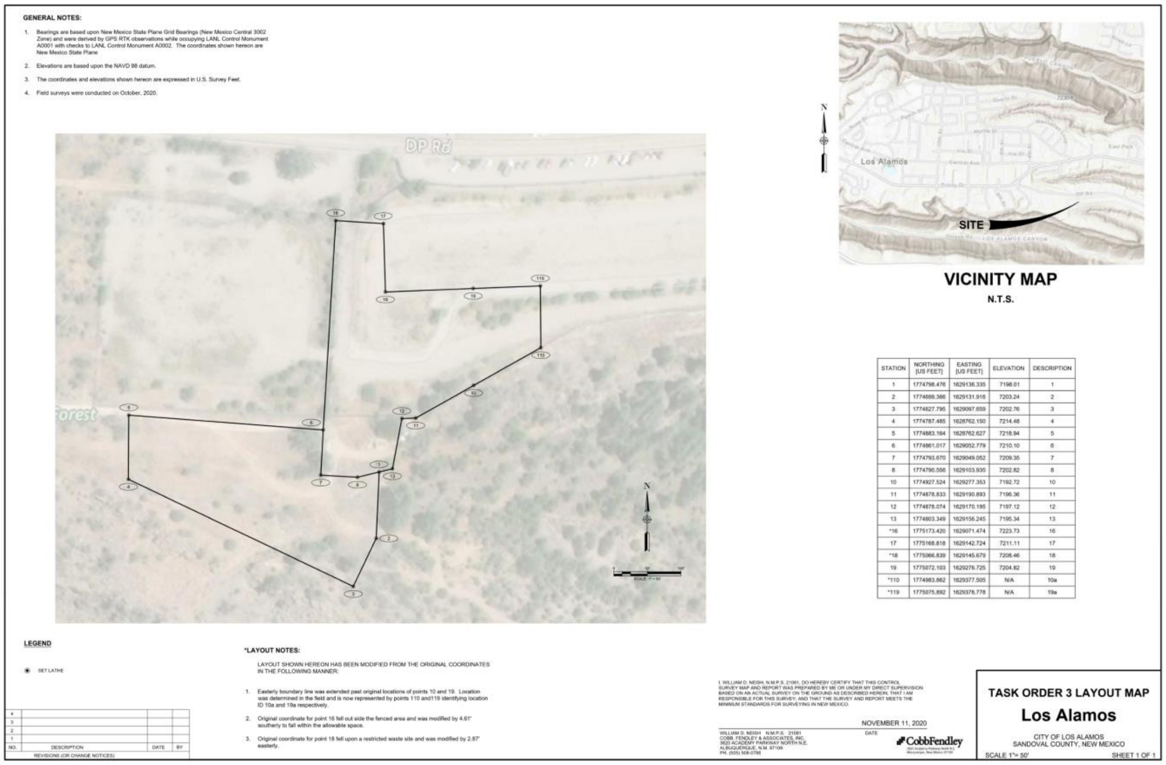

Figure 2. MDPR Site AOI (black outline) as provided by BGI.

Data Acquisition

As outlined in the geophysical work plan, the geophysical data were acquired in three phases: 1) acquire electromagnetic (EM) and magnetic data over 100% of the MDPR Site AOI using Time Domain Electromagnetics (TDEM), Frequency Domain Electromagnetics (FDEM), and Vertical Gradient Magnetometry (VGM); 2) acquire 2D ground penetrating radar (GPR) transects over anomalies identified in the phase 1 data and other areas of interest designated by BGI; 3) perform multiple 2D seismic refraction tomography (SRT) transects across the AOI to create 2D compressional wave velocity (Vp) sections. Based on the size of the AOI and surface conditions at the site, all geophysical data were collected using portable instrumentation. A brief description of each method is proved below. For further information regarding the details of these techniques, Collier can submit a method addendum to this report upon request.

Time Domain Electromagnetics (TDEM)

TDEM data were acquired using an EM61-MK2, by Geonics Limited. The EM61-MK2 instrument is a high-sensitivity metal detector and is an industry standard instrument for shallow metal detection (i.e. UXO surveys, landfill investigations, UST locates, etc.). The EM61 will detect most electrically conductive metals (i.e. copper, aluminum, brass, steel, etc.). The effective depth of detection varies with the size (mass and surface area) of the buried metal object. As a general reference range, the EM61-MK2 can typically detect a one-inch diameter steel pipe four inches in length up to maximum burial depth of about 16 inches, while a 55-gallon steel drum has a maximum detection depth of about 10 feet.

The EM61 consists of a coincident transmitter/receiver main coil 1 m by 0.5 m in size, and an equivalent-sized second receiver coil mounted approximately 0.5 m above the primary coil. A

primary magnetic field is generated by imparting a current through the primary coil which is then shut off (unipolar rectangular current), resulting in decaying eddy currents in the subsurface. These eddy currents decay over time, generating a decaying secondary magnetic field. The instrument records the response induced in the coils generated by the secondary magnetic fields in millivolts (mV) in a series of four time-gates up to 1,266 µs after the primary shutoff. The instrument continuously repeats this process and records data at a rate of 10 Hz. The instrument is highly sensitive to all metallic objects in the subsurface, whether ferrous or non-ferrous, as its primary sensitivity is to electrical conductivity. GPS position data were logged simultaneously recording the NEMA string output from a Trimble Geo7x GPS into the EM61 Allegro data logger. GPS data were logged at a rate of 1 Hz. EM61 data were acquired along roughly parallel profile lines with a nominal 8-foot spacing and along-line data spacing of approximately 0.1 ft.

Frequency Domain Electromagnetics (FDEM)

An FDEM instrument consists of at least one pair of transmitting and receiving coils. A primary magnetic field of a constant frequency is generated using an alternating current in the transmitter coil, and a secondary magnetic field is detected in the receiving coil as a result of the interaction of the primary field with the subsurface. The FDEM instrument allows for simultaneous measurements of both the in-phase and quadrature components of the secondary magnetic field. The in-phase component is measured in parts-per-thousand (ppt) of the amplitude of the primary magnetic field. The in-phase response is primarily sensitive to magnetic susceptibility, generally due to the presence of metallic or ferromagnetic material in the subsurface. The quadrature component (90-degrees out of phase with the primary signal) is primarily sensitive to electrical conductivity due to changes in lithology, moisture, and/or fines (clay) content. The quadrature response is calibrated and measured as apparent bulk conductivity in milliSiemens per meter (mS/m). Note that these are the primary sensitivities, but that both components can be affected by buried metal or geologic features.

FDEM data were acquired using a CMD-Explorer, by GF Instruments. The CMD-Explorer consists of a boom with three sets of FDEM coil pairs, at three separations; 1.4 m (4.5 ft), 2.8 m (9.2 ft), and 4.5 m (14.8 ft). The effective depth of sensitivity of the FDEM method is a function of the antenna spacing between the transmitter and receiver, the antenna orientation, the frequency of the primary field, and the bulk electromagnetic properties of the subsurface. Data were acquired using a vertical dipole orientation, which results in the greatest depth of investigation. The depth of investigation is not precise, but as a rule of thumb when using a vertical dipole orientation, is approximately equal to the antenna spacing. In this case using the CMD-Explorer, the values recorded would correspond to the bulk electromagnetic properties in approximately the upper 5 feet, 10 feet, and 15 feet, of the subsurface respective to each antenna separation. CMD-Explorer data were collected at a rate of 10 Hz, using a primary field frequency of 10 kHz at all three antenna spacings simultaneously. GPS position data were logged simultaneously recording the NEMA string output from a Trimble Geo7x GPS into the CMD data logger. GPS data were logged at a rate of 1 Hz. CMD data were acquired along roughly parallel profile lines with a nominal 8-foot spacing and along line data spacing of approximately 0.1 ft.

Vertical Gradient Magnetometry (VGM)

Magnetometry data were acquired using a Geometrics G-858 magnetometer system. The magnetometer was configured with two sensors mounted on a vertical aluminum pole with a separation of 2.4 feet. Each magnetometer sensor measures the strength of Earth's magnetic field in nanoteslas (nT), called the Total Field Intensity (TFI). With two sensors, the difference in the TFI is calculated to obtain the vertical gradient (VGM). The advantage of measuring the vertical gradient is the elimination of the need for a base magnetometer station to provide drift corrections for the diurnal variation in the total magnetic field intensity. The presence of ferrous materials causes distortions in the magnetic field that are detected by the sensors. The effective depth of investigation of the G858 is highly variable as it

depends on the cumulative effect of many factors including the size, mass, shape and orientation of the metal object, the orientation of the remnant magnetic field of the object and the magnetic properties of the materials surrounding the object. In general, the G-858 is capable of detecting large ferrous metal objects, such as pipelines, well casings and tanks, at significantly greater depths than either the EM61 or CMD.

VGM data were collected at a sample frequency of 10 Hz. GPS position data were logged simultaneously recording the NEMA string output from a Juniper Systems Geode GPS into the G-858 console data logger. GPS data were logged at a rate of 1 Hz. VGM data were acquired along roughly parallel profile lines with nominal 8-foot spacing and along line data spacing of approximately 0.1 ft.

Ground Penetrating Radar (GPR)

The GPR method is based on the recording of reflected electromagnetic waves that are transmitted into the subsurface using a transmitter (TX) and receiver (RX) antenna pair (*inset image, below*).

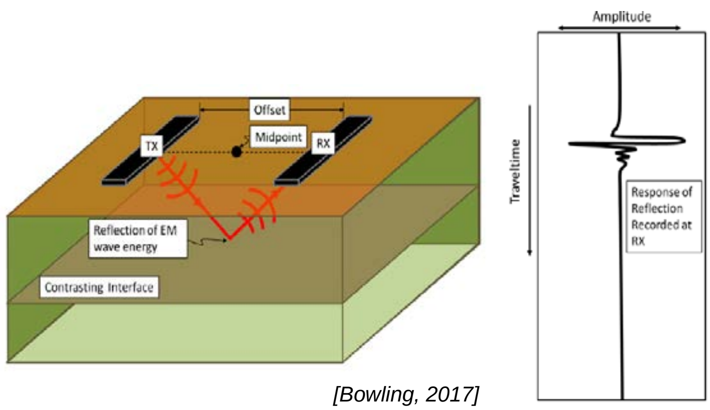

[Bowling, 2017]

The reflections are stored as a time series (known as traces) representing reflection "strength" or amplitude as a function of travel-time. Travel-time is the time required for the transmitted energy to travel down from the transmitting antenna into the subsurface, reflect off an interface of contrasting electromagnetic impedance, and travel back up to the surface to be recorded by the GPR receiver antenna. Therefore this time is often referred to as two-way travel-time (TWT).

As the GPR instrument is moved to different locations on the surface, different reflection series are recorded which represent changes in the subsurface EM impedance/reflectivity distribution. GPR signals are sensitive to the presence of a variety of subsurface materials including: buried objects (metallic and nonmetallic), air-filled voids, water saturated sediments, and geologic boundaries.

For this project GPR data were acquired over geophysical anomalies selected from the TDEM, FDEM and VGM datasets, and in other areas of concern as delineated by BGI onsite personnel. Spacing between GPR transect lines varied depending on ground conditions and the area to be covered. The in-line trace spacing was nominally 1 inch.

A GSSI SIR-4000 GPR system with a digital monostatic 350 MHz antenna was utilized for the data acquisition. GPS position data were logged simultaneously recording the NEMA string output from a Juniper Systems Geode GPS into the SIR4000 GPR console and written into the trace headers. The GPS antenna was mounted on a tripod directly over the center of the 350 MHz GPR antenna. GPS data were logged at a rate of 1 Hz. The effective depth of investigation is strongly affected by the site-specific soil properties such as clay content, water content and metal content. In areas where the bulk conductivity of the soils is greater than about 25 - 30 milliSiemens/meter, GPR effective depth of investigation will be severely limited. The manufacturer's specification for depth of investigation range for the digital 350 MHz antenna is listed as 0 to 40 feet; however, the high end of this range is only possible under ideal conditions. For typical good soil site conditions, the maximum effective depth of investigation is generally 5 -10 ft.

Seismic Refraction Tomography (SRT)

Seismic data were collected using a gimballed land streamer receiver array. Three seismic profile lines were surveyed within the AOI. The land streamer consists of twenty-four 30 Hz geophones suspended within a metal cylindrical enclosure at 3.3 ft (1 meter) spacing. The land streamer is ideally suited to work on smooth ground surfaces, as the weighted gimballed sensors provide good coupling to the ground without the need for inserting a metal spike, and the entire array can be advanced along the profile line by dragging the assembly.

Seismic data were acquired using a Geometrics Geode 24 channel seismograph. This recording system utilizes a state-of-the-practice seismograph connected to a field laptop via an ethernet cable. Analog data from the geophones are collected in the seismograph where the data are digitized, transmitted to the laptop computer, and then recorded on the computer's hard drive. Geophone positions were measured with a Trimble Geo7x, a handheld GPS unit with sub-meter accuracy.

SRT data were acquired using an active seismic impact source (16-lb sledgehammer and HDPE strike plate). Shot points were spaced every 13.1 feet (four receiver stations) along line. Off-end shots for each profile line were also collected to increase ray path coverage beneath the ends of the line(s). Each seismic profile was recorded in overlapping individual segments (24-channel spreads). After source data were recorded at 13.1 feet spacing along each 24-channel spread up through geophone #13 of 24 active, the land streamer was advanced half the spread length (39.4 ft [*12 geophone stations*]) and source recording was repeated at 13.1 ft intervals. This progression continued until the end of the profile line was reached.

The maximum depth of investigation for SRT is a function of the size of the active receiver array (23 meters), the seismic source (sledgehammer) and the subsurface velocity structure, in particular the depth to the top of the first refractor. Additionally, the seismic refraction method assumes the seismic velocity increases with depth. If a high velocity layer overlies a lower velocity layer, the low velocity layer will not be directly detected by refraction methods. Generally, maximum depth of investigation using these acquisition parameters is up to 30 ft.

Data Processing

Time Domain Electromagnetics (TDEM)

The raw TDEM data were downloaded and converted to tabular data files using TrackMaker61 MK2 (version 1.65), by Geomar Software Inc. All further data processing and gridding of the TDEM data was performed using Geosoft Oasis montaj, version 9.3 (Seequent). Within Geosoft, data were analyzed for instrument latency, the presence of drop-outs or spikes, and any drift in the background readings over time (instrument drift), which can be produced by changes in ambient conditions during operation. Data quality for the TDEM data was fair to good, with significant amounts of background electromagnetic noise that required filtering. In order to maximize the data quality, data from each of the four time gates was leveled using the following procedure: First surgically edit outlier data points from the dataset, then fit the remaining data using a smooth curve (via a BSpine filter), and finally remove the smooth curve from the full dataset.

Following the steps described above, the four different time gates were summed together. Geosoft was then used to grid and view the summed TDEM data using the minimum curvature method, and export the result as a plan view map image.

Frequency Domain Electromagnetics (FDEM)

Raw FDEM data were exported in tabular format using CMD Data Transfer, version 1.6.1, by GF Instruments. Positions for each measurement are interpolated for each record from GPS positions using the data transfer software. The data were then processed using Geosoft Oasis montaj, version 9.3 (Seequent). Data were checked for quality then gridded using a minimum curvature method, and export the result as a plan view map image.

Aarhus Workbench, version 5.9.3.0 was used to generate an earth resistivity model based on the FDEM bulk conductivity values. This process includes: decoupling the recorded EM response from surface features by removing affected data, using a 4-meter moving-window average to generate a pseudo-FDEM sounding every 25 cm along the acquired transects, and geophysical inversion of the processed pseudo-soundings. The geophysical inversion process iteratively fits a subsurface electrical resistivity model to each of the pseudo-soundings generated from the first processing steps, subject to lateral smoothing constraints (i.e., along data collection profiles). Resistivity models from the geophysical inversion are then exported in x-y-z-v format (3D position and value) to Geosoft Oasis montaj for final visualization.

Vertical Gradient Magnetometry (VGM)

The VGM raw data were positioned and converted to tabular data files using MAGMAP 2000 (version 5.04), by Geometrics, Inc. All further data processing and gridding of the VGM data was performed using Geosoft Oasis montaj version 9.7.1, by Seequent. The primary step required for VGM data processing is to remove data dropouts that can occur during data acquisition. These data dropouts occur when the magnetometer is aligned at a particular angle with respect to the Earth's magnetic field, or is very close to a large above ground metal object. These occurrences are typically less than one second in duration, and can be easily removed from the data with no detrimental effects on the final results. No further corrections or filtering were required, as the data quality was good to very good. Geosoft was used to grid the VGM data using the minimum curvature method. In addition, an analytic signal (AS) filter was applied to the VGM data grid. AS is an amplitude gradient computation which effectively compensates for the positive/negative magnetic dipole effects in raw VGM data, in order to place magnetic anomalies over their causative bodies.

Ground Penetrating Radar (GPR)

The GPR data processing was performed using Radan v.7 by GSSI Inc. GPR Data processing followed a standard workflow, taking the raw data and applying several filtering and gaining procedures to produce interpretable images. These steps included:

- Mute the direct wave
- Apply exponential gain function
- Apply background removal filter

Seismic Refraction Tomography (SRT)

The 2D refraction data from this investigation were processed using Rayfract®, version 4.01, by Intelligent Resources Inc. The two processing steps involved with SRT processing are first arrival picking and tomographic inversion. The first arrival picking step consists of picking the time on each signal trace where the first arrival energy from the seismic source is observed at each geophone position for each shot record . After picking is completed, a data inversion is performed generating a two-dimensional (2D) P-wave velocity (Vp) model that best fits the arrival picks by iteratively modifying an initial velocity grid model until the misfit between the modeled and measured travel-time values is minimized, subject to smoothing constraints.

GPS Surveying and Positional Data

The location of the surface features were surveyed on the first day of geophysical data acquisition using a Trimble Geo7x handheld GPS. The surface feature GPS data, and the SRT survey data, were differentially corrected in post-processing using Trimble Pathfinder and local permanent GPS base data. GPS data differentially corrected in post-processing typically has a horizontal accuracy better than 0.5 meters under good conditions. A number of control points were GPS surveyed by Collier on the first field day and post-processed as part of the surface feature survey. Comparing Collier's GPS surveyed locations of the control points with BGI's provided locations show that most (9 control points) are within 0.5 ft, one is within 0.75 ft and two outliers are offset by approximately 3 ft. There is approximately a 1.5 meter average offset to the northwest between the real-time GPS positions and the Trimble Pathfinder post-processed GPS positions for the surface feature GPS survey dataset.

GPS positional data recorded simultaneously with instrument data (TDEM, FDEM, VGM and GPR data) were linked in real-time and as such were not differentially corrected in post-processing. The real-time GPS survey data will typically have sub-meter horizontal accuracy or better under good conditions.

Results and Discussion

Time Domain Electromagnetics (TDEM)

A color contoured plan view map of the summed TDEM response for all four time gates is shown in Figure A-1 in the upper left-hand plot window and in Figure A-2. The color contours range from blue to red (low mV response to high mV response). In this plot blue contours represent areas with background readings and little or no buried metal detected. Color contours from green to red represent areas where the EM61 instrument detected the likely presence of metal. The darkest red areas, representing the largest TDEM response, indicate areas containing metal – above or below ground. The detected metal could range from a single large metal object, such as a steel drum, to a number of smaller individual metallic objects clustered beneath or adjacent to the TDEM instrument. Distinguishing between a single large metallic object and a cluster of smaller metallic objects, using only the TDEM data, is difficult. Burial pits or trenches filled with debris containing metallic objects will typically appear in the TDEM plan map as broad areas with variability of the elevated response, and often with vague outlines in shape or a group of irregular clusters of smaller anomalies. Smaller isolated anomalies are generally associated with individual random pieces of buried metal and would not be considered high priority anomalies if searching for a metallic debris-filled burial pit.

As discussed in the Data Acquisition section above, the maximum depth of investigation using the EM61-MK2 instrument varies depending on the mass of the metal object, and other factors. However, this instrument is generally not significantly affected by soil conditions, except in unusual circumstances which are not expected at this site. The only buried metal object at this site of known depth was the culvert beneath the access road (labeled “Buried Metal Culvert” near the northeast corner of Figure A-22). The maximum burial depth to the top of this culvert is approximately 4-5 ft-bgs and this feature was easily detected by the EM61-MK2 creating a high amplitude response (Figure A-2). Large metal surface objects, such as construction vehicles or metal chain link fences, may obscure the signal from buried objects in the TDEM data when those data are acquired within 5 – 10 ft of the surface metal object. Even though they are not beneath the sensor, these surface metal features are also detected by the instrument, which records the sum of all the responses to metal within the volume of the active EM field.

Frequency Domain Electromagnetics (FDEM)

A color contoured plan view map of the FDEM In-Phase and Quadrature response is shown in Figure A-1 in the lower left- and lower right-hand plot windows, respectively, with full page plan maps shown in Figures A-3 and A-4. The In-Phase response is primarily sensitive to larger volume or linear metallic features, while the Quadrature Phase (Bulk Conductivity) is primarily sensitive to ground conductivity (which can also be elevated due to the presence of metal in the subsurface). In Figure A-4, note that the Bulk Conductivity data (mS/m) have been converted to Bulk Resistivity (ohm-m) for easier comparison with the inverted FDEM earth model shown in Figure A-5. The FDEM data identified multiple linear anomalies. Long linear anomalies that appear in both the In-Phase and Bulk Conductivity are likely associated with buried metallic pipes or electrical utilities. However, the east-west and north-south large and obvious response anomalies along the edges of the south and north areas, respectively, are located relatively close to the perimeter fence. The FDEM anomalies do not exactly mimic the fence position, nor do they have equal response along the entire length of the fence; therefore, they are called out as FDEM anomalies (Figures A-3, A-4 and A-22). Linear anomalies that are only evident in the Bulk Resistivity may represent non-metallic pipes or excavations that have been backfilled with non-native soil or trapped moisture in the fill materials.

A pseudo-3D resistivity earth model was developed from the FDEM quadrature data and is presented in Figure A-5 as resistivity depth slices (i.e., 2D plan maps) at 2.5-foot depth intervals. The earth resistivity model was affected by the significant presence of metal at this site, both surface metal and subsurface metal. This impact to the FDEM data required increased smoothing to minimize the localized effects of metal on the measurements. While this improves the inversion results for the resistivity earth model in terms of characterizing the bulk soil electrical properties (vertical variation), it also limits the lateral resolution of small-scale features or objects of interest such as buried debris. Linear features are better represented in the plan view map of the bulk resistivity data (Figure A-4).

As discussed in the Data Acquisition section above, the maximum depth of investigation using the CMD instrument is generally about 15 ft for the largest transmitter – receiver coil separation. This may be reduced if the near surface soils are very conductive (low resistivity). Significant amounts of subsurface or surface metal in close proximity to the instrument can affect the depth of investigation due to their influence on the measured bulk conductivity. As with the EM61-MK2, the known culvert was easily detected by the CMD resulting in strong lows in both the In-Phase and bulk resistivity measurements (Figures A-3 and A-4).

Vertical Gradient Magnetometry (VGM)

Two different color contoured plan view maps of the VGM data are presented to highlight the use of magnetometry surveys. Figure A-1 presents the vertical gradient in the upper right-hand plot; and, Figure A-6 presents a full page plan view map of the VGM analytic signal result. The vertical magnetic gradient is the difference in the total magnetic field intensity measurements between two magnetic sensors relative to the vertical offset distance between the sensors. VGM is only sensitive to magnetic objects, predominantly ferrous metals, unlike TDEM which is sensitive to all conductive metallic objects. Comparison of the responses of larger anomalies in the TDEM and VGM data are used to provide some differentiation between ferrous metal objects and non-ferrous metallic objects. Using VGM data, magnetic anomalies typically appear as dipoles (a magnetic low “blue” adjacent to a magnetic high “red” - see Figure A-1), the orientation of a dipole depends on the shape and orientation of the ferrous metal object. Figure A-6 shows the vertical magnetic gradient data after applying the analytic signal filter, as discussed in the data processing section above. In the AS plot (Figure A-6), the location of the detected ferrous metal object would theoretically be directly beneath the peak amplitude of the anomaly (for an isolated subsurface target passing directly beneath the magnetometer sensors).

VGM is a potential field method which does not use an active signal source; therefore, the depth of investigation is dependent on the magnitude and orientation of the variation (vector property) in the remnant magnetism of ferrous metal objects at the site. Additionally, as a potential field method, the instrument is sensitive to the local perturbations of the earth’s magnetic field caused by all ferrous metal objects, both above ground and below ground, within the detection limit of the instrument. Therefore, the measured total field data at each sensor are the sum of all of the vector contributions of the earth's magnetic field and all the remnant magnetic fields of magnetic objects within the detection limits of the sensors. Using the magnetic vertical gradient will help to reduce the effects of offline surface ferrous metal objects adjacent to the sensor location to some degree, but the VGM data are more sensitive to surface metal features than the TDEM or FDEM data. The location of the known metal culvert correlates with a strong response in the VGM AS data (Figure A-6); however, the shape of the feature is not as well defined as in the TDEM and FDEM data. This may be due to the geometry of the data collection line paths over the culvert or to other ferrous metal objects (surface and/or subsurface) located in the vicinity of the culvert.

Ground Penetrating Radar (GPR)

Figure A-7 shows a plan view map with the locations of the GPR scan lines. The GPR profile sections are shown in Figures A-8 through A-19. GPR data collected over a known buried metal culvert in the North Zone did not detect the culvert at an estimated burial depth of 3 to 4 ft-bgs. The GPR data collected in the vicinity of SRT Line 3 (GPR Line 32) shows a clear shallow reflection to a maximum depth of approximately 3 ft-bgs. This reflection horizon likely represents a layer change within the unconsolidated overburden, possibly the contact between surface fill materials and native soils. Therefore, with the exception of the area around GPR Line 32, the effective depth of investigation for GPR at this site was limited to less than 2 ft-bgs. The GPR data in this excepted area also show some distinct diffractions in multiple parallel GPR profiles. These diffractions likely represent buried pipelines.

The GPR data collected along the SRT profile lines (GPR Lines 32, 36, and 38) are shown in Figures A-12, A-13 and A-14 respectively, and with the SRT profiles in Figure A-21. The plots in Figure A-21 show that the GPR data do not image to the depth of the interpreted top of bedrock horizon (dashed black contour) shown in the SRT Vp sections (Figure A-20). SRT results are discussed in the following section.

To a much greater degree than any of the other geophysical methods deployed at this site, the effectiveness of GPR is heavily dependent on the site-specific ground conditions. Therefore, the effective depth of investigation cannot be determined prior to data collection at a given site. Typically, high bulk ground conductivity, often due to high clay content in the soils, is a common limiting factor in GPR depth of investigation. At this site, the mean bulk conductivity of the surface soil layer is approximately 24 mS/m, as measured by the shortest offset receiver coil (1.4 meter separation) of the CMD instrument which is most sensitive to the upper few feet of soil. This value is approaching the general rule of thumb limit of 25 – 30 mS/m and is likely a contributing factor in limited GPR depth of investigation at this site. This is also supported by the observation that the best GPR data were collected in an area where the near surface bulk conductivity (measured by the 1.4 m separation coils on the CMD) was less than 14 mS/m. Based on approximately 5,930 linear feet of GPR data collected at this site, we have not fully identified the boundaries of areas where near-surface soil properties limit the depth of investigation when using a new, state-of-the-art, 350 MHz GPR digital antenna. This antenna was selected to identify the depth of buried objects in the overburden soils, and had an anticipated depth of investigation of 5 to 10 feet bgs.

Seismic Refraction Tomography (SRT)

The SRT results are shown as color contoured 2D P-wave velocity (Vp) cross sections beneath the three seismic lines in Figure A-20. Horizontal and vertical scales and color contour scales for each line are the same. An inset image showing a 3D perspective view of the 2D lines (as viewed from the southeast) is included in Figure A-20. The P-wave velocity (Vp) results tie very well at the line intersections, based on the 3D seismic fence diagram. Cool colors show low velocities (i.e., blues) which are generally loose, unconsolidated and unsaturated soils. Hot colors (i.e., orange/red) show more competent, generally harder materials, which can be interpreted as bedrock. Vp values are an indication of the bulk compressibility of the subsurface materials.

Based on information provided by BGI, bedrock (Upper Bandelier Tuff) was anticipated to be shallow beneath the SRT profile lines but with a variable thickness. Based on the good signal quality and SRT model results, a Vp of 2,300 ft/s has been selected to represent the transition from unconsolidated or weathered materials to bedrock. Borehole geologic information is not yet available to confirm this velocity interface as bedrock; that is, to calibrate these model results with the interpretation. But, based on experience and the high gradient in the Vp contours, we are led to this interpretation, which is shown as the black-dashed lines on each 2D SRT section. The three lines of SRT show an interpreted overburden soil layer (undifferentiated fill and native materials) that ranges from less than 5 feet thick (Line 1 – distance ~0-20 ft) to a maximum observed thickness of just greater than 20 feet (Line 1 – distance ~340 ft). This interpreted bedrock velocity is quite low for competent bedrock, indicating the tuff is either poorly welded, highly fractured and/or a thick weathering zone is present. Drill hole information will be valuable to confirm the Vp interpretation. However, the general shape / geometry of the soil-rock interface, and the overall depth will not be expected to change significantly. Bedrock outcrops at the surface along the southern edge of the South Zone in the AOI (i.e., beyond the southern extent of SRT Line 2). The thickest section of overburden observed beneath both Lines 1 and 2, in the southern part of the AOI, is easily observed in the 2D seismic sections and the inset 3D perspective view (Figure A-20).

The depth of investigation of the SRT method is primarily controlled by the length of the active receiver array (75.5 ft) and the subsurface velocity structure (Vp). At this site, the first refractor encountered in the data, indicated by a change in slope of the first arrivals of signal from the sledgehammer at each receiver, is interpreted as the dashed black line (2,300 ft/s Vp contour) in Figures A-20 and A-21. In the refraction method, the highest ray path density will be associated with this boundary and the highest subsurface resolution will be in the area with the highest raypath data density. Beneath this impedance boundary, raypath density is lower and results in a reduction of resolution. The depth to this interpreted refractor in the SRT profiles ranges from about 5 ft to 20 ft-bgs. This is within the normal depth range expected for this array geometry and thin overburden over bedrock site conditions.

Anomaly Selection

Figure A-22 shows a combined layer map of the interpreted TDEM (red), FDEM (yellow) and VGM (dark blue) data overlain on the Google Earth site image, with posted surface features. Based on the observed trends in each data set, anomaly identification and selection was prioritized for overlapping TDEM and VGM anomalies (e.g., isolated areas), and then FDEM anomalies (e.g., linear features). In Figure A-22, the selected and co-located TDEM and VGM anomalies are outlined in light blue; and the selected linear FDEM anomalies are shown as yellow lines. These selected anomalies are listed below in Tables 1A and 1B:

Table 1A. Center location of selected & co-located TDEM and VGM anomalies (WGS84, DD.dd)

TDEM/VGM Anomaly	Center Latitude	Center Longitude
A	35.87761504	-106.28821691
B	35.87792493	-106.28806758
C	35.87879473	-106.28822083
D	35.87845266	-106.28792178
E	35.87759928	-106.28872777

Table 1B. End points of selected FDEM linear anomalies (WGS84, DD.dd)

FDEM Anomaly	Latitude	Longitude
F (west end)	35.87775373	-106.28905950
F (east end)	35.87772656	-106.28862619
G (west end)	35.87796342	-106.28955097
G (bend)	35.87784105	-106.28912646
G (east end)	35.87785909	-106.28820294
H (west end)	35.87806432	-106.28932634
H (east end)	35.87798395	-106.28820621
I (south end)	35.87810284	-106.28830189
I (north end)	35.87882467	-106.28821913

FDEM Anomaly	Latitude	Longitude
J (west end)	35.87850304	-106.28749026
J (east end)	35.87852784	-106.28728092
K (west end)	35.87846560	-106.28750909
K (east end)	35.87843543	-106.28727387

The selected TDEM and VGM anomalies represent areas with a coincident and larger lateral extent and are apparent in both the TDEM and VGM data. These anomaly areas are of the size and shape generally associated with burial pits and/or trenches. Anomaly A may represent a single buried metal object or a small number of clustered buried metal objects. Anomalies B, C and D are interpreted to reflect multiple metallic objects within the outlined area. While Anomalies B, C and D have marked above-ground metallic surface features and/or marked buried utilities within the anomaly extent, these known cultural features alone do not fully account for the elevated instrument response or spatial extents for these anomalous locations. Anomaly E may represent a single buried metal object based on the shape of the TDEM anomaly.

The selected FDEM linear anomalies represent long linear features typical of narrow trenches or buried utilities (e.g., non-metallic or low conductivity pipe). Over the majority of the extents of these linear FDEM anomalies shown in Figure A-22, there are no apparent or corresponding TDEM/VGM anomalies. This indicates that these features do not likely contain significant amounts of conductive metal. These linear FDEM anomalies, most apparent in the FDEM bulk resistivity measurements (Figure A-4), suggest that the native in-situ soils along these alignments may have been disturbed and possibly replaced with non-native or backfilled materials characterized by a difference in bulk resistivity. Two of these linear higher bulk resistivity anomalies are very close to the boundary fence on the north edge of the southern AOI and the west edge of the northern AOI (previously discussed); as such, their proximity is noteworthy for investigation. Linear Anomaly H is in close proximity, and roughly parallels the mapped alignment of a buried sewer utility shown in Figure A-22. However, the western end of Anomaly H diverges from the mapped sewer utility to the north and then fades out, suggesting that this anomaly may not be fully attributable to the buried sewer utility as mapped. Anomaly I is located between the alignments of a mapped electrical utility and a mapped sewer utility (Figure A-22); however, the shape, character and length of Anomaly I may not totally be attributable to these buried utilities. Linear Anomalies F, G, and K are not located near known or mapped buried utilities. The western portion of Anomaly J is likely associated with the buried corrugated metal culvert, while the eastern portion of the anomaly is not located near any mapped buried utility or linear surface metal features. Elsewhere, the in-phase FDEM data (Figure A-3) clearly detects the buried corrugated metal culvert and detects the perimeter metal fencing at this site, which generally impacts the quadrature values next to the fences as well.

One GPR anomaly is identified on the eastern end of the North AOI Zone, in an area with better depth of investigation (green line, Figure A-22). This anomaly is listed in Table 1C below.

Table 1C. Center location of selected GPR anomaly (WGS84, DD.dd)

GPR Anomaly	Center Latitude	Center Longitude
L	35.8783617	-106.287448

This anomaly has a length of approximately 30 ft and is characterized by a cluster of irregularly spaced small diffractions located beneath a reflecting horizon at a depth of approximately 3 ft-bgs (GPR Line 32, Figures A-12 and A-21). The width of the anomaly (off-line extent) cannot be determined from the single GPR profile. This GPR anomaly has the general in-line extent and characteristics of a potential debris pit. In this location, the VGM shows only background response, indicating no ferrous metal was detected. The TDEM plan map for this area shows two small clusters of low to moderate response above background indicating the presence of metal. The TDEM metal detector is a profiling tool (mapping in X, Y), such that the size and depth of the metal detected cannot be directly determined from the instrument data.

The selected geophysical anomalies discussed above represent the most likely locations of potential debris filled pits or trenches, if present, identified in the geophysical data. An intrusive field investigation is necessary to determine the nature and cause of these geophysical anomalies. The site, in general, contains an abundance of metal, both above and below ground surface that was detected by the geophysical instruments. Geophysical coverage gaps are present beneath the existing debris piles, large surface metal and surface obstructions which are noted on Figure A-22.

Closure

Overall FDEM and VGM data quality were very good, with high signal-to-noise data acquired over the AOI. TDEM data quality was good, although intermittent noise was detected during static instrument testing at a location near the parking area, east of the North AOI Zone. This type of TDEM noise may have been a result of nearby radar (airport) and/or radio signals. SRT data quality was very good with high signal-to-noise levels recorded for most records. SRT Line 1 data had some elevated ambient noise from an operating generator located just north of the fence line in the South AOI Zone, but this did not significantly impact data processing. While GPR data quality was moderate to good, the effective depth of investigation was variable across the site, with the best depth penetration in the southwest corner of the North AOI Zone over regions covered by fill materials. It is determined that the GPR signal penetration of 2 to 3 feet bgs, renders much of the GPR data ineffective for depth imaging of buried objects/debris. Apart from the GPR data/results, there is a high degree of confidence in the results presented herein.

The geophysical methods and field procedures defined in this report were applicable to the project objectives and have been successfully applied by Collier geophysicists to investigations of similar size and nature. However, sometimes field or subsurface conditions are different from those anticipated and the resultant data may not achieve the investigation objectives. Collier warrants that our services were performed within the limits prescribed for this project, with the usual thoroughness and competence of the geophysical profession. Collier conducted this project using the current standards of the geophysical industry and utilized in house quality control standards to produce a reliable geophysical survey.

Collier is very appreciative of the support provided by BGI staff and for the assistance in data collection and site logistics. If you have any questions regarding the field procedures, data analyses, or the interpretive results presented herein, please do not hesitate to contact us. We appreciate working with you and look forward to providing BGI with geophysical services in the future.

Respectfully Submitted,

Collier Geophysics, LLC

J. Pfeiffer

Jim Pfeiffer, PGp, PG
Senior Geophysicist

Phil Sirles

Phil Sirles
Senior Geophysicist

(1 copy e-mailed PDF format)

FIGURES

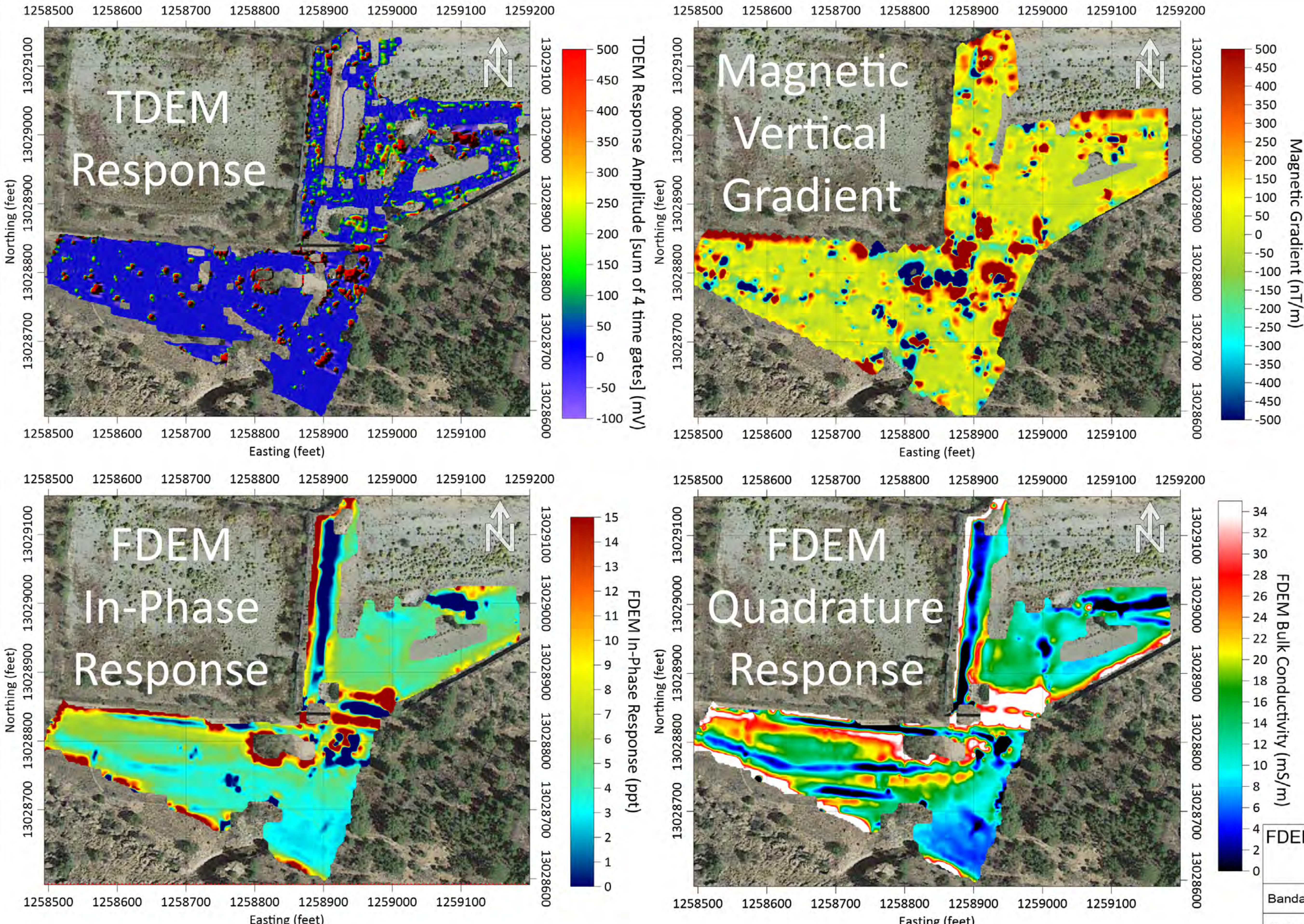

UTM 13N NAD83 Feet

FDEM, TDEM and VGM Results
MDPR Site Investigation
Los Alamos, NM

Banda Group International, LLC

Project #: 20-184 | January 2021

Drafted by: J. Sheehan | Checked by: P. Sirles

COLLIER GEOPHYSICS

Fig. A-1

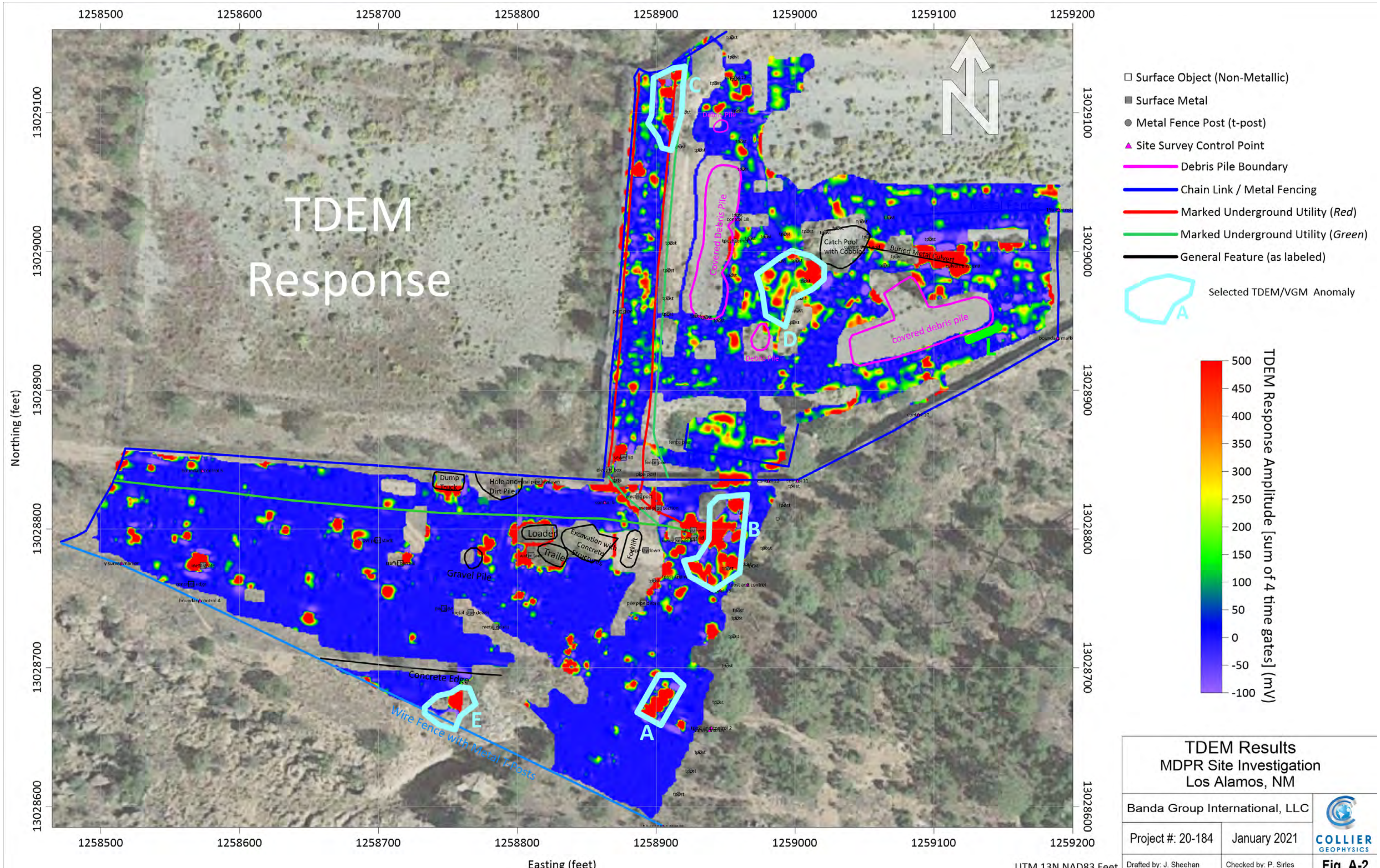
TDEM Response
Surface Object (Non-Metallic)
Surface Metal
Metal Fence Post (t-post)
Site Survey Control Point
Debris Pile Boundary
Chain Link / Metal Fencing
Marked Underground Utility (Red)
Marked Underground Utility (Green)
General Feature (as labeled)
Selected TDEM/VGM Anomaly
TDEM Response Amplitude [sum of 4 time gates] (mV)
500
450
400
350
300
250
200
150
100
50
0
-50
-100
A
B
C
D
E
Covered Debris Pile
covered debris pile
Debris Pile
Catch Pool with Cobble
Buried Metal Culvert
Dump Truck
Hole and Dirt Pile
Loader
Excavation with Concrete Structure
Trailer
Forklift
Gravel Pile
Concrete Edge
Wire Fence with Metal T-posts
Easting (feet)
Northing (feet)
1258500
1258600
1258700
1258800
1258900
1259000
1259100
1259200
13029100
13029000
13028900
13028800
13028700
13028600
UTM 13N NAD83 Feet
TDEM Results
MDPR Site Investigation
Los Alamos, NM
Banda Group International, LLC
Project #: 20-184
January 2021
Drafted by: J. Sheehan
Checked by: P. Sirles
COLLIER GEOPHYSICS
Fig. A-2

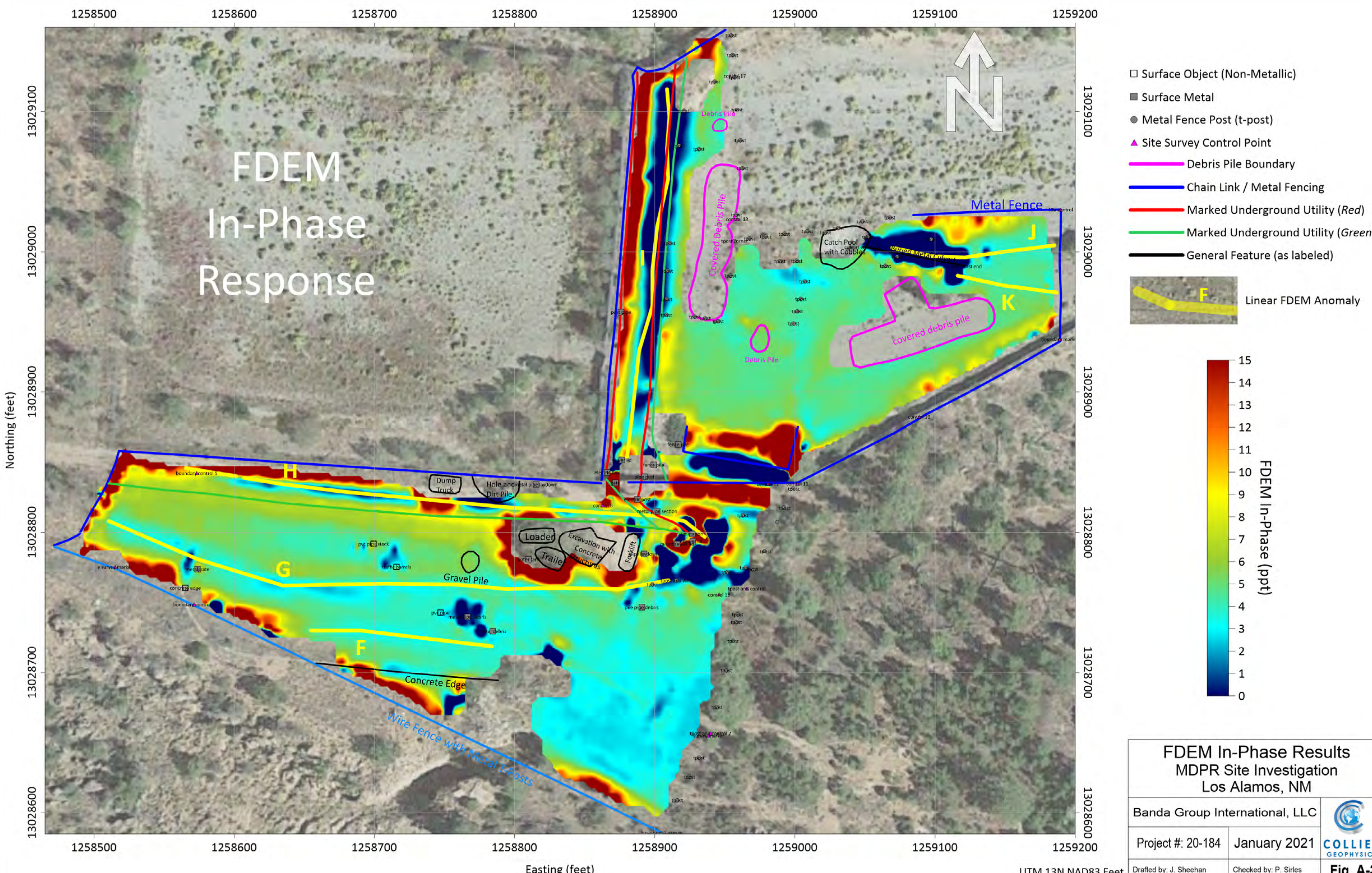

FDEM In-Phase Results
MDPR Site Investigation
Los Alamos, NM

Banda Group International, LLC

COLLIER GEOPHYSICS

Project #: 20-184

January 2021

Drafted by: J. Sheehan

Checked by: P. Sirles

Fig. A-3

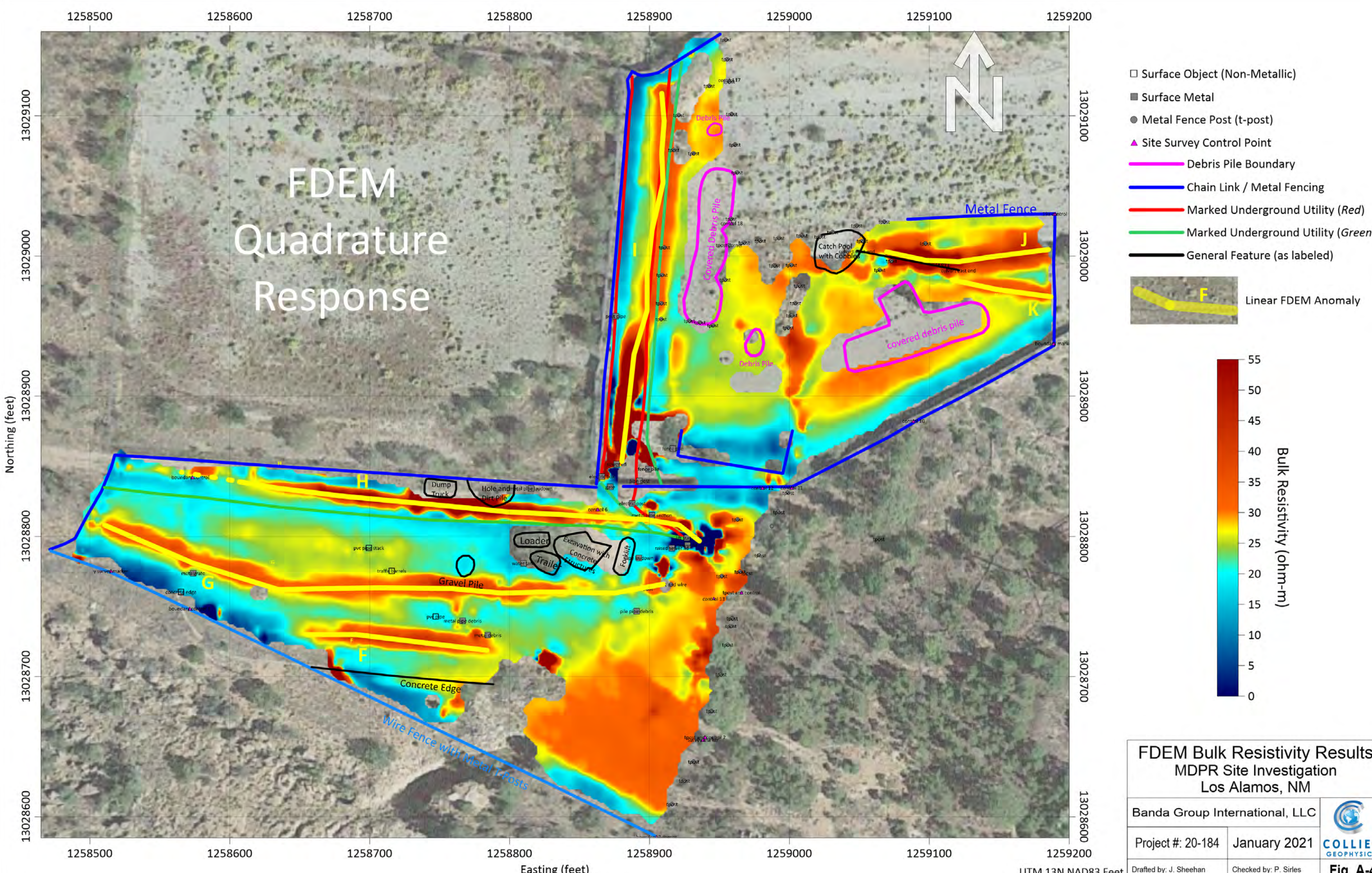

FDEM Bulk Resistivity Results
MDPR Site Investigation
Los Alamos, NM

Banda Group International, LLC

Project #: 20-184 | January 2021

Drafted by: J. Sheehan | Checked by: P. Sirles

COLLIER GEOPHYSICS

Fig. A-4

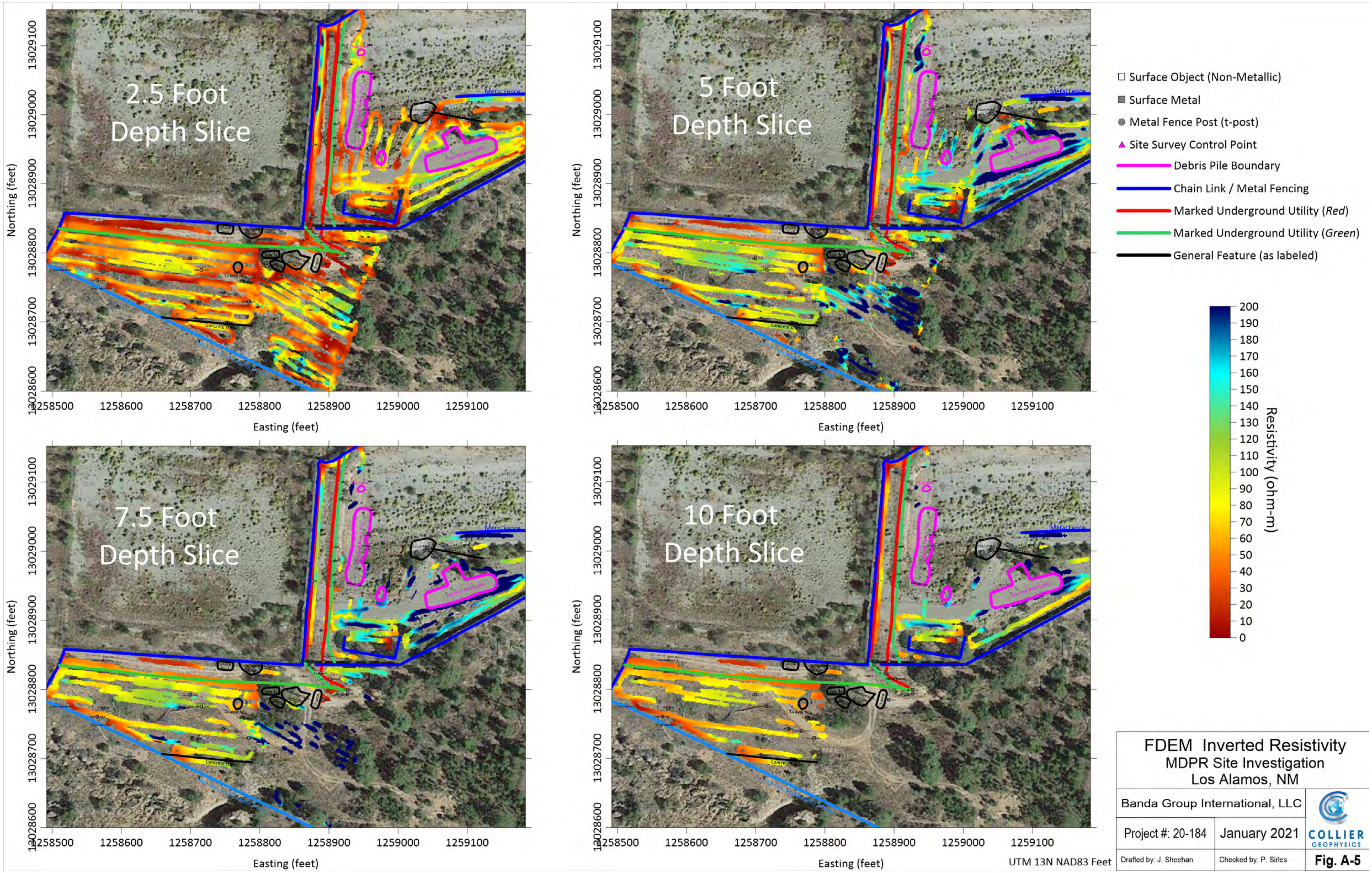
2.5 Foot Depth Slice
5 Foot Depth Slice
7.5 Foot Depth Slice
10 Foot Depth Slice
Northing (feet)
Easting (feet)
13028600
13028700
13028800
13028900
13029000
13029100
1258500
1258600
1258700
1258800
1258900
1259000
1259100
Metal Fence
Surface Object (Non-Metallic)
Surface Metal
Metal Fence Post (t-post)
Site Survey Control Point
Debris Pile Boundary
Chain Link / Metal Fencing
Marked Underground Utility (Red)
Marked Underground Utility (Green)
General Feature (as labeled)
Resistivity (ohm-m)
200
190
180
170
160
150
140
130
120
110
100
90
80
70
60
50
40
30
20
10
0
UTM 13N NAD83 Feet
FDEM Inverted Resistivity
MDPR Site Investigation
Los Alamos, NM
Banda Group International, LLC
Project #: 20-184
January 2021
COLLIER GEOPHYSICS
Drafted by: J. Sheehan
Checked by: P. Sirles
Fig. A-5

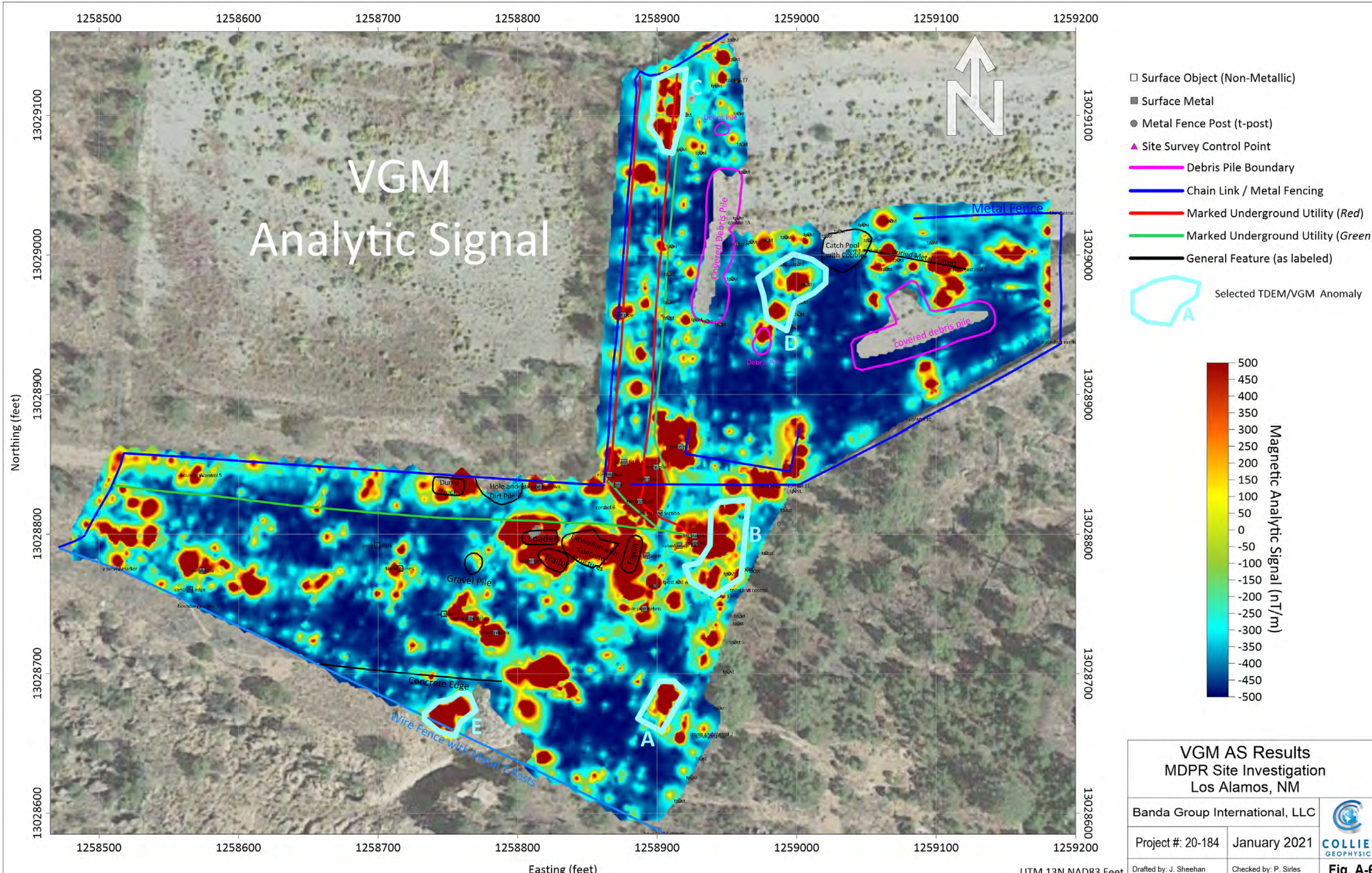

VGM AS Results
MDPR Site Investigation
Los Alamos, NM

Banda Group International, LLC

Project #: 20-184 | January 2021

Drafted by: J. Sheehan | Checked by: P. Sirles

COLLIER GEOPHYSICS

Fig. A-6

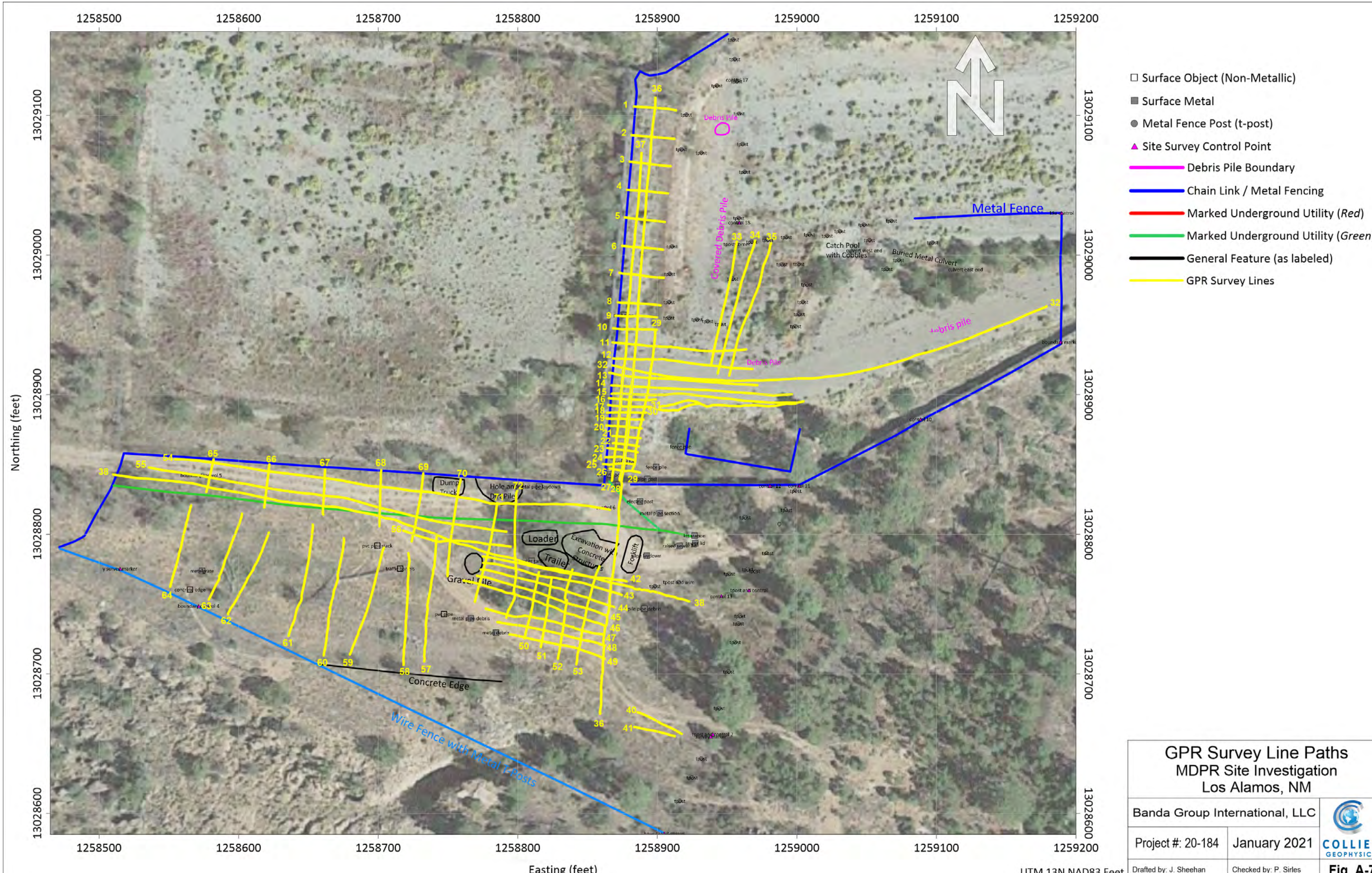

GPR Survey Line Paths
MDPR Site Investigation
Los Alamos, NM

Banda Group International, LLC	COLLIER GEOPHYSICS
Project #: 20-184	January 2021
Drafted by: J. Sheehan	Checked by: P. Sirles

Fig. A-7

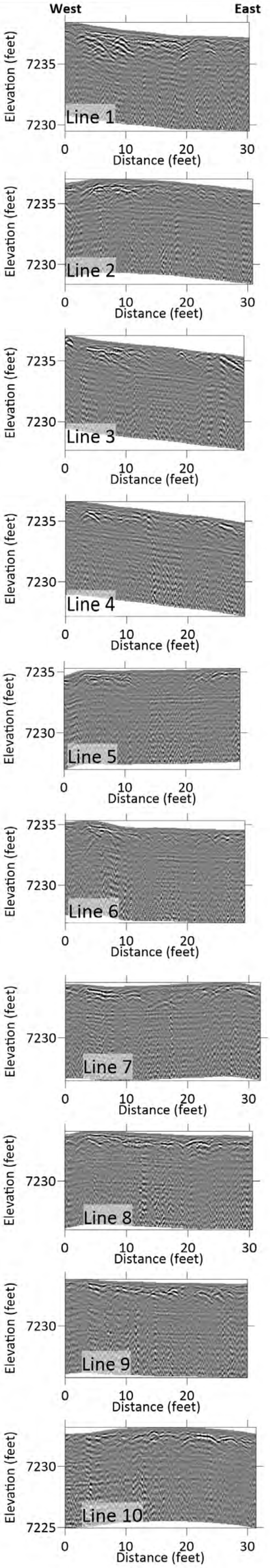

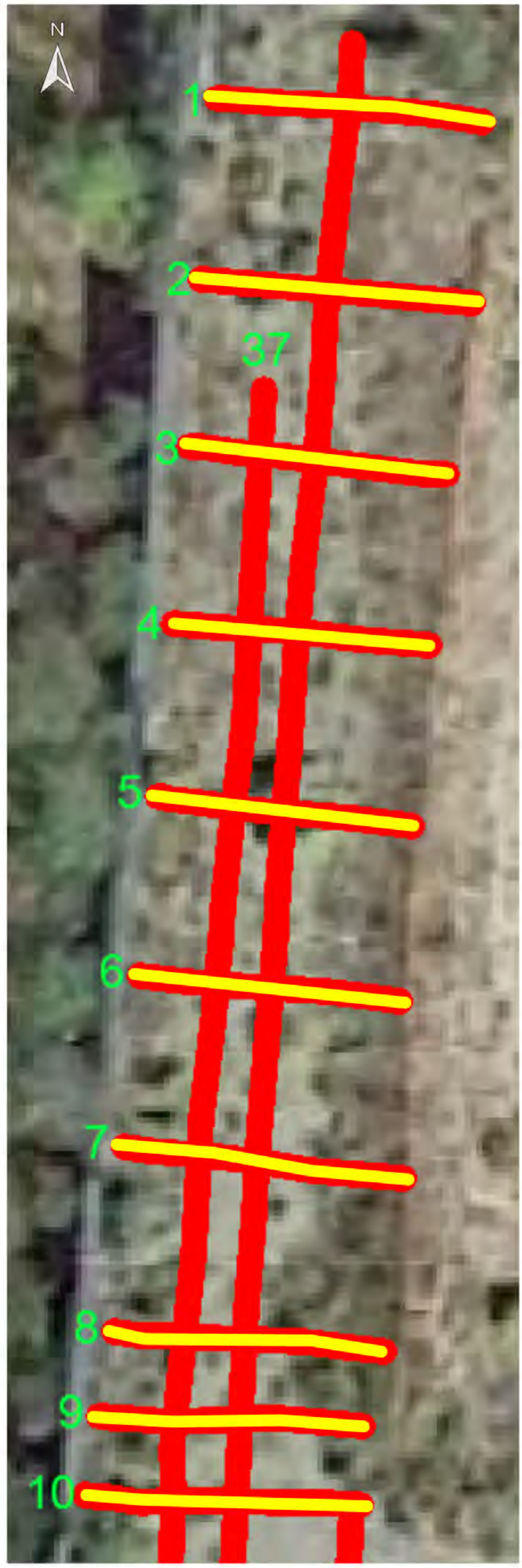

GPR Results (1 of 12)
MDPR Site
Los Alamos, NM

Banda Group International, LLC		COLLIER GEOPHYSICS
Project #: 20-184	January 2021	
Drafted by: J. Sheehan	Checked by: P. Sirles	Fig. A-8

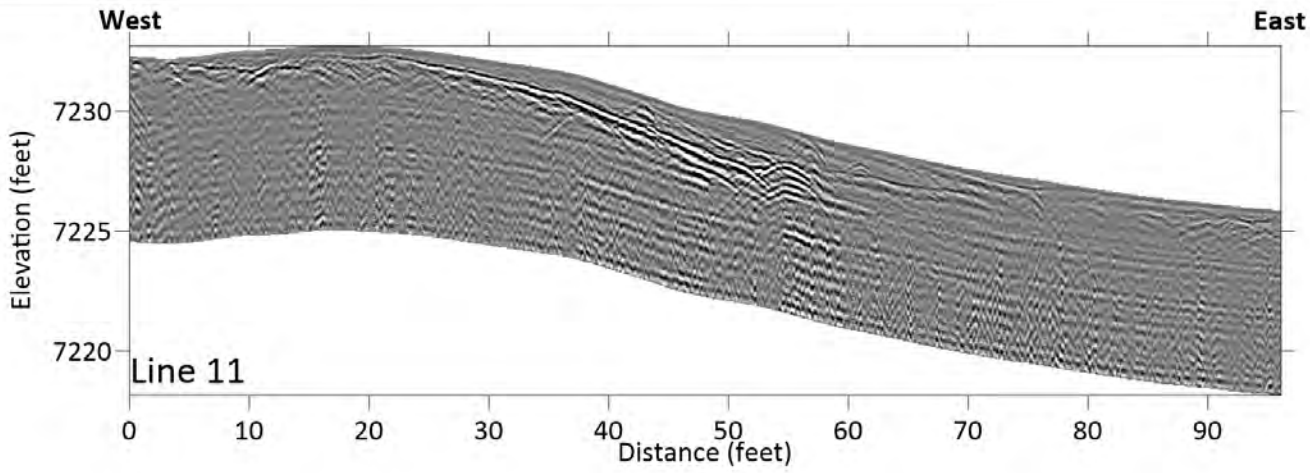

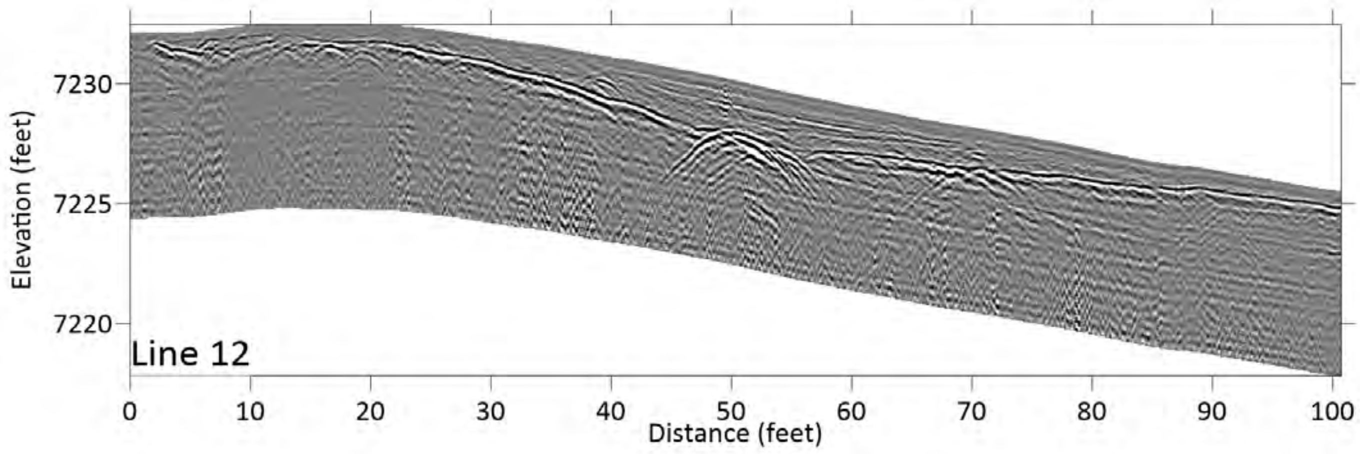

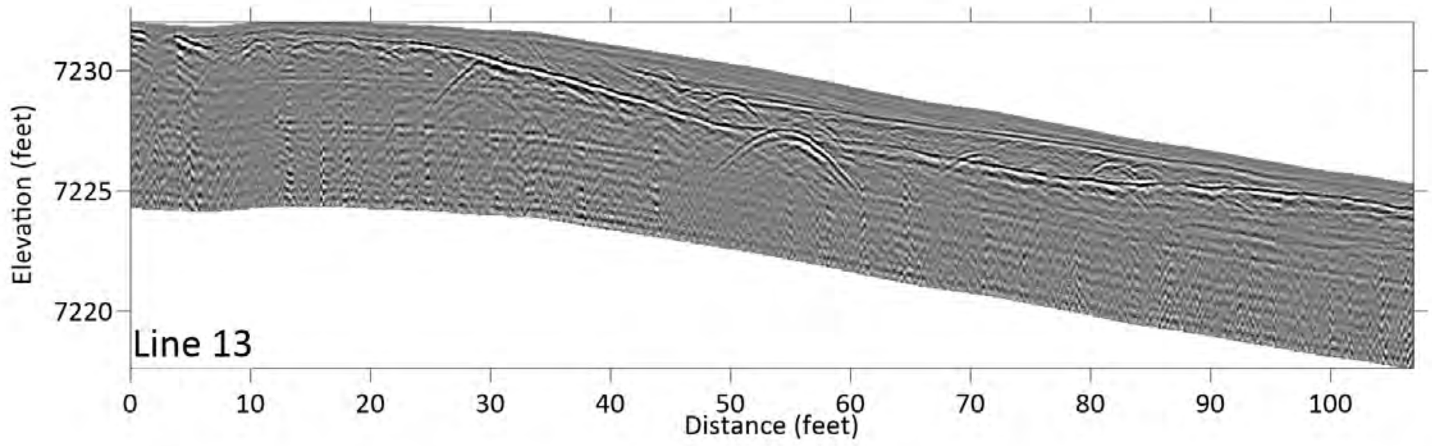

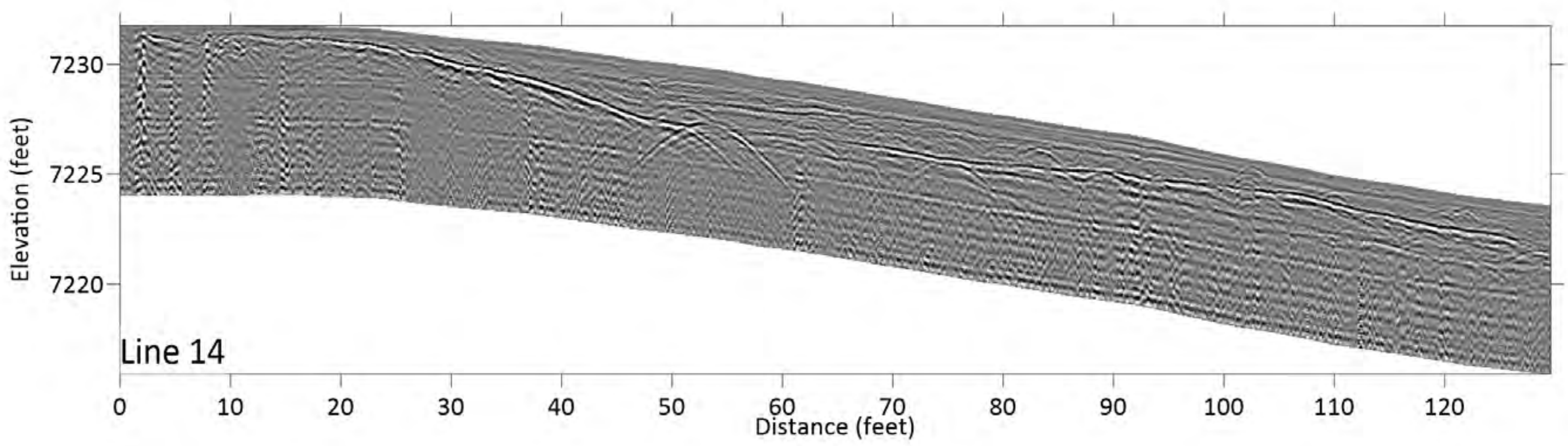

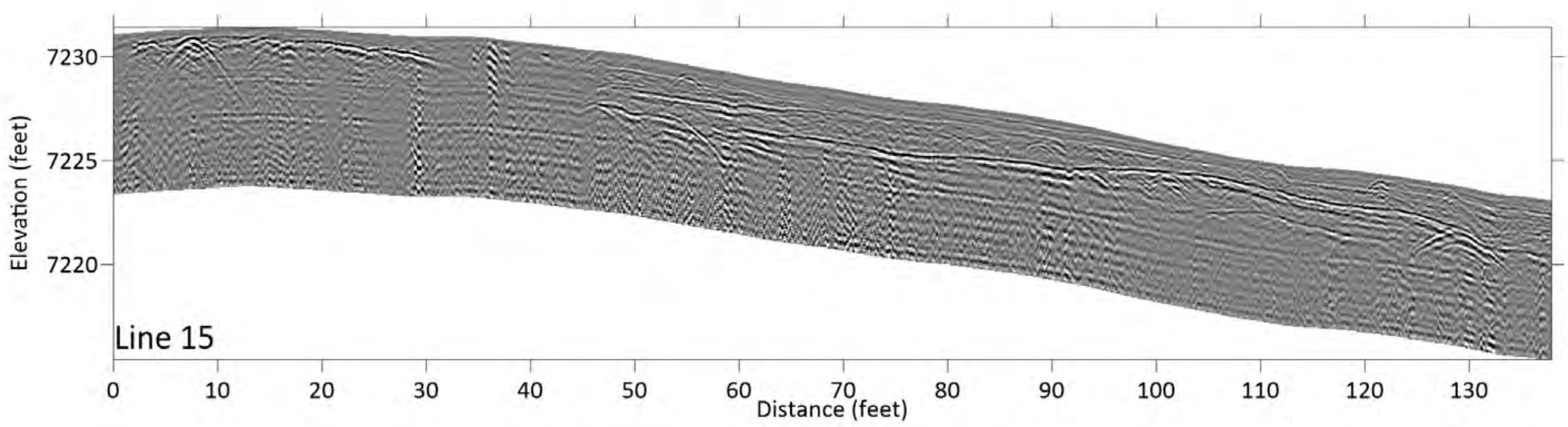

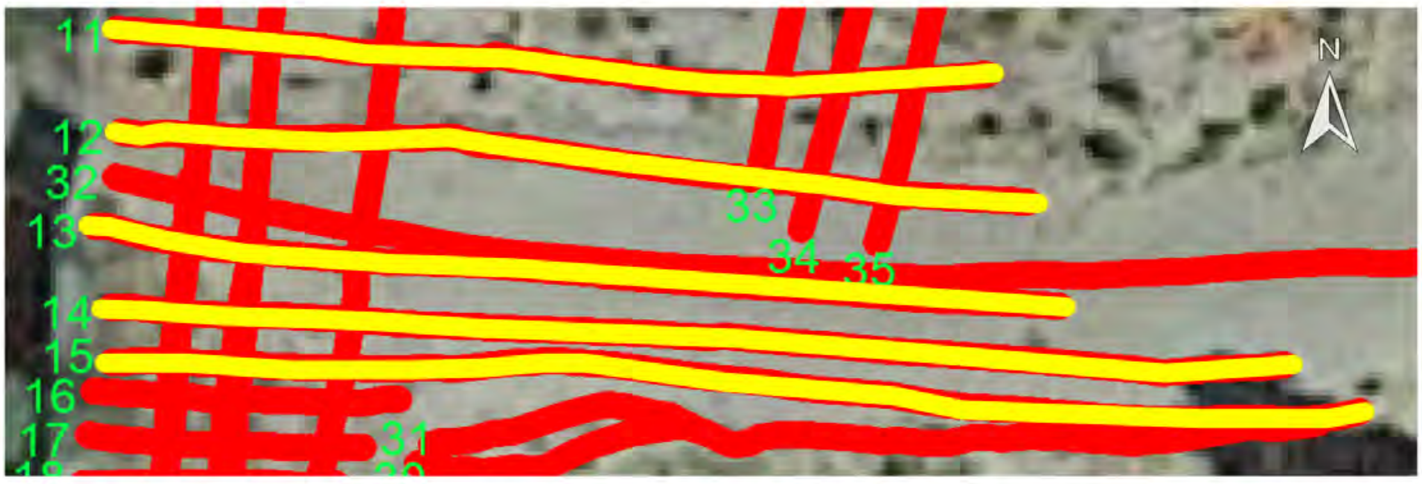

GPR Results (2 of 12)
MDPR Site
Los Alamos, NM

Banda Group International, LLC

Project #: 20-184 | January 2021

COLLIER GEOPHYSICS

Drafted by: J. Sheehan | Checked by: P. Sirles

Fig. A-9

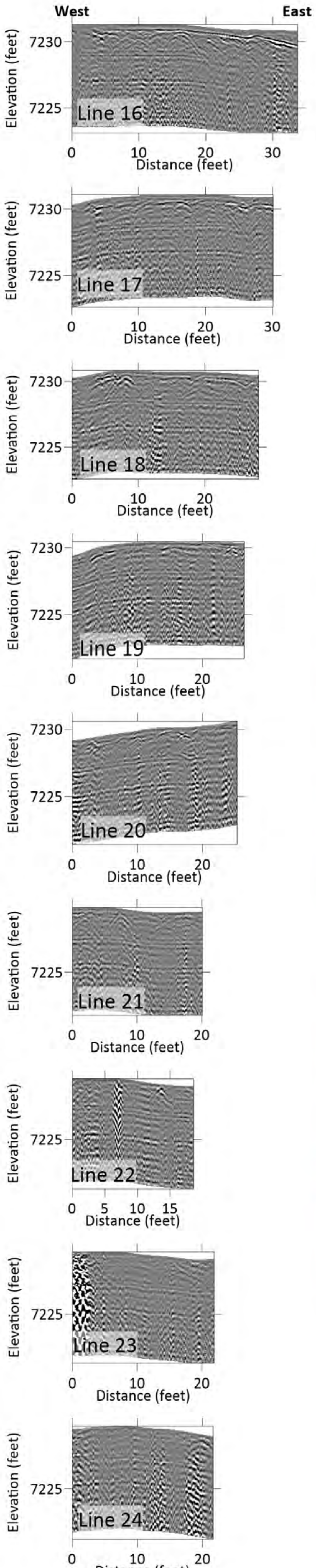

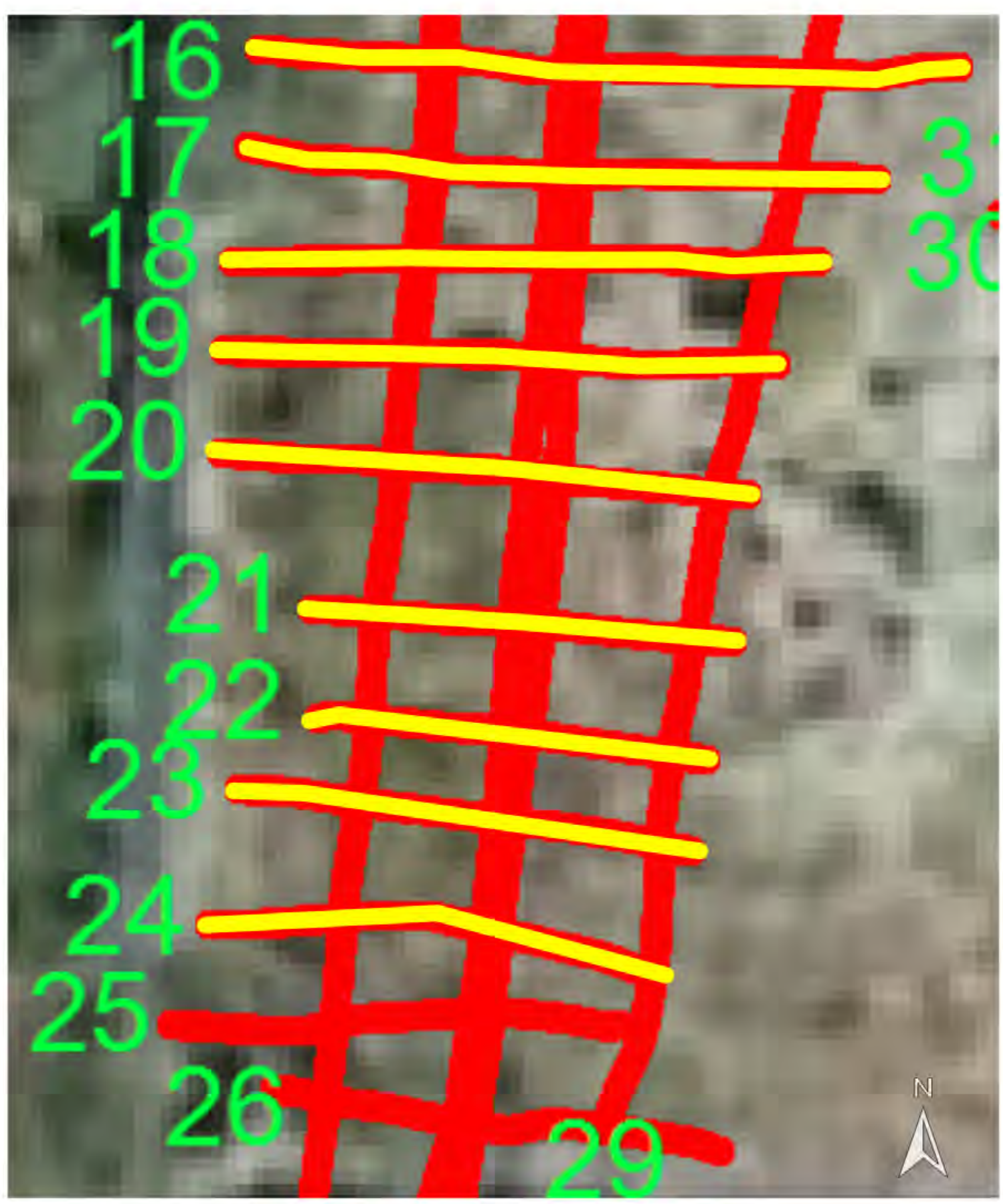

GPR Results (3 of 12)
MDPR Site
Los Alamos, NM

Banda Group International, LLC

COLLIER GEOPHYSICS

Project #: 20-184	January 2021
Drafted by: J. Sheehan	Checked by: P. Sirles

Fig. A-10

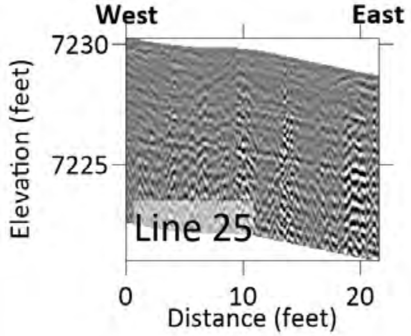

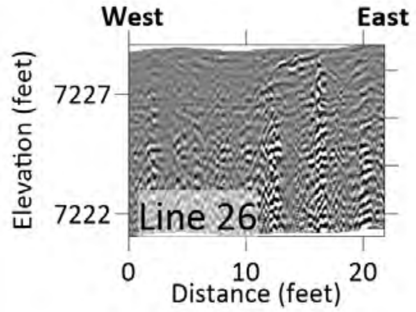

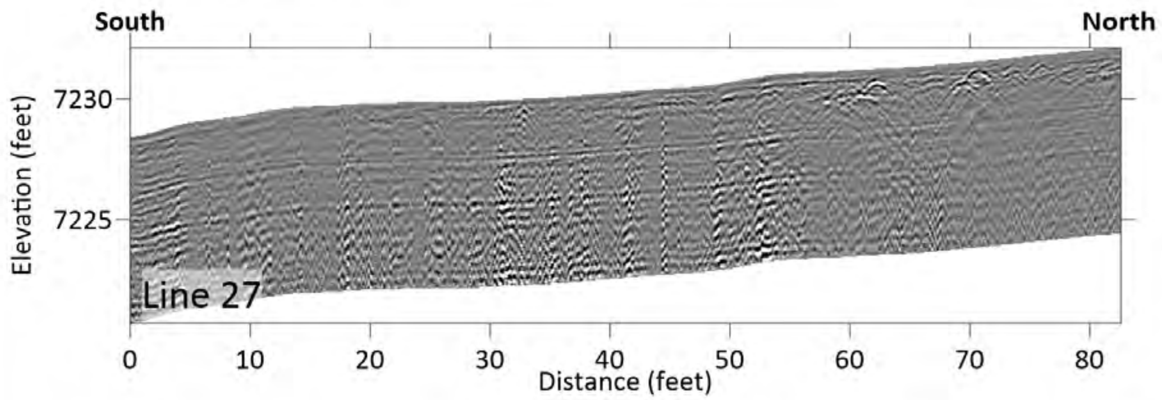

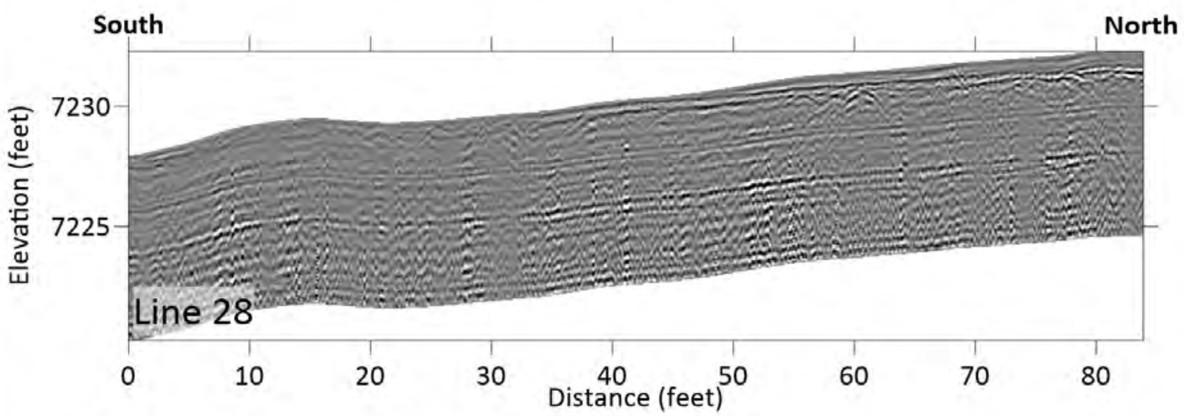

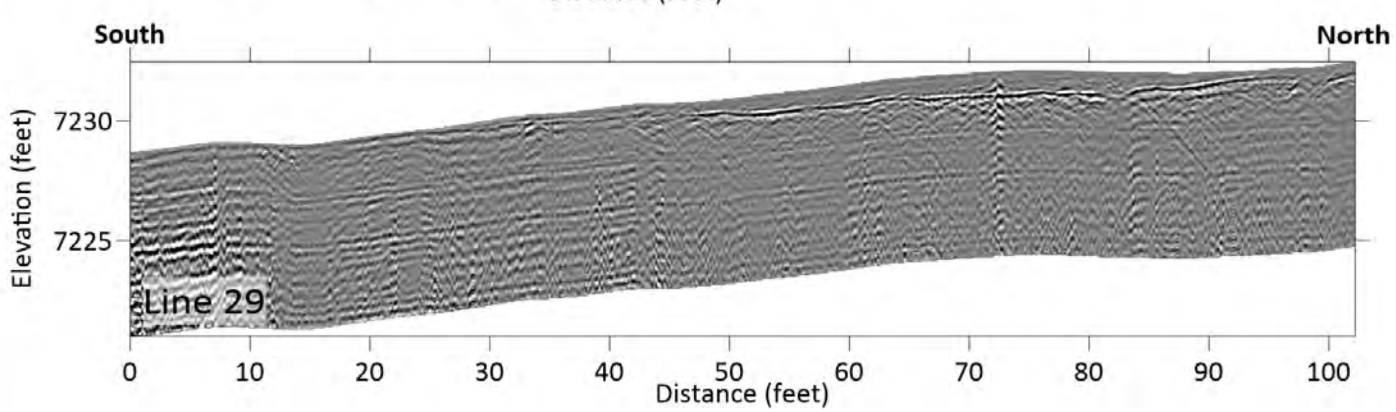

GPR Results (4 of 12)
MDPR Site
Los Alamos, NM

Banda Group International, LLC

Project #: 20-184 | January 2021

COLLIER GEOPHYSICS

Drafted by: J. Sheehan | Checked by: P. Sirles

Fig. A-11

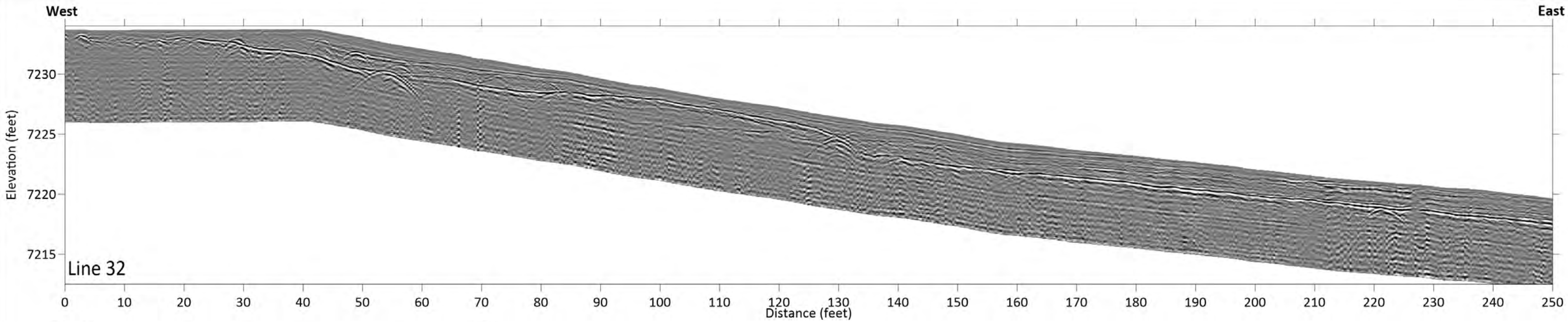

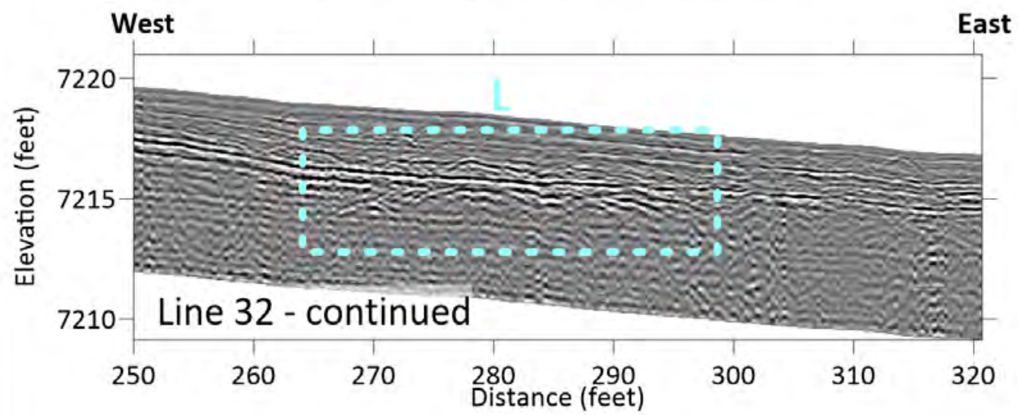

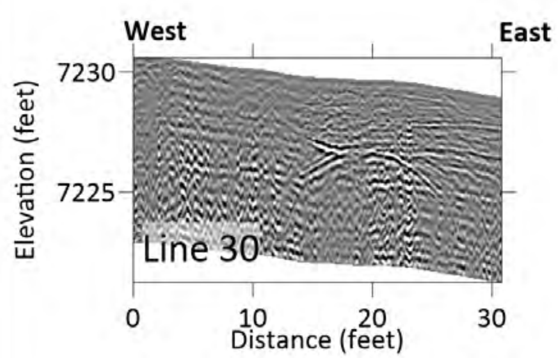

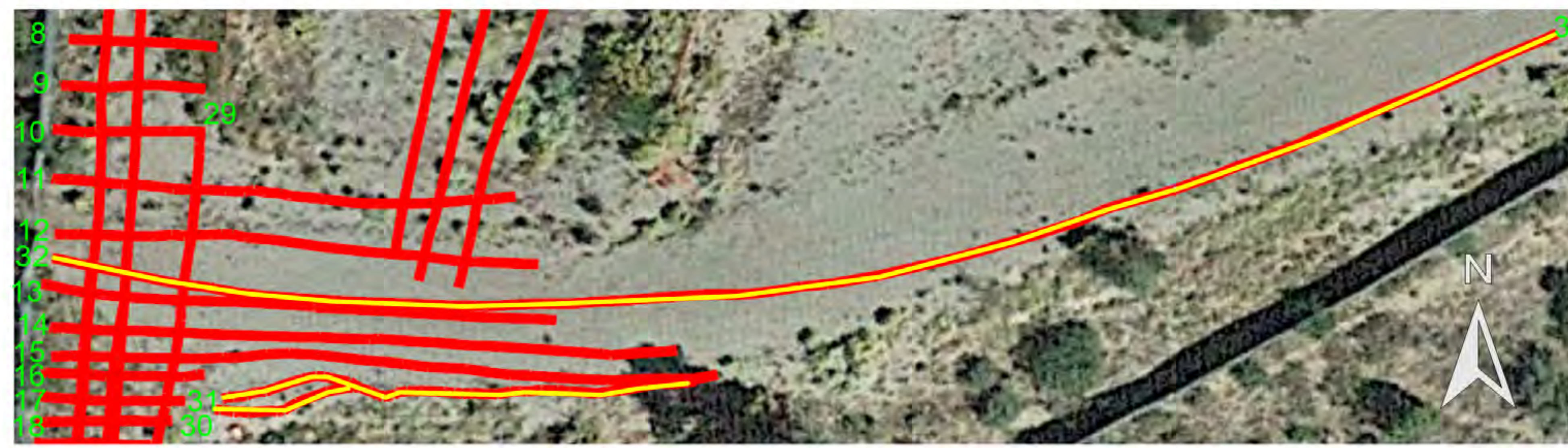

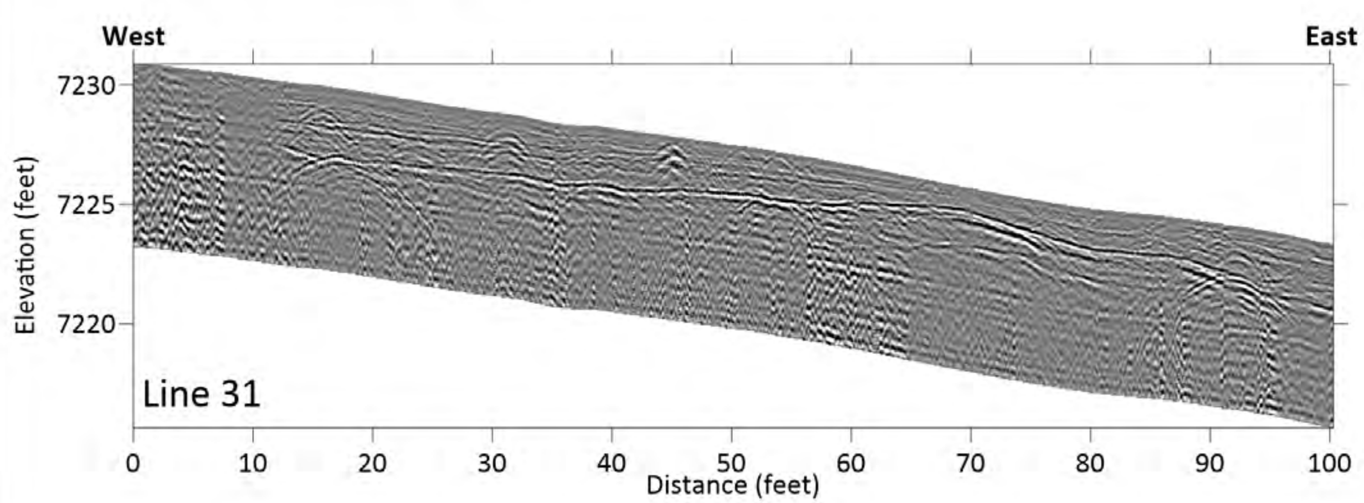

L Selected GPR Anomaly

GPR Results (5 of 12) MDPR Site Los Alamos, NM	
Banda Group International, LLC	COLLIER GEOPHYSICS
Project #: 20-184	January 2021
Drafted by: J. Sheehan	Checked by: P. Sirles
	Fig. A-12

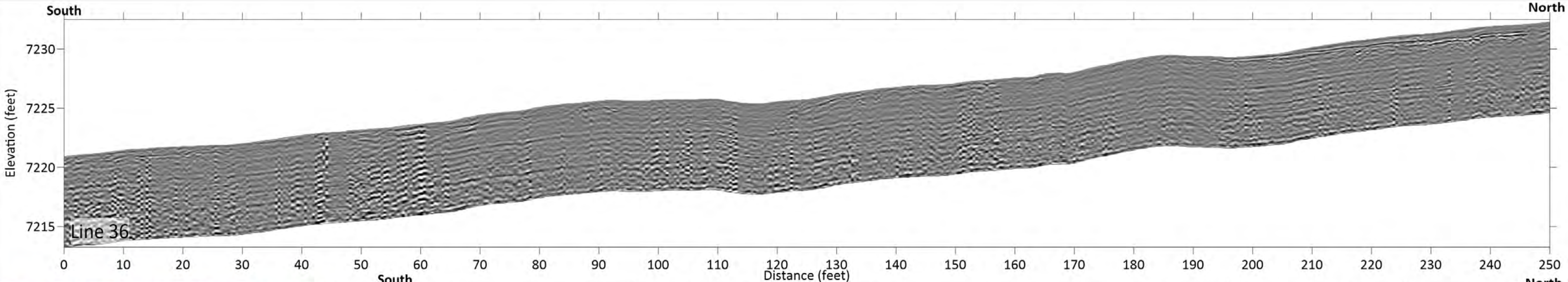

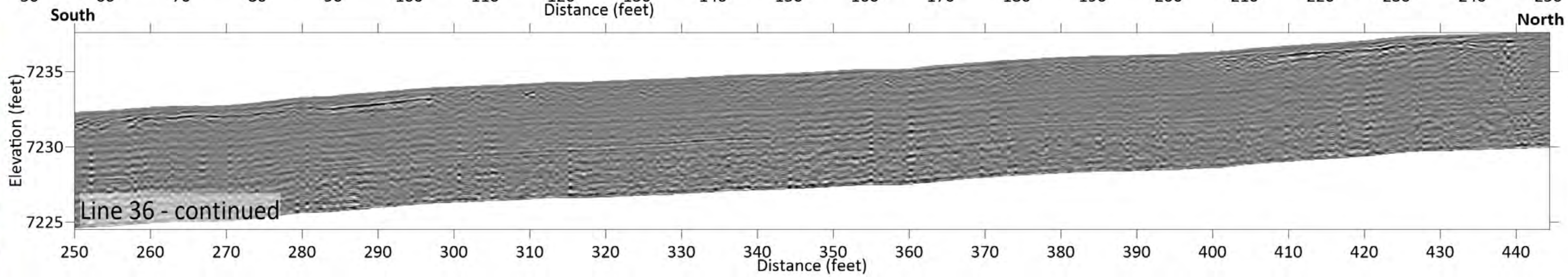

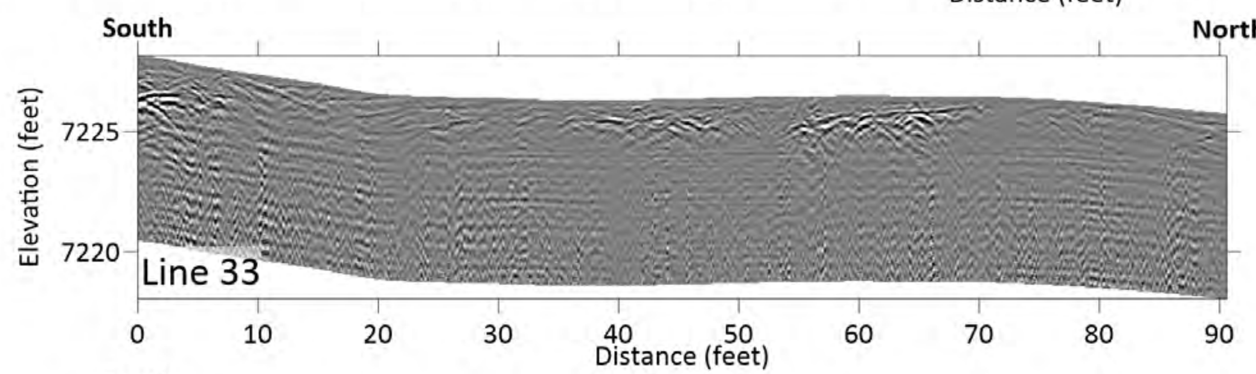

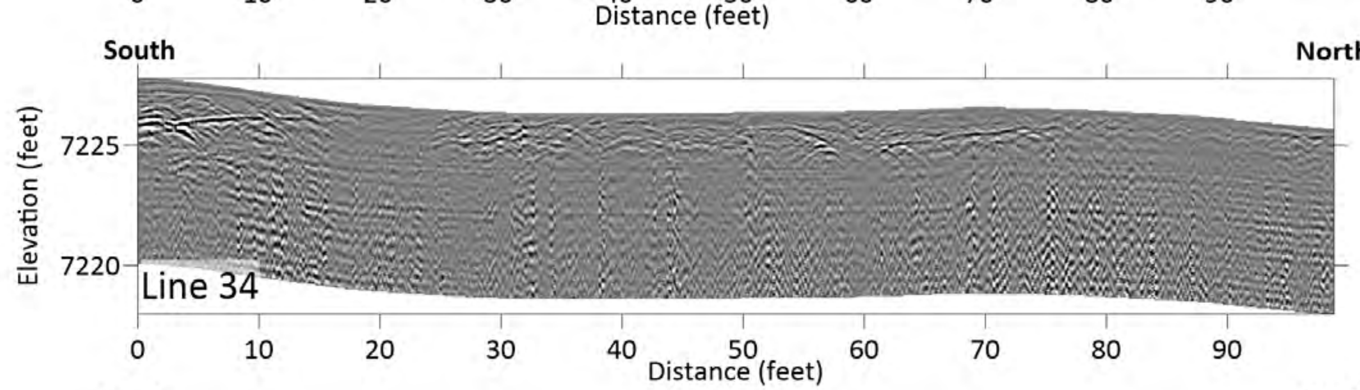

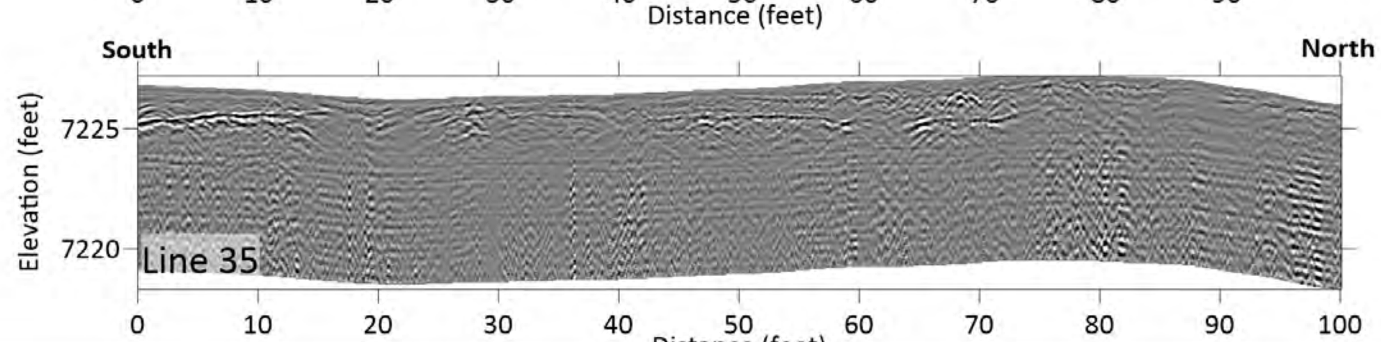

GPR Results (6 of 12) MDPR Site Los Alamos, NM	
Banda Group International, LLC	COLLIER GEOPHYSICS
Project #: 20-184	January 2021
Drafted by: J. Sheehan	Checked by: P. Sirles
	Fig. A-13

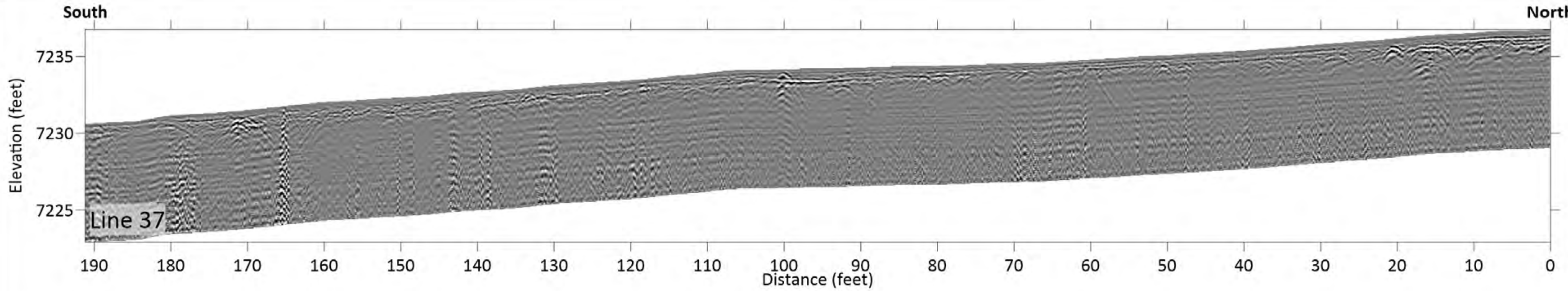

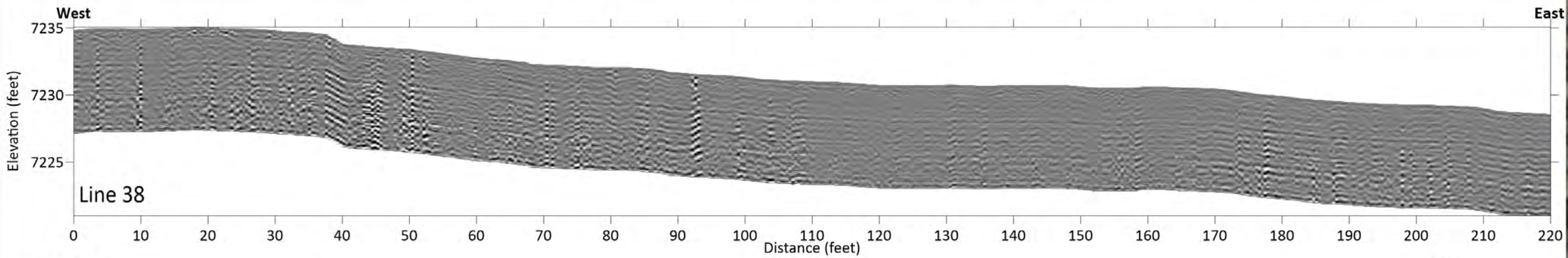

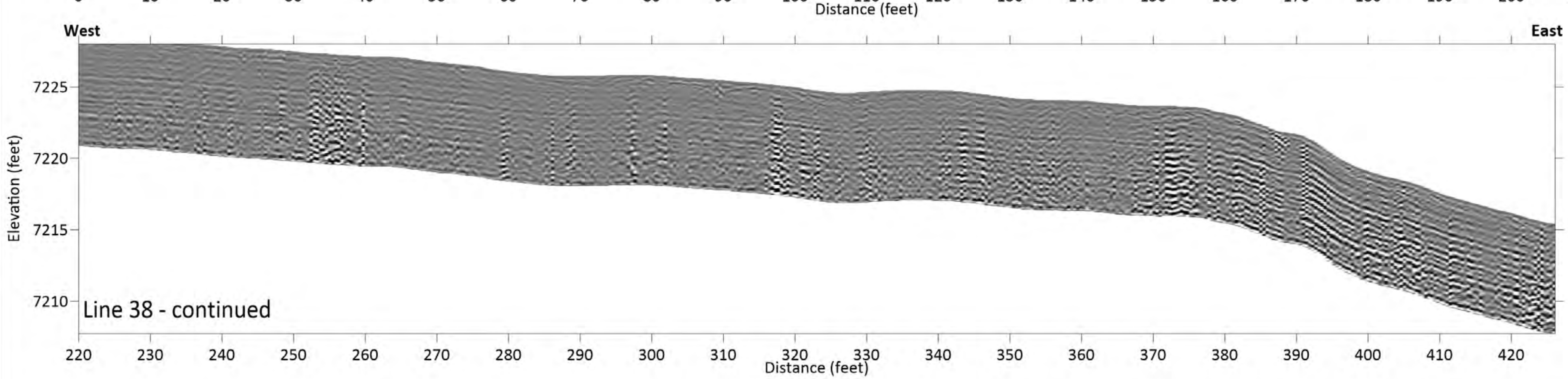

GPR Results (7 of 12)
MDPR Site
Los Alamos, NM

Banda Group International, LLC

COLLIER GEOPHYSICS

Project #: 20-184	January 2021
Drafted by: J. Sheehan	Checked by: P. Sirles

Fig. A-14

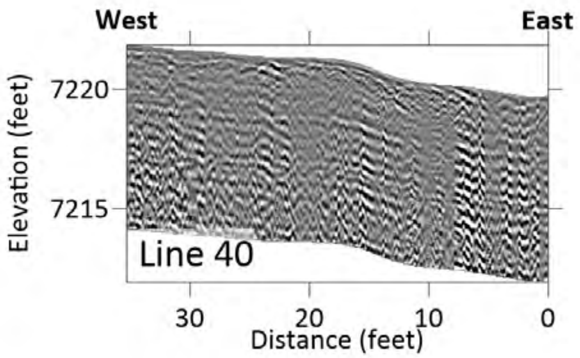

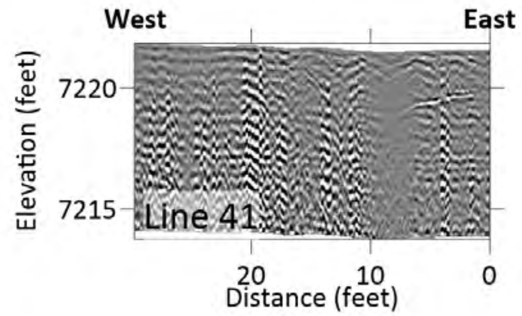

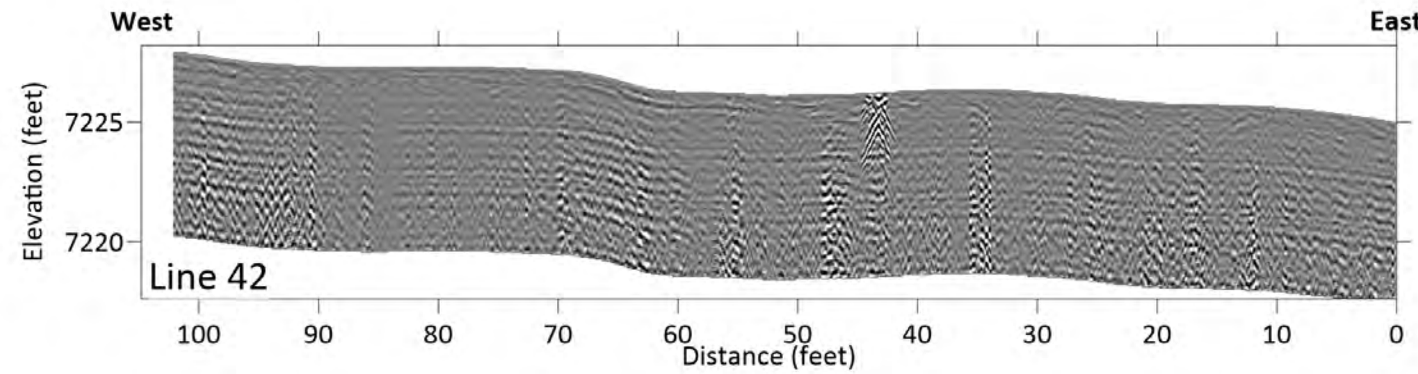

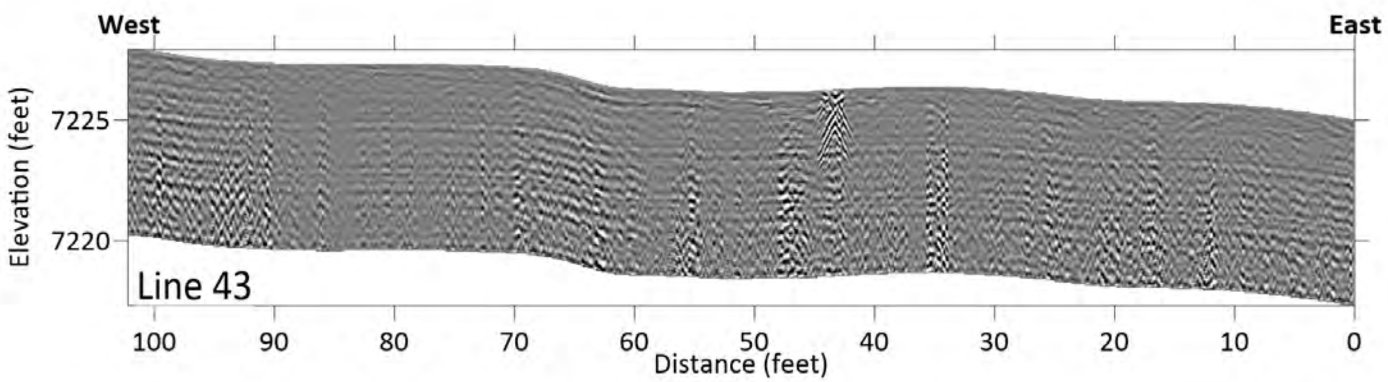

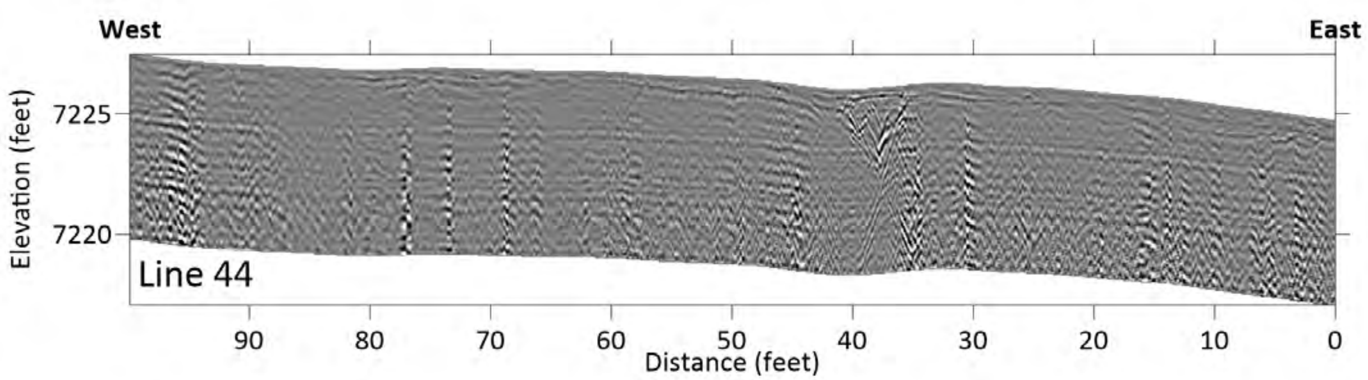

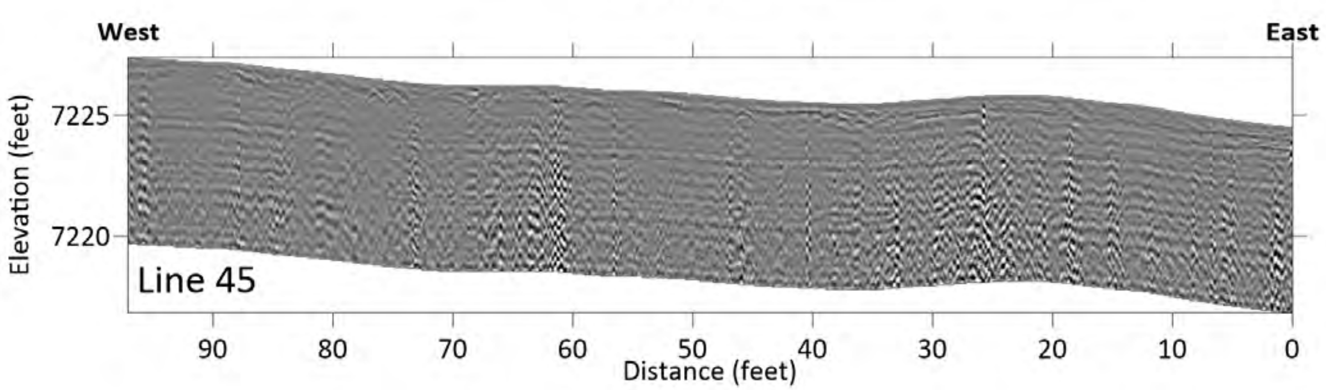

GPR Results (8 of 12)
MDPR Site
Los Alamos, NM

Banda Group International, LLC

Project #: 20-184	January 2021
Drafted by: J. Sheehan	Checked by: P. Sirles

COLLIER GEOPHYSICS

Fig. A-15

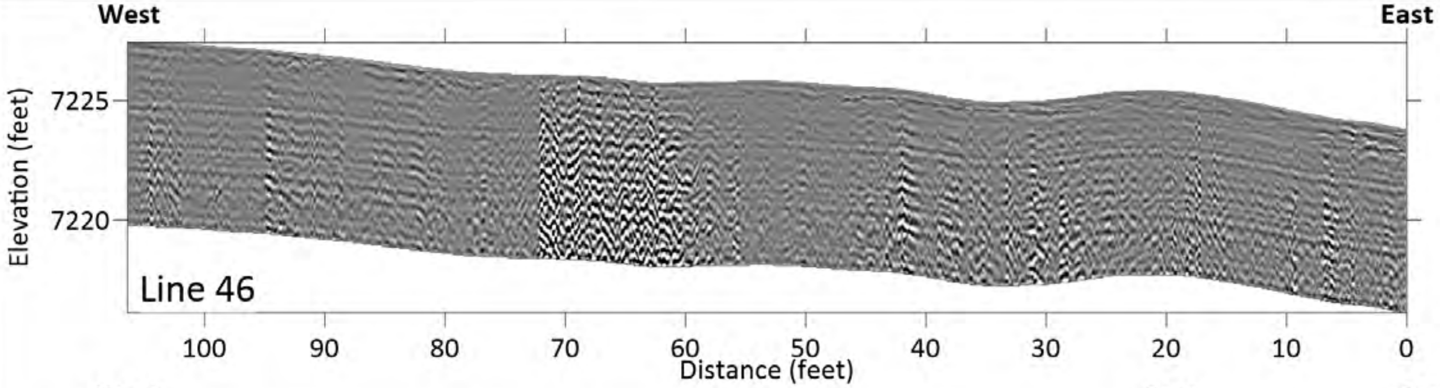

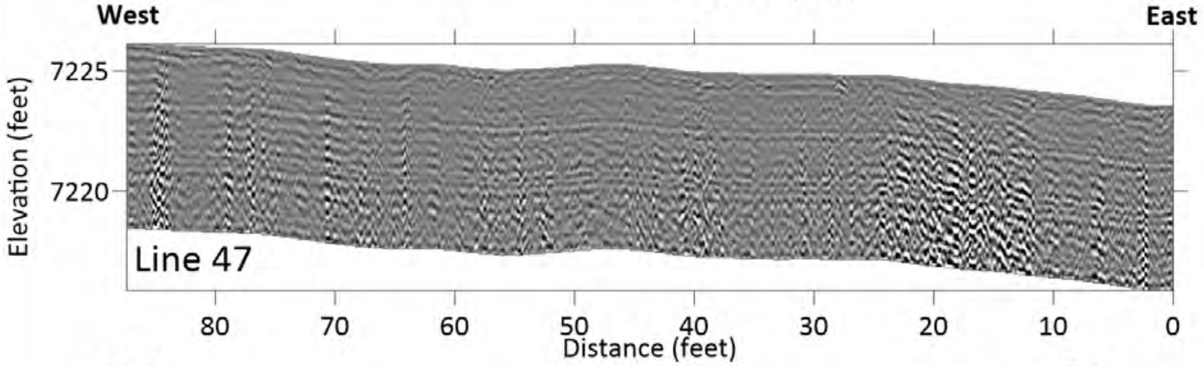

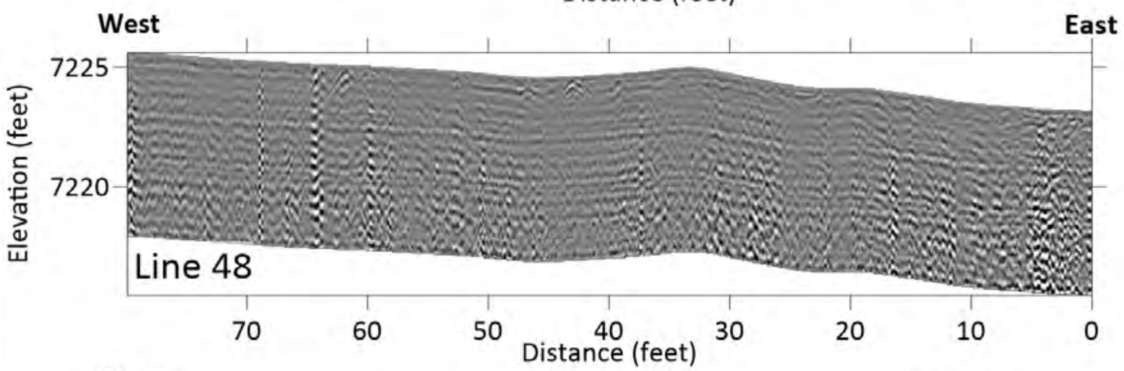

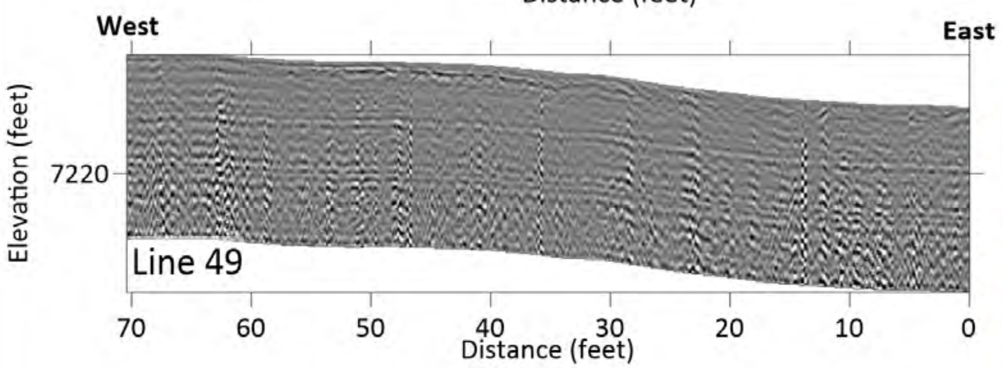

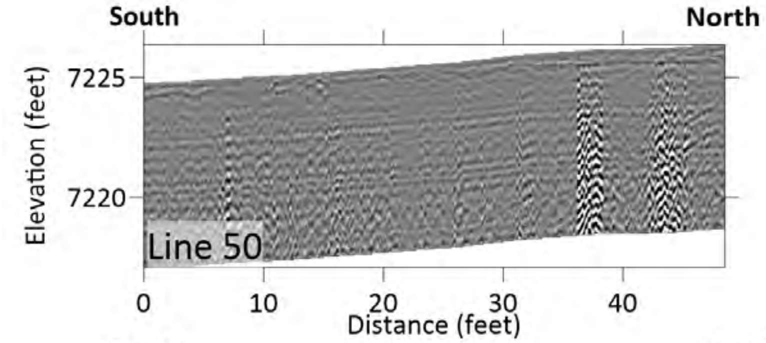

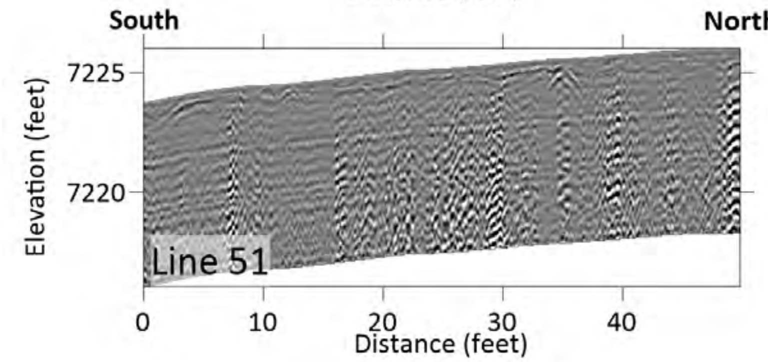

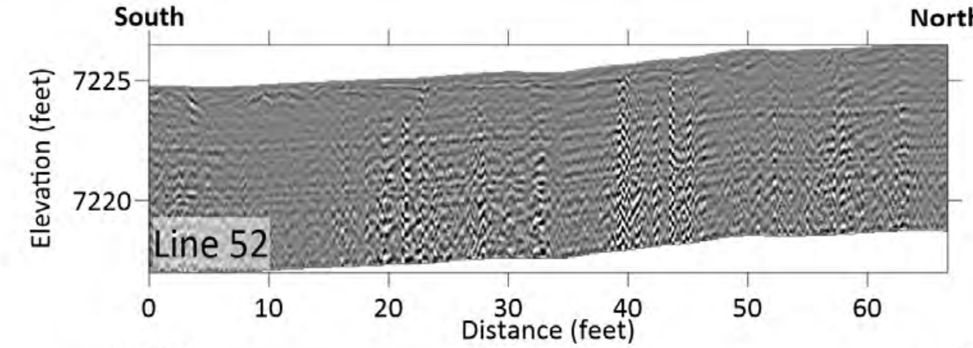

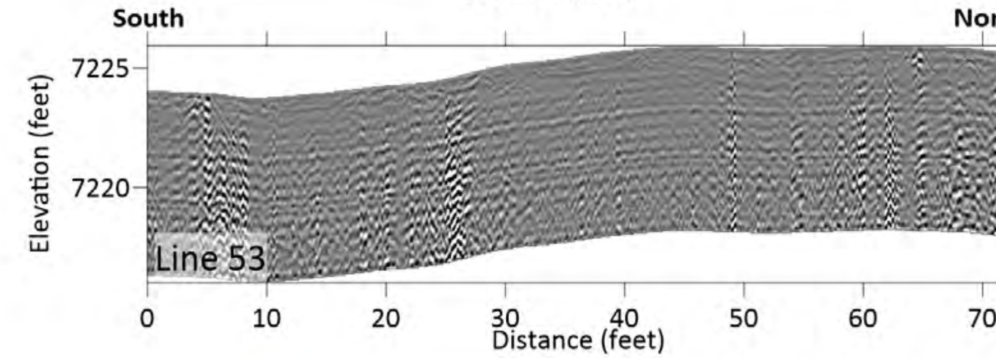

GPR Results(9 of 12)
MDPR Site
Los Alamos, NM

Banda Group International, LLC

COLLIER GEOPHYSICS

Project #: 20-184

January 2021

Drafted by: J. Sheehan

Checked by: P. Sirles

Fig. A-16

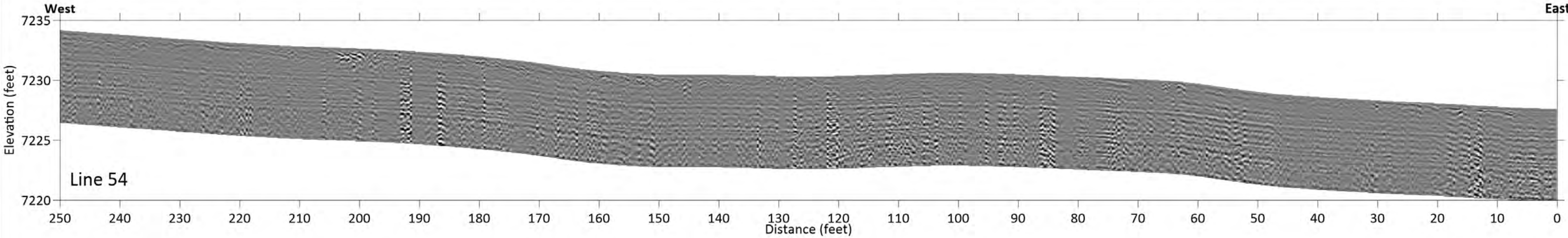

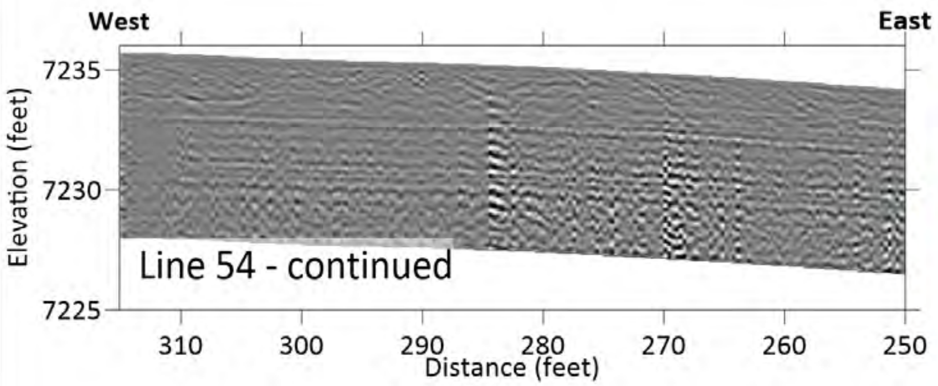

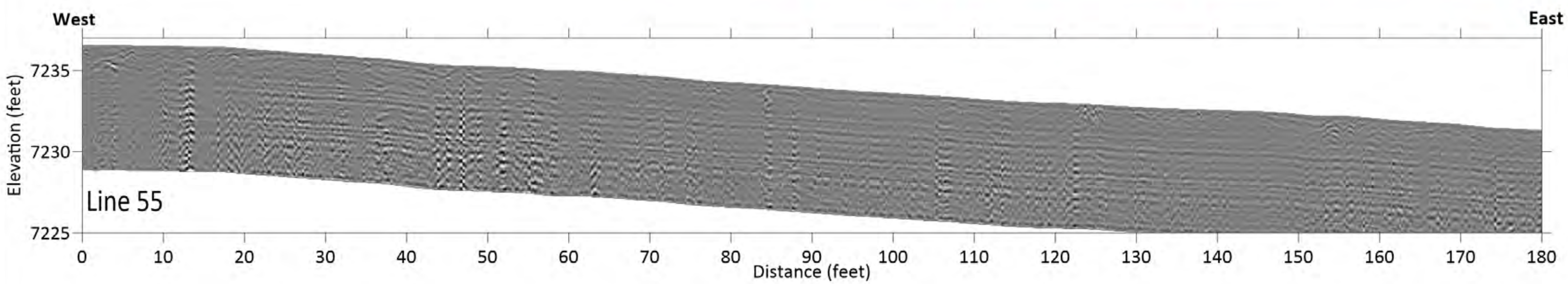

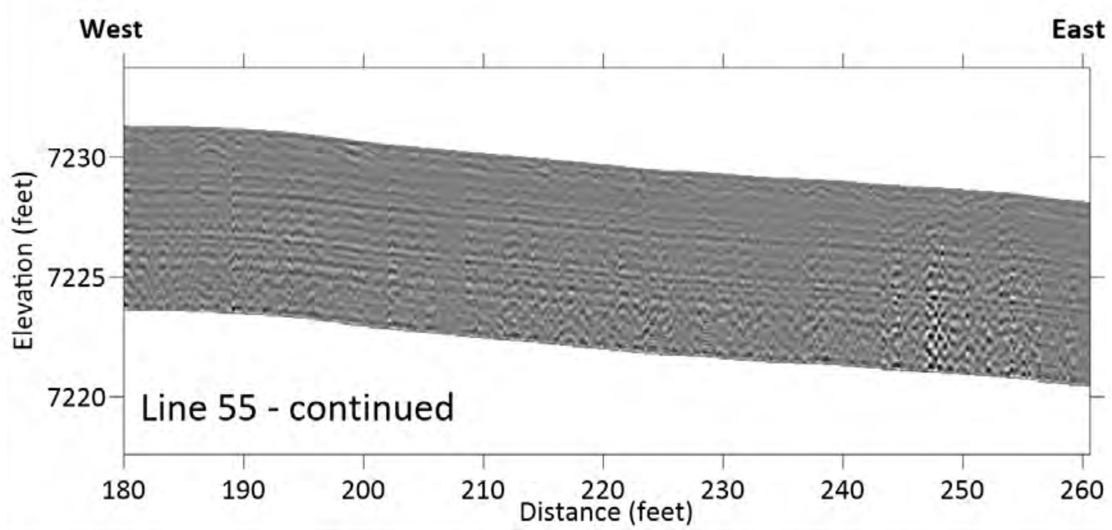

GPR Results (10 of 12)
MDPR Site
Los Alamos, NM

Banda Group International, LLC

COLLIER GEOPHYSICS

Project #: 20-184	January 2021
Drafted by: J. Sheehan	Checked by: P. Sirles

Fig. A-17

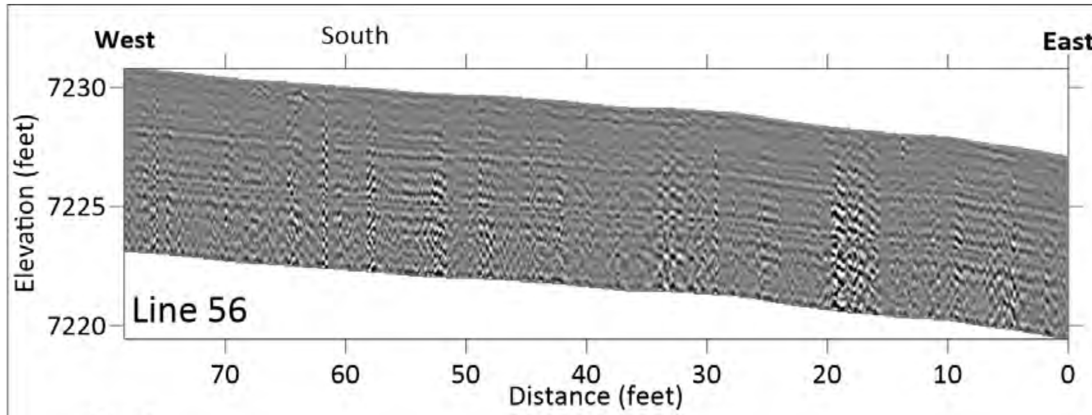

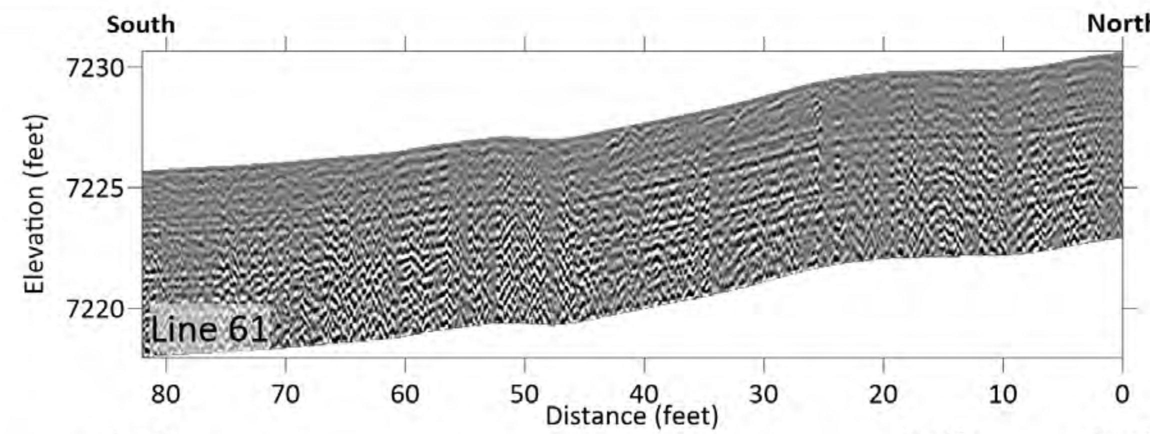

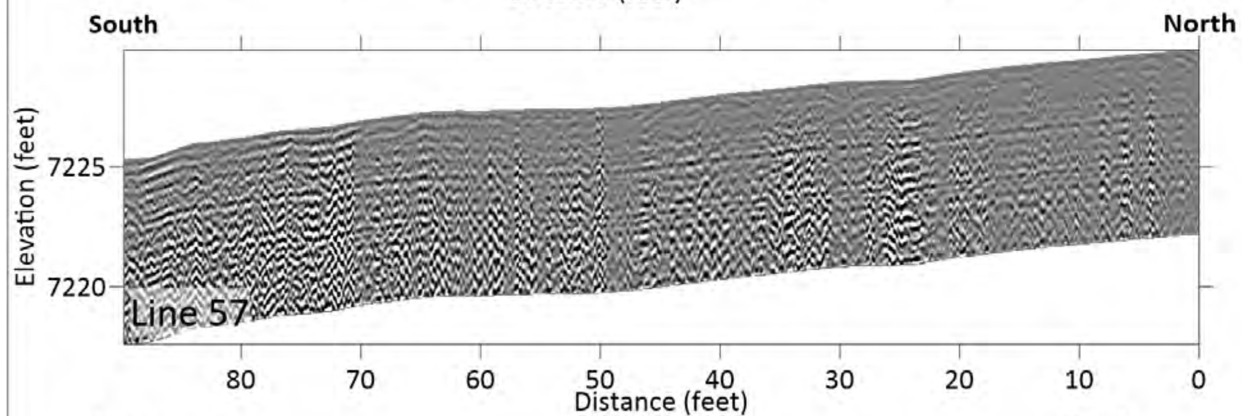

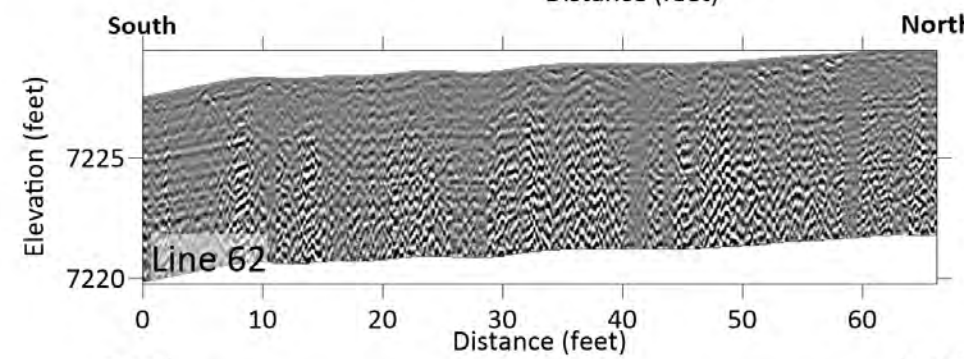

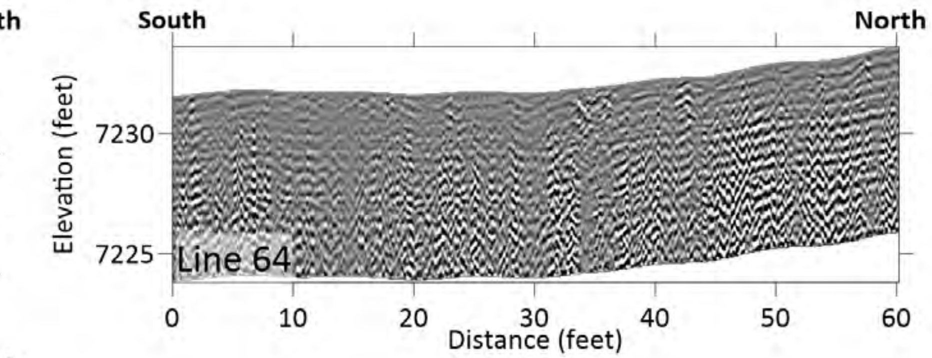

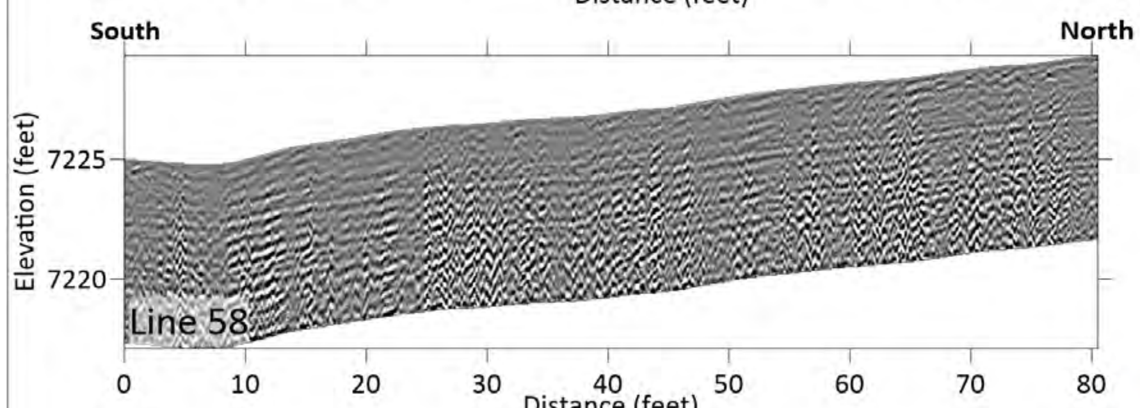

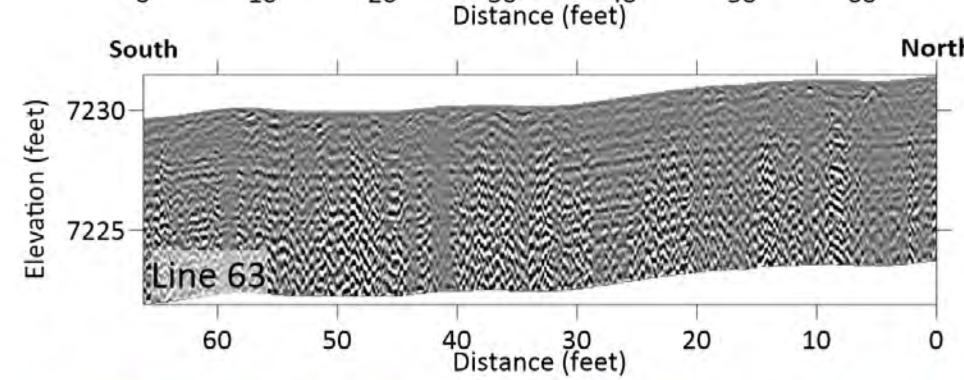

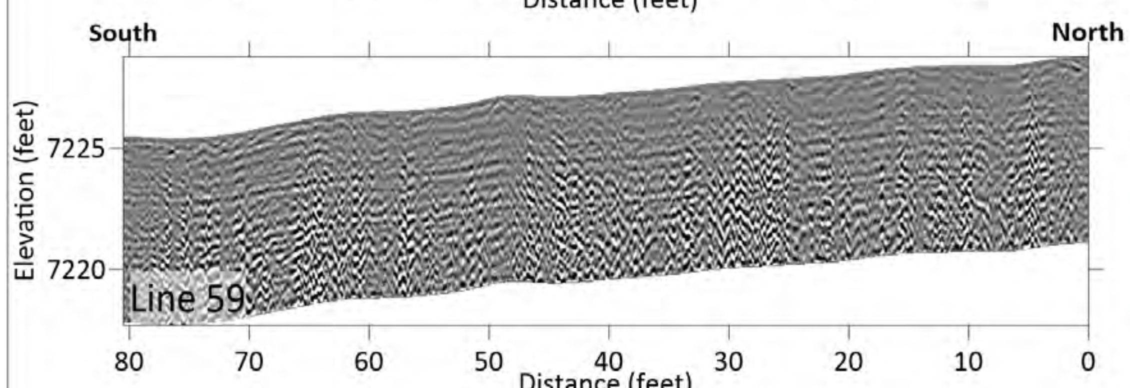

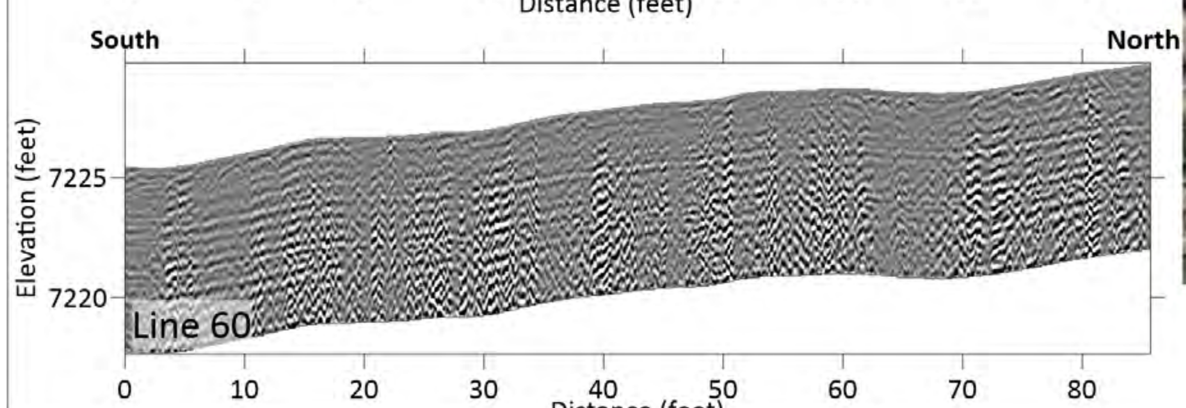

GPR Results (11 of 12)
MDPR Site
Los Alamos, NM

Banda Group International, LLC	COLLIER GEOPHYSICS
Project #: 20-184	January 2021
Drafted by: J. Sheehan	Checked by: P. Sirles

Fig. A-18

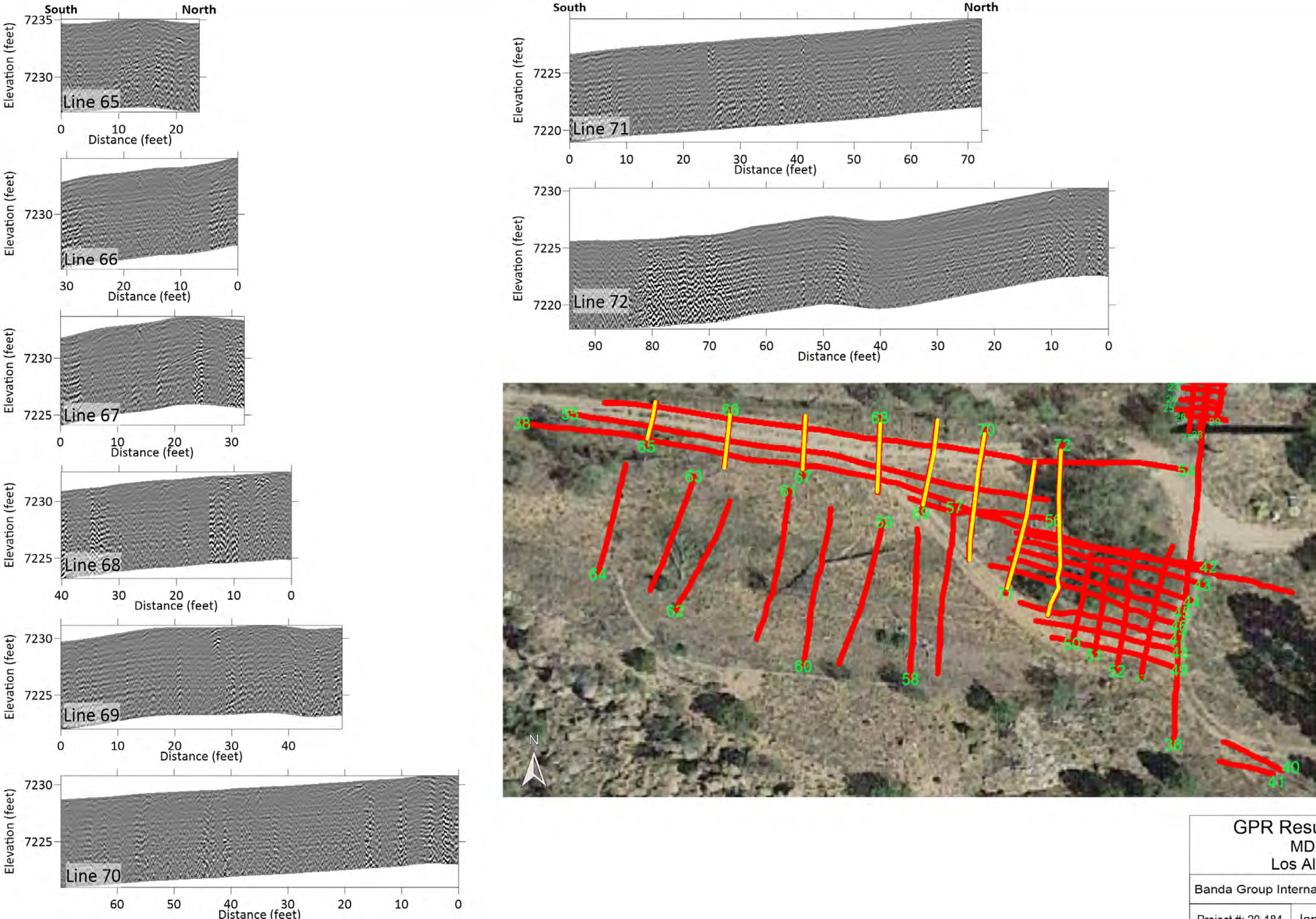

GPR Results (12 of 12)
MDPR Site
Los Alamos, NM

Banda Group International, LLC		COLLIER GEOPHYSICS
Project #: 20-184	January 2021	
Drafted by: J. Sheehan	Checked by: P. Sirles	Fig. A-19

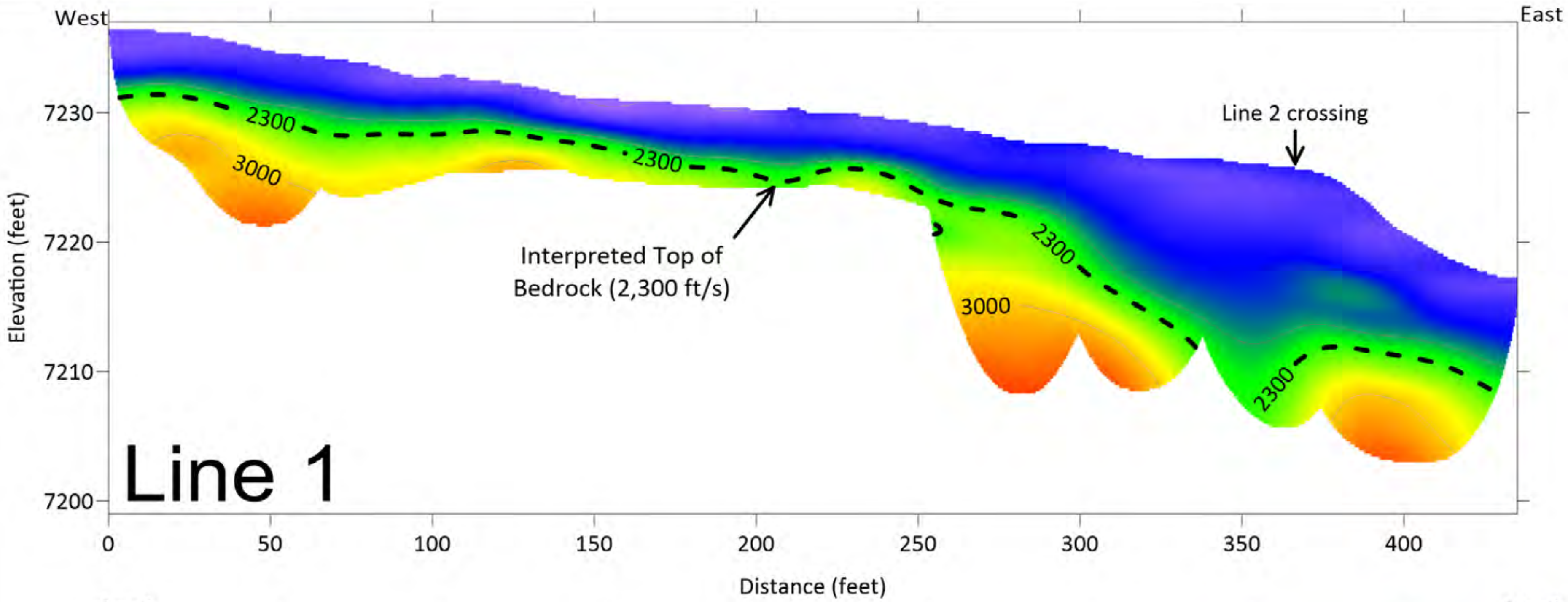

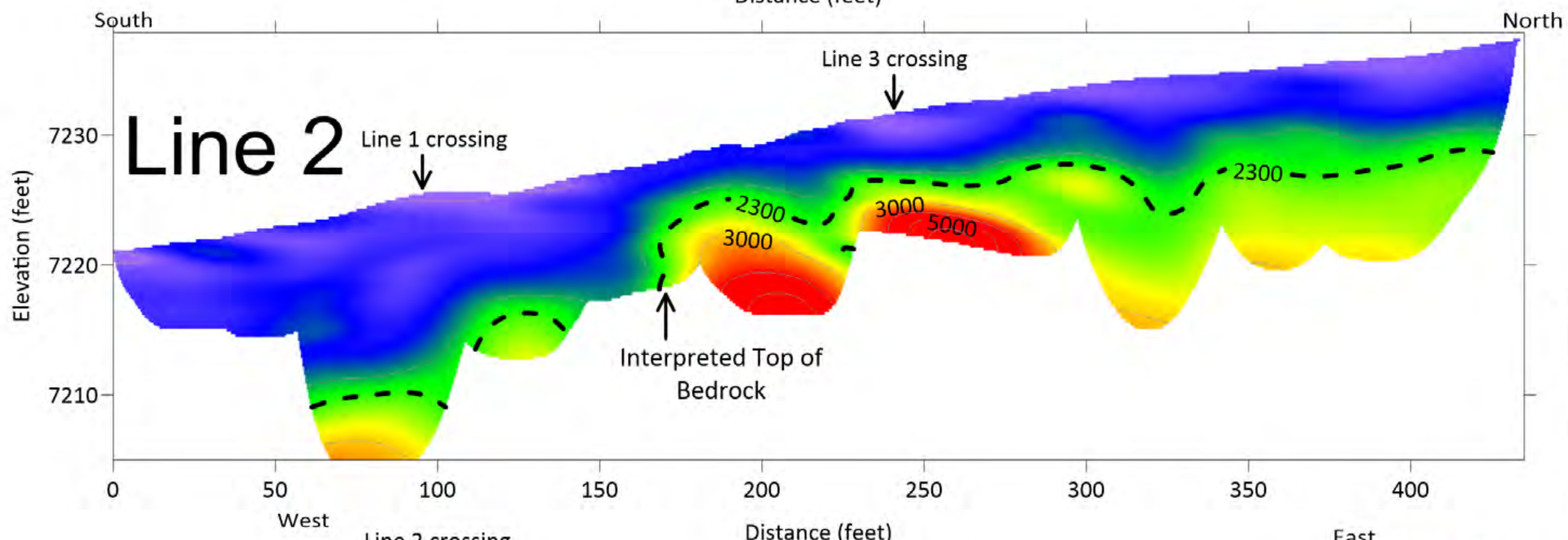

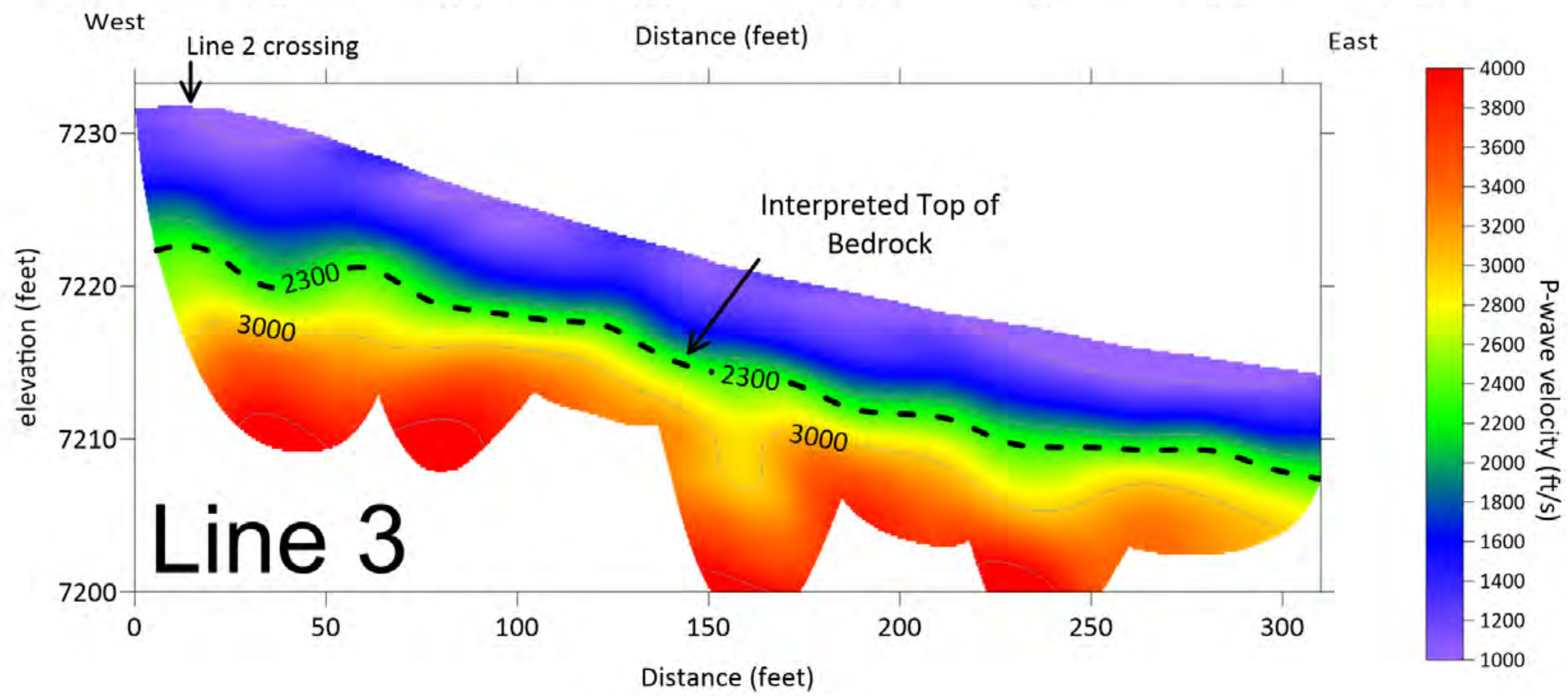

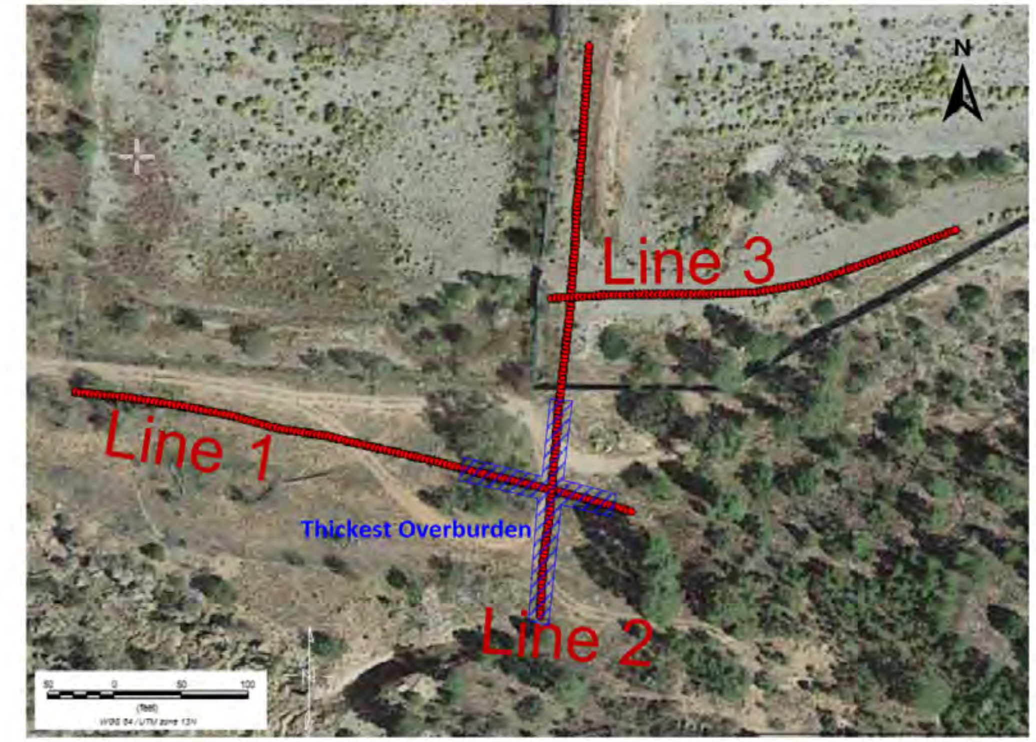

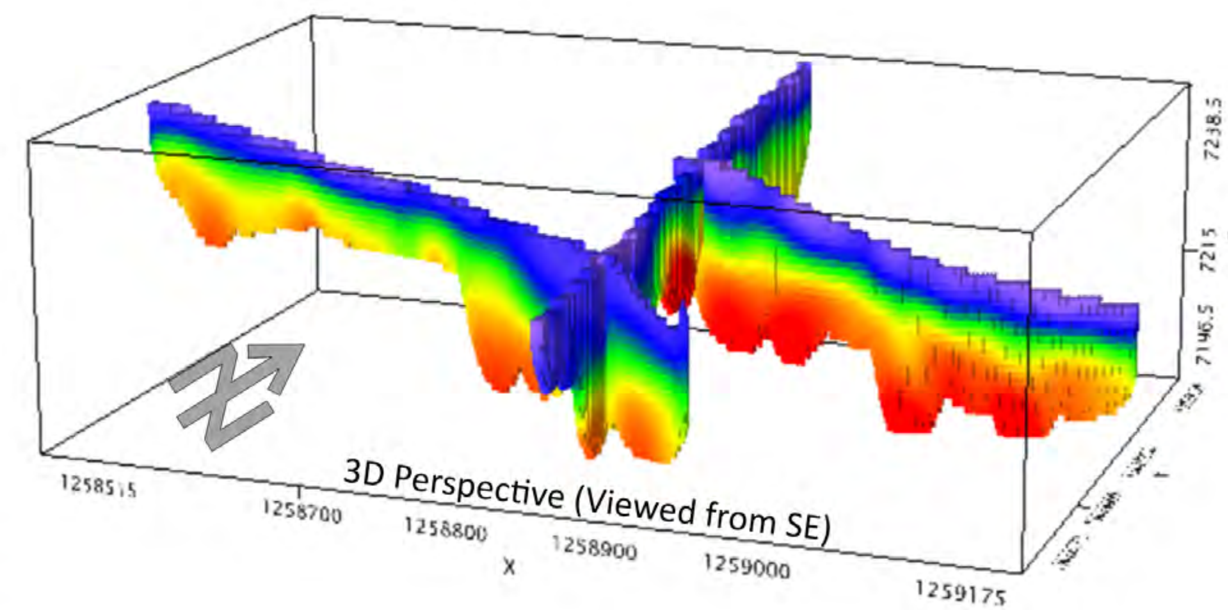

Seismic Results
MDPR Site Investigation
Los Alamos, NM

Banda Group International, LLC

Project #: 20-184 | January 2021

COLLIER GEOPHYSICS

Drafted by: J. Sheehan | Checked by: P. Sirles

Fig. A-20

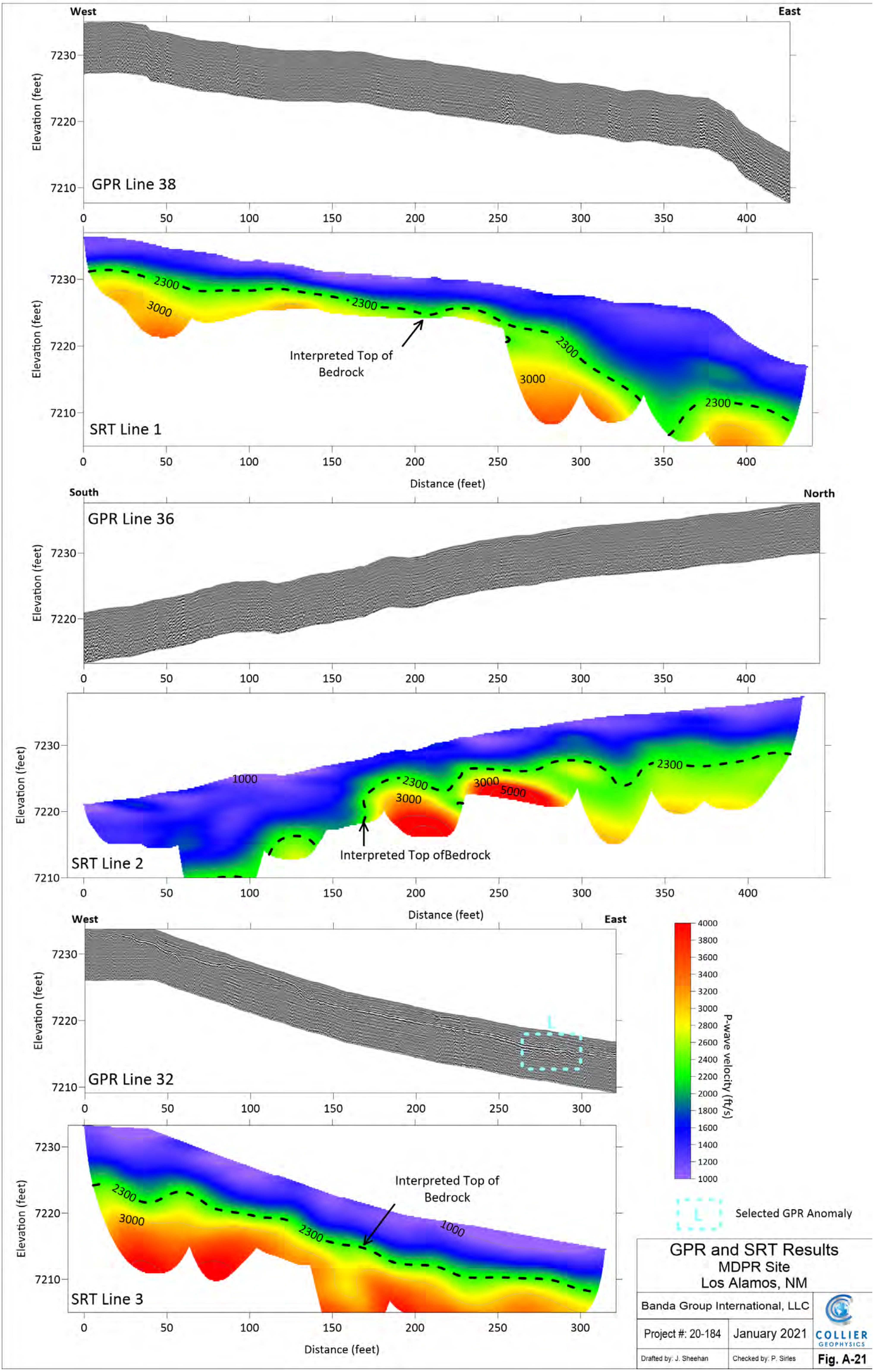

West
East
GPR Line 38
Elevation (feet)
SRT Line 1
Interpreted Top of Bedrock
2300
3000
Distance (feet)
South
North
GPR Line 36
SRT Line 2
1000
Interpreted Top ofBedrock
5000
GPR Line 32
SRT Line 3
P-wave velocity (ft/s)
Selected GPR Anomaly
GPR and SRT Results
MDPR Site
Los Alamos, NM
Banda Group International, LLC
Project #: 20-184
January 2021
Drafted by: J. Sheehan
Checked by: P. Sirles
COLLIER GEOPHYSICS
Fig. A-21

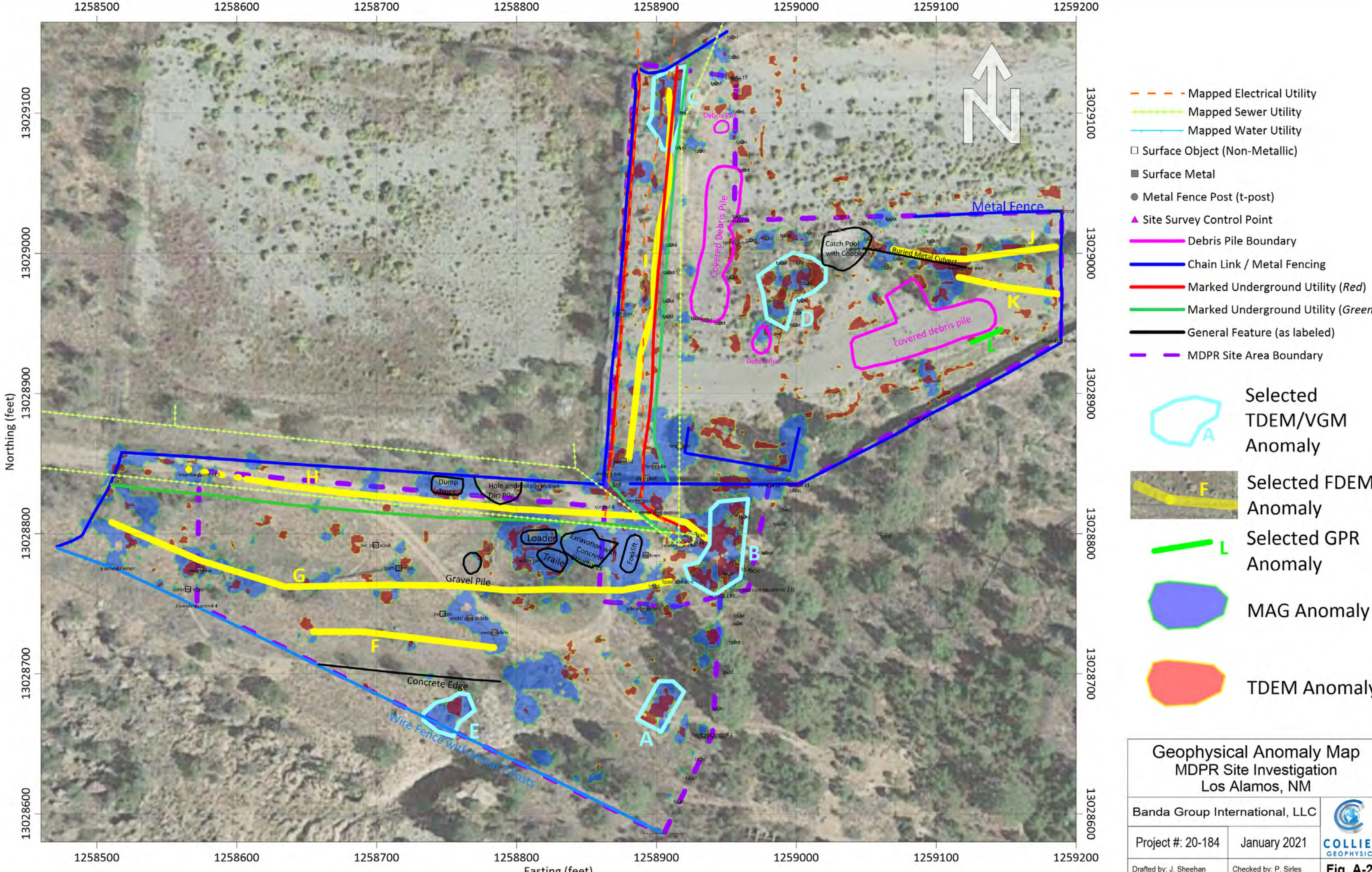

Geophysical Anomaly Map
MDPR Site Investigation
Los Alamos, NM

Banda Group International, LLC

Project #: 20-184 | January 2021

Drafted by: J. Sheehan | Checked by: P. Sirles

COLLIER GEOPHYSICS

Fig. A-22

Enclosure 2

Figure 4.1-1, Proposed potholing locations
and excavation areas at Tract A-8-a

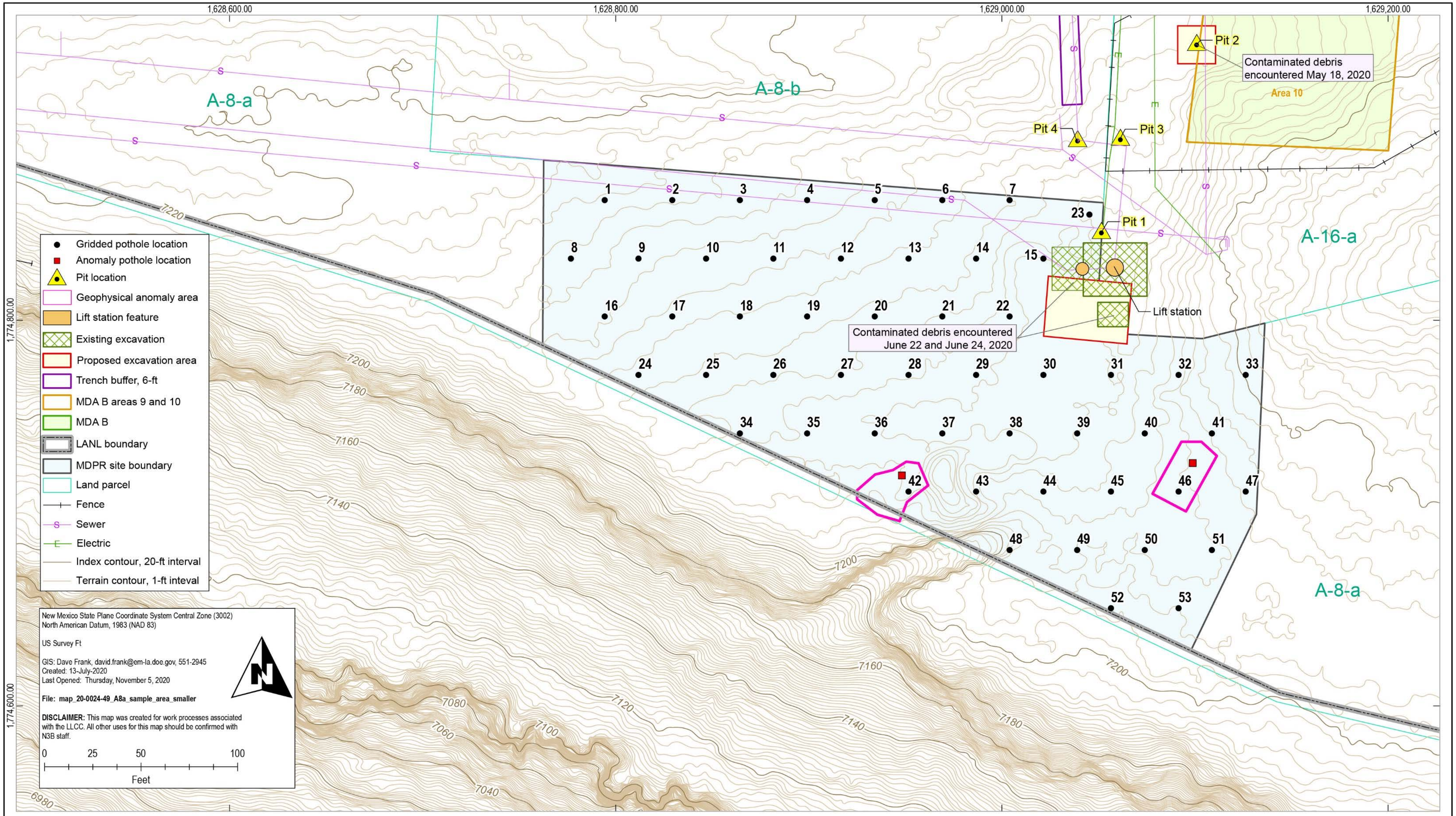

Figure 4.1-1 Proposed potholing locations and excavation areas at Tract A-8-a

Enclosure 3

Figure 4.2-2, Proposed potholing locations and excavation areas at Tract A-16-a

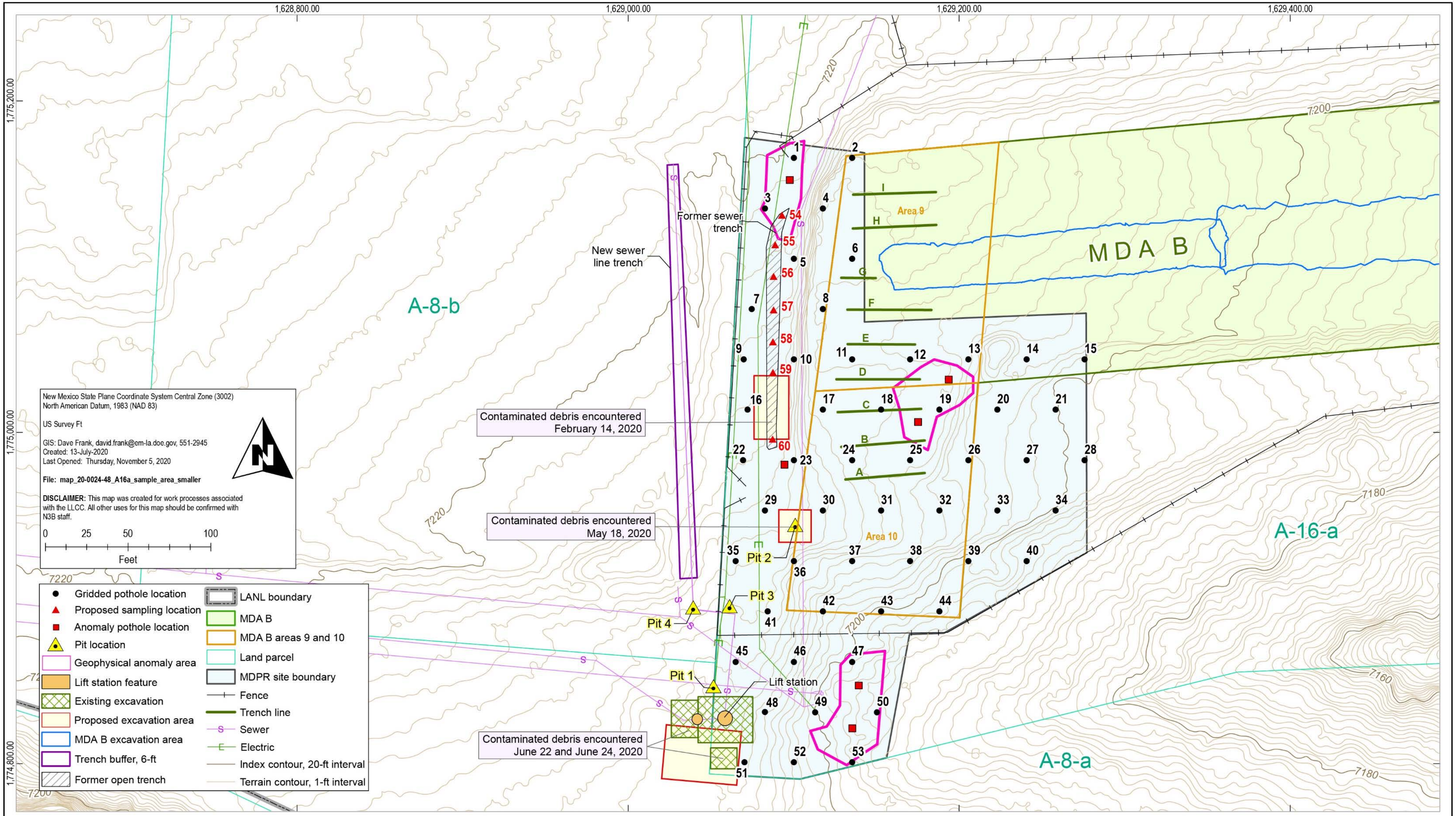

Figure 4.2-2 Proposed potholing locations and excavation areas at Tract A-16-a

Enclosure 2

Figure 4.1-1, Proposed Potholing Locations and Excavation Areas at Tract A-8-a

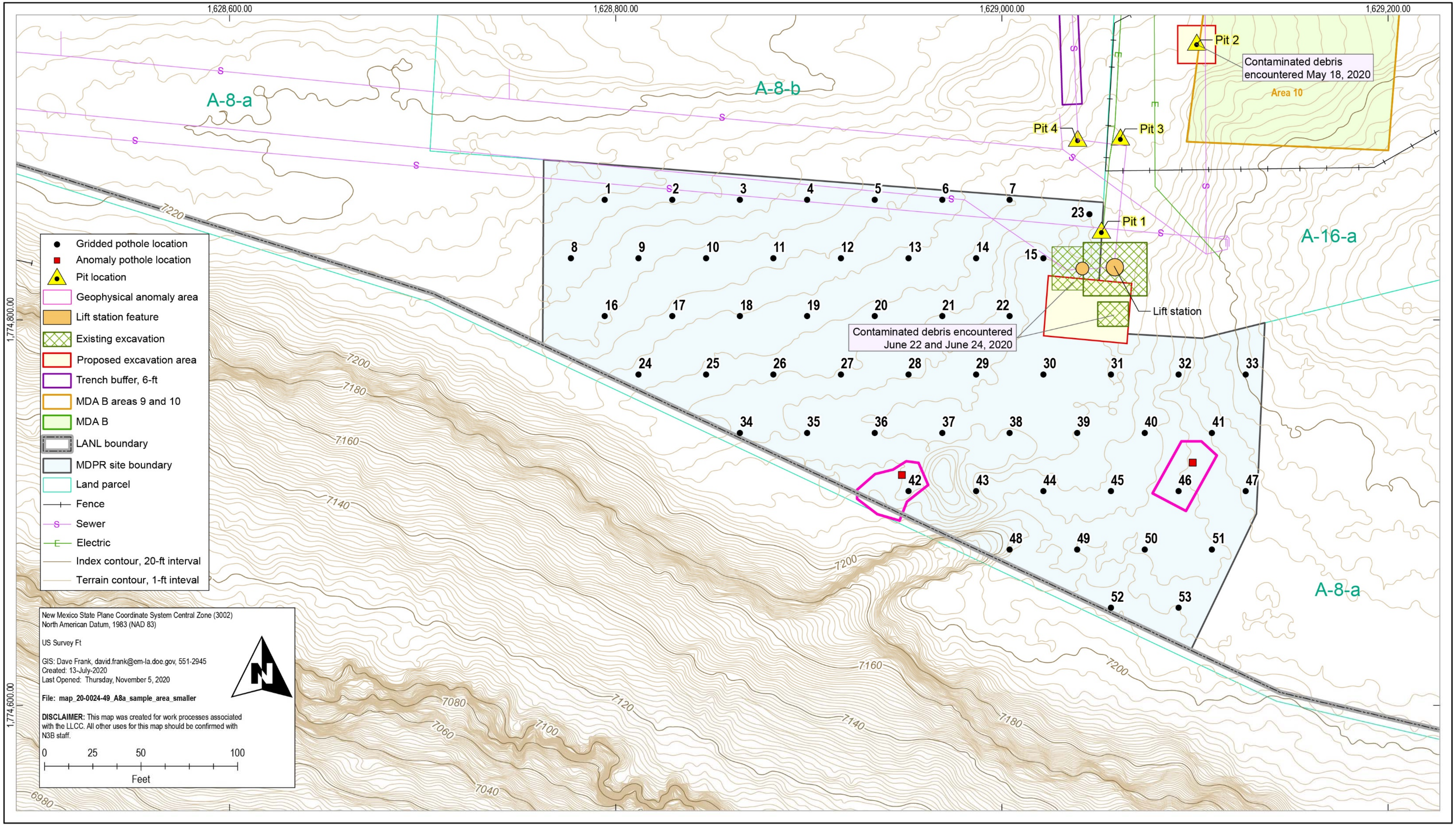

Figure 4.1-1 Proposed potholing locations and excavation areas at Tract A-8-a

Enclosure 3

Figure 4.2-2, Proposed Potholing Locations and Excavation Areas at Tract A-16-a

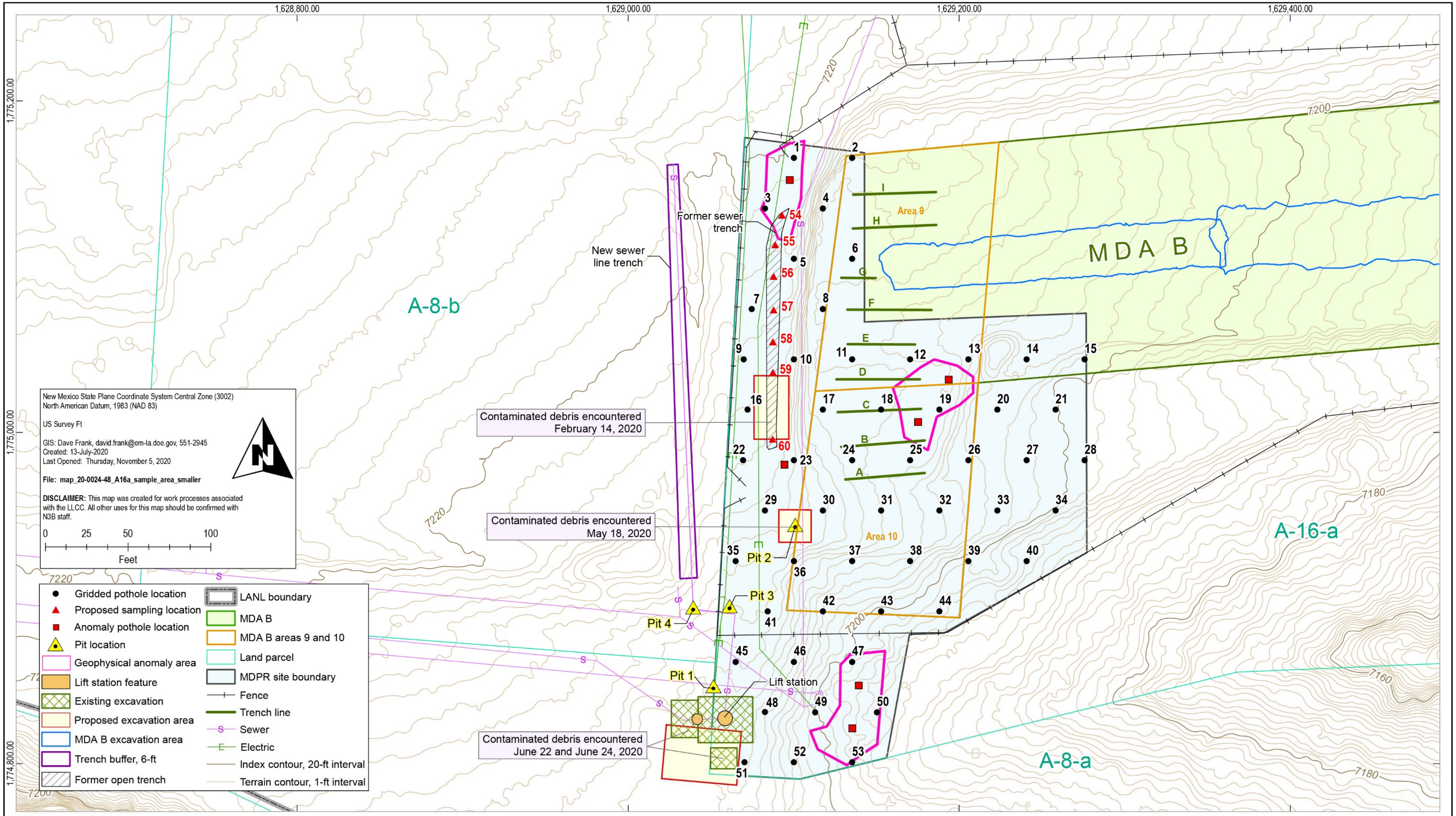

Figure 4.2-2 Proposed potholing locations and excavation areas at Tract A-16-a

Enclosure 4

Independent Review of the Solid Waste Management Unit Assessment Work Plan for Middle DP Road Site Associated with the Los Alamos National Laboratory, Los Alamos, New Mexico, DCN 5352-LT-02-0

December 18, 2020

Mr. Brian Harcek
Senior Health Physicist
Department of Energy, Environmental Management, Los Alamos Field Office
1200 Trinity Dr.
4th Floor
Los Alamos, NM 87544

SUBJECT: **INDEPENDENT REVIEW OF THE SOLID WASTE MANAGEMENT UNIT ASSESSMENT WORK PLAN FOR MIDDLE DP ROAD SITE ASSOCIATED WITH THE LOS ALAMOS NATIONAL LABORATORY LOS ALAMOS, NEW MEXICO**
DCN 5352-LT-02-0

Dear Mr. Harcek:

The Oak Ridge Institute for Science and Education (ORISE) is pleased to provide the enclosed comments detailing review of the subject document. In summary, the survey design presented in the work plan appears sufficient for identifying the presence/absence of contamination of a specified area. However, the associated threshold for the presence/absence determination is not specified and supporting data assessment methods are not presented. Specific ORISE comments are provided in the attached table.

Please feel free to contact me at 865.574.6273 or Erika Bailey at 865.576.6659 should you want to further discuss the enclosed comments.

Sincerely,

Nick Altic, CHP
Health Physicist/Project Manager
ORISE

NAA:jlc

Attachment

Electronic distribution: D. Hagemeyer, ORISE E. Bailey, ORISE
File/5352

Distribution approval and concurrence:	Initials
Group Manager Review	
Technical Review	ENB

ATTACHMENT A – COMMENT TABLE FOR INDEPENDENT REVIEW OF THE SWMU ASSESSMENT WORK PLAN

Table A.1. ORISE Comments on the SWMU Assessment Work Plan			
Comment No.	**Section**	**Page**	**Comment**
1	General		This is not a comment related to the technical aspect of the Solid Waste Management Unit Assessment (SWMU) Work Plan (WP), but rather ORISE staffs' interpretation of the survey design and objectives. This interpretation will frame the basis for the specific comments below. Per section 1.2 of the WP, the project decision is whether or not to include the subject land area as a newly discovered (SWMU) or Area of Concern (AOC) or if no further action is required. Therefore, if the collected data satisfy specific criteria then the project will make a no further action decision; otherwise, the area will receive a SMWU/AOC classification. ORISE staffs' interpretation of the survey design is that the survey will address the question of whether or not contamination is present in the study area. The sampling approach is basically a presence/absence survey design (often referred to as compliance sampling), where the resulting data will demonstrate that a high percentage of the decision area does not contain contamination above a specified threshold. A secondary, and related, objective of the study is to establish the nature and extent of contamination—when identified during the initial presence/absence investigations (i.e., potholing, geophysical surveys, visual inspections, and field surveys).
2	2.5.4	13	It is unclear how the collected survey data will be assessed against the referenced cleanup levels. ORISE interprets that the referenced cleanup levels are used as screening levels for determining whether there is a need for additional evaluations assessing human health consequences (i.e., the classification as SWMU/AOC vs NFA decision). In this decision scenario, collected data would be assessed against the screening levels through the appropriate statistical method (e.g. hypothesis testing or direct comparison of the appropriate population parameter—such as the upper confidence limit of the mean). Data assessment methods would be a critical component of the plan if the data are to be used for a NFA decision. The WP text indicates that samples are collected for determining contamination extent and are only collected if contamination is identified during the field screening. This conclusion is based on

Table A.1. ORISE Comments on the SWMU Assessment Work Plan			
Comment No.	**Section**	**Page**	**Comment**
			language within the plan, such as that found in Section 4.2.3.3 that states: *"Confirmation sampling results will be used to define the lateral and vertical extent of potential contamination associated with the debris. If no debris is encountered, the pothole will be backfilled and samples will not be collected."* Therefore, in the event debris is not identified, samples will not be collected (with the noted exception of the 28 samples in tract A-16-a, as noted in Table 4.1-1). The WP should clarify how the presence/absence survey results will be assess against the referenced cleanup levels, particularly in the event samples are not collected from a large portion of the survey area. Note, ORISE staff are not indicating that a presence/absence survey design is not appropriate for this study. The cleanup levels may serve as the threshold for the binary decision of whether a potential contaminant is "present" or "absent."
3	2.5.4	13	For the potential radionuclides, it is unclear if the conceptual model under which the cleanup levels were derived matches the conceptual model outlined in the WP. The WP should clarify the applicability of the cleanup levels to this conceptual model.
4	4.1.3.3, 4.2.3.3	18, 22	The WP states the layout of potholing locations will provide 100% confidence that contamination will be identified. ORISE staff agrees that the proposed potholing layout has a 100% probability of intersecting contamination in the horizontal direction. However, the probability of correctly determining the presence/absence of contamination is not 100%. This probability could only be applicable to visible debris criteria, not whether a contaminant of concern is present/absent from the media. The implementation of field screening activities and assessment of analytical data results in the potential for decision errors, i.e. there is the chance of false-negative (concluding contamination is not present when it actually is present) and false positive (concluding contamination is present when it is actually not present) decisions. These type of conditions are not described in the plan. This comment also relates back to Comment 2 regarding the uncertainty in the decision objectives and how data may ultimately be assessed. As currently written, the only decision is a presence/absence determination for a given area and that absence of visible debris appears to preclude the collection of any samples for quantitatively demonstrating compliance. Furthermore, the activity/concentration threshold for determining whether or not contamination is present is not explicitly stated. If this threshold is the cleanup levels, then this determination can

Table A.1. ORISE Comments on the SWMU Assessment Work Plan			
Comment No.	**Section**	**Page**	**Comment**
			only be made quantitative analytical soil sample data. Once this threshold is defined, then the appropriate field screening procedures, sample sizes, and analytical assessment methods can be defined.
5	5.4	23	The basis for the stated field screening action level is not presented, in terms the SWMU/AOC or NFA decision. If the decision at each potholing location is whether or not contamination is present, the field investigation level should adequately reflect this decision. For example, analytical detection limits are based on the critical level of the instrument background distribution. An analogous threshold for field surveys should be defined in terms of acceptable false positive/negative decision error rates. Furthermore, this threshold is directly related to the probability of identifying contamination discussed in Comment 4. If the threshold for classifying material as contaminated is below the detection limit for the field instrumentation, assessment methods may rely solely on analytical data. Additionally, specific instrumentation should be listed and evaluated as acceptable for satisfying survey objectives.
6	5.9	25, 26	Assessment methods of the collected analytical data are not presented. Similar to Comment 5 above, it is not clear how the analytical data will be interpreted, in terms of a presence/absence decision. In part this comment is related to Comment 2, as the applicable presence/absence threshold has not been defined. If the intention is to base this determination on background, then the appropriate threshold would be a parameter that is a function of the background distribution for either: a) the laboratory instrument—if the radionuclide is not naturally present in the environment, or 2) the background concentration of the radionuclide in the environment. Alternatively to the use of background as a threshold, Comment 2 provides additional discussion related to how the cleanup levels may be applicable to soil sample analytical results.

Table A.1. ORISE Comments on the SWMU Assessment Work Plan			
Comment No.	**Section**	**Page**	**Comment**
7	5.9	25, 26	Preparation methods of the samples submitted for laboratory analysis are not presented. For example, will the entire core increment be submitted for analysis? If not, how will the sample be segregated prior to laboratory submittal?